THE UNIVERSITY OF CHICAGO

ABERRANT SYNAPTIC PLASTICITY UNDERLYING PARKINSONIAN MOTOR BEHAVIORS

A DISSERTATION SUBMITTED TO

THE FACULTY OF THE DIVISION OF THE BIOLOGICAL SCIENCES

AND THE PRITZKER SCHOOL OF MEDICINE

IN CANDIDACY FOR THE DEGREE OF

DOCTOR OF PHILOSOPHY

COMMITTEE ON NEUROBIOLOGY

BY

MEERA JANAK PATEL

CHICAGO, ILLINOIS

DECEMBER 2019

TABLE OF CONTENTS

LIST OF FIGURES

LIST OF ABBREVIATIONS

A2AR	adenosine A2A receptor
AAV	adeno-associated virus
AC5	adenylyl cyclase type 5
ACSF	artificial cerebrospinal fluid
AMPA	α-amino-3-hydroxy-5-methyl-4-isoxazolepropionic acid
BAC	bacterial artificial chromosomal
cAMP	3',5'-cyclic adenosine monophosphate
CB1R	cannabinoid type 1 receptor
ChR2	channelrhodopsin-2
D1-MSN	D1-receptor-expressing medium spiny neuron
D1R	D1 dopamine receptor
D2-MSN	D2-receptor-expressing medium spiny neuron
D2R	D2 dopamine receptor
DARPP-32	dopamine- and cAMP-regulated phosphoprotein 32 kDa
DBS	deep brain stimulation
DLS	dorsolateral striatum
DMS	dorsomedial striatum
eCB	endocannabinoid
eCB-LTD	endocannabinoid-mediated long-term depression
EGFP	enhanced green fluorescent protein
EPSC	excitatory postsynaptic current
GABA	*gamma*-aminobutyric acid
GPCR	G-protein-coupled receptor
GPe	globus pallidus external segment
GPi	globus pallidus internal segment
IEG	immediate early gene
IT	intratelencephalic
L-DOPA	levodopa
LDR	long duration response
LFS	low-frequency stimulation
LTD	long-term depression
LTP	long-term potentiation
mEPSC	miniature excitatory postsynaptic current
mGluR	metabotropic glutamate receptor
MSN	medium spiny neuron
nAChR	nicotinic acetylcholine receptor
NMDA	*N*-methyl-D-aspartate
PKA	protein kinase A
PD	Parkinson's disease
PPR	paired pulse ratio
PT	pyramidal tract
RGS4	regulator of G protein signaling 4

SDR	short duration response
SNc	substantia nigra pars compacta
SNr	substantia nigra pars reticulata
STDP	spike-timing-dependent plasticity
STN	subthalamic nucleus
TRAP	targeted recombination in active populations
VTA	ventral tegmental area

ACKNOWLEDGMENTS

I would like to thank my advisor, Xiaoxi Zhuang, for his support and patience throughout the course of my graduate training. With his encouragement, I was able to learn a remarkable range of concepts and techniques which has been truly invaluable in my research. I have been very fortunate to work in a lab with a mentor as dedicated, enthusiastic, and kind as Xiaoxi, and for that I am very grateful.

Next, I want to thank the other members of the Zhuang lab, both past and present. In particular, I thank Jessica Koranda, Jary Delgado, Wanhao Chi, Qian Yang, Lee Vaasjo, Susie Turkson, and Jason Thome for providing me with various forms of support, whether through technical assistance or friendship. All of them helped make the lab a fun and collaborative environment.

I would also like to acknowledge my thesis committee, Dan McGehee, Nicho Hatsopoulos, and Christian Hansel, for providing valuable guidance throughout this project. Each of them taught courses during my first year that expanded my approach to neuroscience and that I continue to refer back to today. I thank Dan especially, who has been a valuable collaborator and whose lab I often sought help from over the years.

I am extremely grateful to Raj Awatramani for the scientific training I received while working as technician in his lab. Raj taught me how to be a thoughtful and diligent scientist and I feel very lucky to have begun my scientific career with him. I would also like to thank all of the exceptional scientists that I worked with in the Awatramani lab who taught me nearly all of the molecular biology techniques that I use today.

Finally, I am grateful to my family and friends who have provided unwavering support

throughout my scientific pursuits. I am thankful to my parents for giving me an excellent education and for fostering in me a passion for learning. I thank my sisters for their encouragement and for taking me on hikes whenever I visited. Finally, I thank my dear friends Dan, Alisa, Pamela, Clarabelle, Mark, Andrés, and Derek for their friendship, humor, and love.

ABSTRACT

The long-lasting deterioration of motor output in Parkinson's disease (PD) is thought to arise from the degeneration of midbrain dopamine neurons and the subsequent loss of dopamine signaling in the striatum. While much is already known about dopaminergic modulation of striatal activity, few studies have directly linked aberrant synaptic plasticity to PD motor symptoms. Here, I examine the striatal synaptic plasticity mechanisms that contribute to parkinsonian motor behaviors. To establish a technique for examining plasticity *ex vivo*, I first characterize an *in vitro* optogenetic long-term depression (LTD) protocol that induces postsynaptic corticostriatal depression in D2 dopamine receptor (D2R)-expressing medium spiny neurons (MSNs). Unlike previously reported forms of striatal LTD, this light-mediated LTD is cannabinoid type 1 receptor (CB1R)-independent and does not alter presynaptic glutamate release. Moreover, I show that it does not require the activation of *N*-methyl-D-aspartate (NMDA) receptors or metabotropic glutamate receptor 5 (mGluR5).

Previous studies from our laboratory have suggested that the loss of dopamine signaling in the striatum may lead to motor decline through aberrant plasticity at corticostriatal synapses in the D2R-expressing indirect pathway. To test this, I use optogenetics and whole-cell recordings to assess changes in corticostriatal plasticity in mice that underwent motor training with a pharmacological D2R blockade. I demonstrate that this treatment results in enhanced *ex vivo* corticostriatal LTD in D2R-expressing MSNs, suggesting that long-term potentiation (LTP) had previously occurred at these synapses *in vivo*. I also show that co-administration of an A2A adenosine receptor (A2AR) antagonist is sufficient to prevent induction of aberrant

corticostriatal potentiation, revealing a potential mechanism for caffeine's protective effects in PD. Finally, I demonstrate that direct *in vivo* corticostriatal stimulation in mice with D2R blockade leads to a lasting impairment in rotarod performance following stimulation. Together, these results implicate aberrant corticostriatal plasticity in the development of parkinsonian motor symptoms and provide support for therapeutic strategies that target altered plasticity in PD and other neuropsychiatric disorders.

CHAPTER 1

INTRODUCTION

1.1 Parkinson's disease

1.1.1 Etiology and symptoms

Parkinson's disease (PD) is a progressive neurodegenerative disease that affects nearly 1% of the overall population (Marras et al., 2018). It is characterized by the selective loss of dopamine neurons in the substantia nigra pars compacta (SNc) which results in the loss of dopamine signaling in the striatum. Symptoms of the disease primarily affect motor function and include resting tremor, bradykinesia, muscular rigidity, and postural instability. Non-motor symptoms include sleep disturbances, cognitive impairments, depression and anxiety, and sensory symptoms (Sveinbjornsdottir, 2016).

The etiology of PD is still poorly understood, but both genetic and environmental factors are thought to contribute. Age is a major factor in the onset of PD, while about 5% of cases occur before the age of 60 with the majority of these cases relating to mutations in familial-PD-associated genes (Wirdefeldt et al., 2011; Reeve et al., 2014). These mutations are thought to be responsible for pathologic features such as mitochondrial dysfunction (*PINK1* and *Parkin*), aggregation of α-synuclein and Lewy bodies (*PARK1*), and oxidative stress (*PARK7*). A number of these mutations have been found in patients with sporadic cases of PD as well (Wirdefeldt et al., 2011). In addition to genetic background, several studies point to exposure to environmental toxins, pesticides, or heavy metals as a risk factor for PD. These environmental factors are not believed to act on their own; rather, the interaction between genetic mutations and exposure to

toxins is viewed as significant contributor to development of PD (Carvey et al., 2006; Sulzer, 2007).

1.1.2 Current treatments

The most commonly used treatment for PD consists of dopamine replacement therapy with levodopa (L-DOPA), the precursor to dopamine. First introduced in 1969 (Cotzias et al., 1969), L-DOPA remains the most effective treatment for PD today. A patient's response to L-DOPA consists of a short duration response (SDR), which is an acute improvement in motor performance that wears off in between doses, and a long duration response (LDR), which is a slower improvement in motor performance that occurs over days or weeks and persists in between doses. Following cessation of treatment, the LDR can take days or weeks to wear off, suggesting that long-term neural plasticity underlies this response (Barbato et al., 1997; Zhuang et al., 2013).

With prolonged use of the L-DOPA, the therapeutic response can become complicated by motor fluctuations and dyskinesia. Dyskinesia typically occurs when L-DOPA and dopamine reach their peak dose concentrations in the brain (Fabbrini et al., 2007; Calabresi et al., 2010), however it is unclear whether the disorder is due to PD progression, long-term L-DOPA use, or both. Dysfunctional striatal circuitry has been implicated in levodopa-induced dyskinesia (Cao et al., 2010; Engeln et al., 2016), and hyperactivity in cholinergic interneurons (Ding et al., 2011) and D1 dopamine receptor (D1R)-expressing medium spiny neurons (MSNs) (Girasole et al., 2018) have been shown to mediate the disorder in mice.

In recent years, deep brain stimulation (DBS) has become a reliable treatment for advanced stages of PD (Herrington et al., 2016). Through surgically implanted electrodes

controlled by a pulse generator implanted under the skin, PD patients receive high frequency stimulation at deep basal ganglia structures such as the subthalamic nucleus (STN) or globus pallidus internal segment (GPi) (Chiken and Nambu, 2016). DBS has been found to be most effective at treating tremor and bradykinesia at higher frequencies (> 130 Hz), while low frequency (< 50 Hz) stimulation has been reported to worsen symptoms (Moro et al., 2002). The proposed mechanisms behind DBS are varied and inconclusive, but it is likely that the treatment acts via several mechanisms including acute activation and inhibition, modulation of network-wide activity, and structural and synaptic plasticity (Herrington et al., 2016). Some studies in animal models have also suggested that DBS may have neuroprotective effects through induction of neurotrophic factors and neurogenesis (Toda et al., 2008; Spieles-Engemann et al., 2011), however DBS has so far not been found to change the progression of PD in human patients. Despite our limited mechanistic understanding of the treatment, advances in DBS continue to progress. Recently, efforts have been made to develop closed-loop or adaptive DBS, which takes feedback from the brain in order to modify stimulation in real time (Little et al., 2016).

1.1.3 Protective effects of caffeine and nicotine

Numerous epidemiological studies have demonstrated a neuroprotective role for caffeine in PD. Chronic intake of caffeine, a nonselective A2A adenosine receptor (A2AR) antagonist, is strongly correlated with a lower incidence of PD in a diverse set of populations (Ross et al., 2000; Ascherio et al., 2001; Tan et al., 2003; Palacios et al., 2012). In men, the reduction in PD risk is striking, with a five times lower risk in those who drink over 4 cups of coffee per day (Ross et al., 2000). These beneficial effects of caffeine are dose-dependent and occur with

several different types of caffeine-containing products. In women, however, the relationship between caffeine and PD risk is not linear. At moderate levels of caffeine consumption, women have a decreased risk of PD, just as in men. However, at high levels of caffeine consumption, women show the same risk of PD as those who consume no caffeine (Ascherio et al., 2001). The difference in caffeine's effectiveness for men and women may be due to the interaction between caffeine and estrogen, particularly in women who use hormone replacement therapy (Pollock et al., 1999; Ascherio et al., 2001, 2004). However, estrogen itself has been shown to have a protective effect against PD (Leranth et al., 2000; Currie et al., 2004; Xu et al., 2006), therefore the beneficial effects of caffeine may simply be occluded in women.

While evidence for caffeine's protection against PD is very strong, the exact mechanism underlying this protection is still unknown. Some studies have suggested that caffeine and its metabolite theophylline can attenuate neurodegeneration in animal models of PD (Chen et al., 2001; Joghataie et al., 2004; Aguiar et al., 2006). Caffeine, theophylline, and other A2AR antagonists have been found to prevent or reduce haloperidol-induced catalepsy in rodents (Casas et al., 1988; Mandhane et al., 1997; Moo-Puc et al., 2003). Similarly, the A2AR antagonist theophylline was shown to prevent aberrant motor learning caused by dopamine receptor blockade in mice (Beeler et al., 2012), suggesting that caffeine's protective effects are primarily mediated by A2AR antagonism. In humans, caffeine's benefits appear to be mainly protective in nature, as a recent study found caffeine to be ineffective at improving motor symptoms in patients already with PD (Postuma et al., 2017). In addition, clinical trials for other A2AR antagonists in treating PD have often failed due to ineffectiveness or inconsistent results (Zheng et al., 2018).

Tobacco use has also been shown to be inversely correlated with risk of PD (Gorell et al.,

1999; Tanner et al., 2002). Nicotine has been identified as the protective factor in cigarettes due to its role in stimulating dopamine release from nigrostriatal dopaminergic terminals via nicotinic acetylcholine receptors (nAChRs) (Lichtensteiger et al., 1982; Grady et al., 1992). The mechanism of nicotine's protective effects is not well understood, and studies on the protection against dopamine neuron degeneration have produced conflicting results (Ferger et al., 1998; Quik et al., 2006; Khwaja et al., 2007). Chronic nicotine treatment has been shown to protect against inhibitory motor learning in mice (Koranda et al., 2016), and studies have highlighted the drug's role in desensitizing β2-subunit-containing nAChRs which may lead to neuroadaptations that prepare the striatum for future dopamine loss (Koranda et al., 2014).

1.2 Anatomy and physiology of the striatum

1.2.1 Basal ganglia overview

The basal ganglia are a set of evolutionarily conserved nuclei that are critical for action selection, habit formation, and motor learning. Dysfunction within the basal ganglia results in a range of psychiatric and movement disorders, such as PD, Huntington's disease, obsessive-compulsive disorder, and addiction. Components of the basal ganglia include the striatum, globus pallidus, substantia nigra, and STN which interact with thalamus and cortex to form a basal-ganglia-thalamocortical circuit (Graybiel et al., 1994; Redgrave et al., 2010; Stephenson-Jones et al., 2011). The striatum, which serves as the main input nucleus of the basal ganglia, is anatomically divided on the dorsal side into the caudate nucleus and putamen in primates, though this division is not distinguishable in rodents. The ventral half of the striatum includes the ventral-most parts of the caudate-putamen, the olfactory tubercle, and the nucleus accumbens, which can be further subdivided into core and shell domains (Heimer et al., 1991; Haber, 2016).

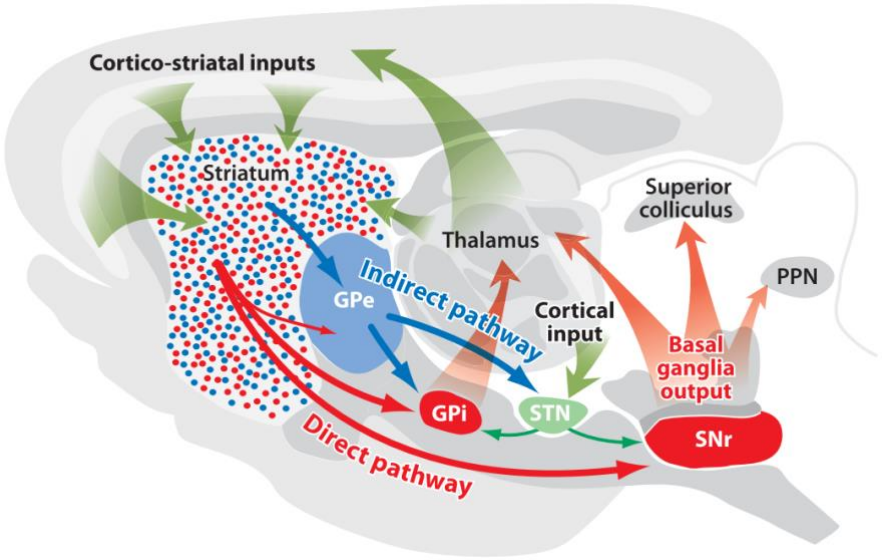

Figure 1.1. Diagram of the basal ganglia.
MSNs in the striatum receive excitatory cortico- and thalamostriatal inputs. Outputs come from the GPi and SNr and are directed to the thalamus, which returns output to the cortex. Additional outputs terminate in the brainstem. D1-MSNs comprise the direct, or striatonigral, pathway while the indirect, or striatopallidal, pathway begins at D2-MSNs that project to the GPe. (Gerfen and Surmeier, 2011.)

The striatum receives abundant excitatory projections from nearly all parts of cortex in addition to a smaller number of excitatory projections from thalamus (Figure 1.1). The striatum also receives significant dopaminergic input from midbrain projections as well as inhibitory inputs from local striatal interneurons (Bolam et al., 2000; Kreitzer, 2009).

The bulk of the striatum—over 90%—is comprised of MSNs that send gamma-aminobutyric acid (GABA)-ergic axonal projections to downstream nuclei of the basal ganglia. The small number of remaining striatal neurons are interneurons that target axons solely within the striatum. MSNs are classified as either direct or indirect pathway neurons, based on their projection targets. D1R-expressing MSNs (D1-MSNs), which make up the direct pathway, send

projections directly to the two basal ganglia output nuclei, the GPi (known as the entopeduncular nucleus in rodents) and substantia nigra pars reticulata (SNr). The indirect pathway begins with D2 dopamine receptor (D2R)-expressing MSNs (D2-MSNs) that project solely to the GPe. GABAergic neurons of the GPe then project to the STN, which sends glutamatergic projections to the GPi and SNr. The outputs from the GPi and SNr then go to thalamus, which completes the circuit by projecting back to cortex. The unique connectivity within the direct and indirect pathways enables each pathway to have distinct effects on basal ganglia output and behavior. The result of direct pathway activation is facilitation of movement, while activation of the indirect pathway results in suppression of movement (Albin et al., 1989; Kravitz et al., 2010; Gerfen and Surmeier, 2011).

1.2.2 Medium spiny neurons

MSNs are the sole output neurons of the striatum and account for over 90% of striatal neurons. The dendrites of these cells are densely populated with spines that receive glutamatergic and dopaminergic input (Wilson and Groves, 1980). While all MSNs share the same morphological features, they can also be divided into two equally distributed subpopulations on the basis of their dopamine receptor expression and axonal targets. D1R-expressing MSNs project directly to the GPi and SNr, while D2-expressing MSNs project to only to the GPe (Smith et al., 1998).

Both D1- and D2-MSNs express an abundance of inwardly rectifying Kir potassium channels that endow a large conductance that drives their membrane potential toward the potassium equilibrium potential (Calabresi et al., 1987; Shen et al., 2007). Because of their acutely hyperpolarized resting state, often referred to as the “down-state,” MSNs depend heavily

on excitatory inputs to drive depolarization to an "up-state" in which action potentials can be generated (Wilson and Kawaguchi, 1996). Both types of MSNs express ionotropic α-amino-3-hydroxy-5-methyl-4-isoxazolepropionic acid (AMPA) and *N*-methyl-D-aspartate (NMDA) type glutamate receptors as well as metabotropic glutamate receptors (mGluRs) 1 and 5. Activation of glutamate receptors leads to depolarization of the MSNs and inactivation of Kir channels which then allows the cells to spike (Wilson and Kawaguchi, 1996).

D2-MSNs are intrinsically more excitable and fire at higher frequencies than D1-MSNs (Cepeda et al., 2008; Gertler et al., 2008). Moreover, synapses onto D2-MSNs show higher release probability and larger NMDAR-mediated currents than D1-MSN synapses, suggesting a natural imbalance in striatal input and output (Kreitzer and Malenka, 2007).

Previous studies characterizing gene expression differences between D1- and D2 MSNs have found several subtype-specific genes that are critical to the function of these two neurons (Lobo et al., 2006; Heiman et al., 2008). More recently, additional molecularly distinct subtypes within the D1- and D2-MSN populations have also been discovered, including those that co-express both D1- and D2-specific genes (Gokce et al., 2016; Stanley et al., 2019). This finding may challenge the canonical view of the basal ganglia circuit if these subtypes are found to give rise to distinct sub-circuits.

1.2.3 Excitatory inputs to striatum

The major excitatory inputs to the striatum come from cortex and thalamus. In cortex, excitatory (glutamatergic) pyramidal neurons projecting to striatum primarily come from layer 5 of most cortical areas (Gerfen et al., 2013). There are two subtypes of corticostriatal projection neurons that are classified on the basis of their main axonal or collateral targets. The first type,

the intratelencephalic (IT) neuron, sends axon collaterals that terminate only within striatum or other parts of cortex. IT neurons originate mainly from upper layer 5 cortical layers with a small population distributed deep within layer 3, and their striatal targets are bilateral (Wilson, 1987). The other subtype of corticostriatal neuron is the pyramidal tract (PT) neuron. PT neurons originate primarily from lower layer 5 cortical areas and send axons to the brainstem or spinal cord as part of the corticobulbar and corticospinal tracts. The striatal input from this tract comes from thin collaterals that branch off the main axon of the PT neuron and terminate in ipsilateral striatum (Donoghue and Kitai, 1981; Cowan and Wilson, 1994; Shepherd, 2013). While previous studies have suggested that PT and IT neurons differentially innervate D1- and D2-MSNs, more recent work has shown that both MSN subtypes receive inputs from both types of cortical neurons (Kress et al., 2013).

Studies from rodents, monkeys, and humans have found that inputs from cortex to striatum are generally topographically organized to provide functional organization to the striatum (Wiesendanger et al., 2004; Pan et al., 2010; Hooks et al., 2018). Sensory and motor cortical areas generally project to the dorsolateral striatum (DLS), association cortical areas project to central striatum, and limbic areas project to ventromedial striatum (Selemon and Goldman-Rakic, 1985; Haber et al., 2006; Kupferschmidt et al., 2017). There is also evidence of integration between different cortical projection types. Sensory and motor axons have been shown to converge in the DLS (Ramanathan et al., 2002). In more medial parts of striatum, projections from the dorsal anterior cingulate cortex, ventromedial prefrontal cortex, and orbitofrontal cortex converge at more rostral levels (Averbeck et al., 2014).

In addition to the topographical organization described above, the striatum may also be subdivided into neurochemically distinct compartments termed patch (also known as striosome)

or matrix. These two compartments can be distinguished by their cortical afferent projections, suggesting possible functional specificity within these regions. Numerous studies from decades ago have suggested that matrix neurons preferentially receive input from sensorimotor cortex, while the patch compartment receives afferents from limbic regions (Donoghue and Herkenham, 1986; Gerfen, 1992; Eblen and Graybiel, 1995; Kincaid and Wilson, 1996). While these previous studies used immunohistochemical methods to roughly define the spatial boundaries of patch and matrix compartments, newer techniques have been able to map patch/matrix input organization and activity with much greater precision. A recent study using transgenic mice and retrograde viral tracing found that patch and matrix compartments integrate inputs from both limbic and sensorimotor cortical areas, contrary to previous studies (Smith et al., 2016). Additional research will be needed to better understand the function of each compartment within the basal-ganglia-thalamocortical circuit.

The thalamus serves as the other source of excitatory input to the striatum. Overall, there are significantly fewer thalamic terminals in striatum than there are cortical terminals (Huerta-Ocampo et al., 2014). Thalamostriatal afferents typically come from the centromedian-parafascicular complex, but other thalamic nuclei have been shown to provide striatal inputs as well (Alloway et al., 2014). Like corticostriatal projections, thalamostriatal projections also retain some topographic organization (Smith et al., 2004).

1.2.4 Dopaminergic inputs to striatum

Dopamine plays and essential role in the striatum where it acts to modulate excitatory signals coming from cortex and thalamus. Midbrain dopamine neurons that project to striatum are typically organized into three distinct regions: SNc, ventral tegmental area (VTA), and

retrorubral field (Björklund and Dunnett, 2007). In addition to their anatomical distinctions, these regions differ in where their axons terminate in the striatum. Anatomical studies have shown that SNc dopamine neurons primarily project to the dorsal striatum to form the nigrostriatal pathway, while VTA dopamine neurons project to the nucleus accumbens via the mesolimbic pathway (Lynd-Balta and Haber, 1994; Prensa and Parent, 2001). While previous studies have found clear functional differences between these two pathways (Kravitz et al., 2010, 2012), more recent studies have also found evidence of molecular and functional heterogeneity within each pathway as well. Recent studies using single-cell gene expression profiling have uncovered the presence of five different dopamine neuron subtypes within the mouse midbrain (Poulin et al., 2014; La Manno et al., 2016). In the SNc, three of these unique subtypes give rise to molecularly distinct nigrostriatal projection patterns that each terminate in a different part of dorsal striatum (Poulin et al., 2018). Uncovering the functional diversity of midbrain dopamine neurons could be an important step towards understanding PD and other disorders of the dopamine system.

Dopamine transmission to striatum occurs by two distinct mechanisms: phasic release caused by transient bursts in dopamine neuron firing, and tonic release which maintains low baseline levels of extracellular dopamine (Grace and Bunney, 1983). Phasic firing is typically induced by rewards or salient stimuli, while adverse events tend to result in a pause in tonic firing (Schultz, 1998; Redgrave and Gurney, 2006). These changes in dopamine neuron firing are thought to represent instructive signals that serve to reinforce or suppress motor actions through modulation of corticostriatal plasticity (see section 1.4).

1.2.5 Striatal interneurons

From within the striatum, cholinergic and GABAergic interneurons, which constitute 5-10% of all striatal neurons, provide important local regulatory input to MSNs. Cholinergic interneurons possess intrinsic membrane currents that allow them to depolarize and fire in the absence of any synaptic input (Bennett et al., 2000). This autonomous activity functions to maintain a cholinergic tone throughout the striatum. Cholinergic interneurons are important for modulating excitability and plasticity in D1- and D2- MSNs through muscarinic receptors on both MSNs and cortical axon terminals (Goldberg et al., 2012; Augustin et al., 2018). Dysfunction in the physiology of these interneurons has been implicated in PD and L-DOPA-induced dyskinesia (Ding et al., 2006, 2011; Lim et al., 2014; Tanimura et al., 2018, 2019).

The most prominent and well-characterized types of GABAergic striatal interneurons include fast-spiking interneurons (FSIs) and low-threshold spiking (LTS) interneurons (Kreitzer, 2009). Others that have long ago been identified but are still poorly characterized include calretinin-positive and tyrosine-hydroxylase-positive interneurons (Dubach et al., 1987; Rymar et al., 2004). More recently, novel subtypes of striatal GABAergic interneurons have been identified and characterized. These include neurogliaform interneurons, fast adapting interneurons, and spontaneously active bursty interneurons (Ibáñez-Sandoval et al., 2011; Faust et al., 2015; Assous et al., 2018). FSI and LTS interneurons are known to engage in feedforward inhibition of MSNs to mediate striatal-dependent learning and behavior (Tepper et al., 2008; Martiros et al., 2018; Owen et al., 2018). Others, however, seem to take part in more complex microcircuitry, receiving either excitation from cholinergic interneurons or inhibitory feedback from MSNs themselves (Tepper et al., 2010). The diversity of GABAergic interneurons alone

suggests a highly important role for local inhibition in striatal function, but more research is required to uncover the unique roles of each subtype.

1.3 Dopaminergic modulation of striatal activity

1.3.1 Acute effects of dopaminergic modulation

Dopamine modulates corticostriatal and thalamostriatal glutamatergic signaling via G-protein-coupled receptors (GPCRs) at striatal MSN synapses. Its effects are bidirectional in that it can enhance or inhibit excitation depending on the receptor type. D1Rs, which are expressed at high levels in direct pathway MSNs, are coupled to $G_{s/olf}$ proteins (Zhuang et al., 2000) that activate adenylyl cyclase type 5 (AC5) and increase intracellular 3',5'-cyclic adenosine monophosphate (cAMP). This results in activation of protein kinase A (PKA), which acts on numerous intracellular targets that influence excitability, glutamatergic transmission, and plasticity (Figure 1.2). One notable target of PKA is the dopamine- and cAMP-regulated phosphoprotein 32 kDa (DARPP-32), which inhibits protein phosphatase-1 (Svenningsson et al., 2004). It is important to note that AC5 activation occurs independently of calmodulin, unlike the calmodulin-sensitive isoform expressed in cortex and hippocampus, AC1 (Sunahara and Taussig, 2002). As a result, cAMP production in the striatum is primarily regulated by GPCR signaling. Among the acute effects of the D1R signaling pathway are changes in ion conductances in D1-MSNs. During the down state, D1Rs cause a reduction in sodium channel conductance (Schiffmann et al., 1995). During the up state, however, D1R signaling increases the opening of L-type calcium channels and closure of hyperpolarizing potassium channels, thereby enhancing excitability (Surmeier et al., 1995; Nisenbaum et al., 1998; Neve et al., 2004). D1R activation also leads to increases in AMPAR and NMDAR surface expression (Svenningsson et al., 2004).

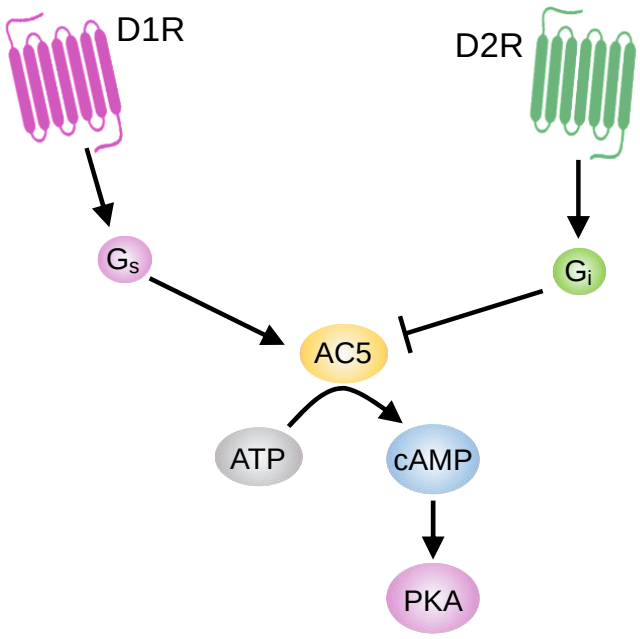

Figure 1.2. Signal transduction pathways for D1 and D2 receptors.
Activation of D1Rs by dopamine stimulates G_s activation of AC5. AC5 catalyzes the conversion of ATP to cAMP, which activates PKA. PKA activity influences excitability and plasticity in MSNs. Activation of D2Rs stimulates G_i which inhibits AC5 activity. The result is suppression of PKA.

D2Rs are expressed at high levels in indirect pathway MSNs and are coupled to $G_{i/o}$ proteins that inhibit AC5 (Figure 1.2). D2R signaling leads to weaker calcium and sodium conductance and increased potassium conductance (Surmeier and Kitai, 1993; Greif et al., 1995; Hernández-López et al., 2000; Higley and Sabatini, 2010). Furthermore, D2Rs have been shown to decrease AMPAR- and NMDAR-mediated currents in MSNs (Hernández-Echeagaray et al., 2004; Higley and Sabatini, 2010). Together, the overall effect of these mechanisms is to weaken the excitability of D2-MSNs.

In the striatum, dopamine receptors are also expressed presynaptically on corticostriatal terminals where they act to modulate glutamate release. D1Rs are expressed on cortical terminals

in the nucleus accumbens, but very sparsely on terminals in the dorsal striatum (Dumartin et al., 2007). D2Rs are expressed in corticostriatal axon terminals and in cholinergic axon terminals in dorsal and ventral striatum, where they decrease the release of glutamate and acetylcholine, respectively (Pisani et al., 2000; Higley and Sabatini, 2010). In addition, dopaminergic axon terminals themselves express D2 autoreceptors to reduce dopamine release (Phillips et al., 2002). The predominant form of D2R expressed on dopaminergic neuron terminals is a distinct isoform encoded by a D2R mRNA splice variant (Giros et al., 1989; De Mei et al., 2009; Ford, 2014).

1.3.2 Dopaminergic modulation of synaptic plasticity

Corticostriatal plasticity plays an essential role in the regulation of striatum-dependent learning and memory. In the striatum, dopamine modulates long-term potentiation (LTP) and long-term depression (LTD) in both D1- and D2-MSNs. Corticostriatal endocannabinoid-mediated LTD (eCB-LTD) is the most thoroughly studied form of striatal plasticity, as it is easy to induce in brain slices (Lovinger et al., 1993; Lovinger, 2010). This form of LTD involves pairing high frequency afferent stimulation with postsynaptic depolarization (Kreitzer and Malenka, 2005). The intended outcome of this stimulation is co-activation of mGluR5 and L-type calcium channels located at MSN synapses (Lovinger et al., 1993; Kreitzer and Malenka, 2005). The subsequent calcium influx into the postsynaptic side triggers the production of a retrograde eCB signaling molecule that diffuses to cannabinoid type 1 receptors (CB1Rs) on the presynaptic side to decrease neurotransmitter release (Augustin and Lovinger, 2018). Therefore, eCB-LTD is postsynaptically induced, but presynaptically expressed. eCB-LTD is primarily expressed at corticostriatal synapses, as thalamostriatal synapses express few CB1Rs (Wu et al., 2015).

eCB-LTD is modulated by D2Rs in indirect pathway MSNs via an AC5-dependent mechanism (Wang et al., 2006; Kreitzer and Malenka, 2007; Kheirbek et al., 2009; Lerner and Kreitzer, 2012). D2R signaling inhibits activation of PKA, which prevents phosphorylation of regulator of G protein signaling 4 (RGS4), an inhibitor of group I mGluR G protein signaling (Lerner and Kreitzer, 2012). Disinhibition of mGluR5 signaling then permits the production and release of eCBs in D2-MSN synapses. Consistent with this, it has also been shown that high levels of intracellular cAMP inhibit induction of eCB-LTD, while low cAMP levels permit it (Kheirbek et al., 2009; Augustin et al., 2014). Interestingly, D1-MSN corticostriatal synapses are also susceptible to eCB-LTD despite their lack of D2R expression (Wu et al., 2015). eCB-LTD in D1-MSNs depends on D2Rs that are expressed on cholinergic interneurons (Augustin et al., 2018). D2R activation reduces acetylcholine transmission and tonic M1 muscarinic receptor activation in both D1- and D2-MSNs, thereby promoting the induction of LTD (Wang et al., 2006; Tozzi et al., 2011; Augustin et al., 2018). LTD expression in D1-MSNs also depends on G_i-coupled M4 muscarinic receptors, which promote LTD by diminishing RGS4 activity (Shen et al., 2015).

Striatal MSNs also express LTP, though the mechanisms behind it are not fully understood. Early studies of striatal LTP showed that it could be induced in brain slices with a magnesium-free extracellular solution combined with postsynaptic depolarization and high frequency afferent stimulation (Calabresi et al., 1992). Removal of magnesium from the recording medium unblocks NMDARs which are necessary for induction of this LTP (Calabresi et al., 2007).

Striatal LTP has also been induced in brain slices under normal magnesium concentrations, where NMDAR-dependence still holds (Shen et al., 2008; Pascoli et al., 2012;

Augustin et al., 2014; Park et al., 2014). Both D1- and D2-MSNs express bidirectional spike-timing-dependent plasticity (STDP) that is regulated by dopamine signaling (Pawlak and Kerr, 2008; Shen et al., 2008). D1R signaling is required for LTP in D1-MSNs, while D2R signaling blocks the induction of LTP in D2-MSNs (Flajolet et al., 2008; Shen et al., 2008; Augustin et al., 2014; Yagishita et al., 2014). In D2-MSNs, high intracellular cAMP paired with low frequency stimulation has been shown to promote LTP, highlighting the importance of the PKA pathway in modulating striatal plasticity (Augustin et al., 2014). Recently, a form of eCB-dependent STDP LTP has been reported in the dorsal striatum (Cui et al., 2015, 2016). This LTP, which is expressed in both D1- and D2-MSNs, depends on dopaminergic activation of D2Rs on corticostriatal terminals (Xu et al., 2018).

1.3.3 Interactions with adenosine signaling

Adenosine signaling in the striatum plays an important role in modulating plasticity alongside dopamine. A2ARs, which are expressed in D2-MSNs, are positively coupled to AC5 and therefore offset the effects of G_i-coupled D2Rs (Surmeier et al., 2014). The significance of striatal A2ARs has been clearly demonstrated in plasticity experiments where A2AR activation not only inhibits the induction of eCB-LTD, but also facilitates LTP in D2-MSNs (Shen et al., 2008; Lerner and Kreitzer, 2012). Tonic activation of A2ARs maintains cAMP levels and facilitates NMDAR-mediated calcium entry to influence excitability and plasticity in D2-MSNs (Higley and Sabatini, 2010). Furthermore, D2Rs and A2ARs can combine to form heteromeric receptors in which A2AR activation can lower the dopamine binding affinity of the associated D2R via allosteric modulation (Ferré et al., 2011; Fernández-Dueñas et al., 2015).

1.3.4 Striatal dysfunction in Parkinson's disease

The loss of dopaminergic innervation to the striatum is considered to be the primary cause of motor symptoms in PD. Studies in animal models of PD have demonstrated that motor impairments are the result of hypoactivity of the direct pathway and hyperactivity of the indirect pathway (Albin et al., 1989; Kravitz et al., 2010). At the level of the synapse, it is clear that both LTP and LTD are affected by the loss of dopamine in the striatum; due to their dependence on dopamine signaling, LTP in D1-MSNs and LTD in D2-MSNs are impaired in the presence of dopamine receptor antagonists in brain slices (Kreitzer and Malenka, 2005; Shen et al., 2008). Following 6-hydroxydopamine (6-OHDA) lesioning of nigrostriatal neurons in mice, the amplitude of corticostriatal responses is increased in D2-MSNs and decreased in D1-MSNs, suggesting the presence maladaptive plasticity changes (Peterson et al., 2012; Fieblinger et al., 2014). Thalamostriatal connectivity is also altered, resulting in a significant and selective reduction of thalamic input to D1-MSNs (Parker et al., 2016).

Following chronic dopamine depletion, MSNs show evidence of homeostatic adaptations intended to mitigate the effects of the disease state. Loss of dopamine signaling results in enhanced intrinsic excitability in D1-MSNs and reduced intrinsic excitability in D2-MSNs (Fieblinger et al., 2014). Dendritic spine loss is observed in both D1- and D2-MSNs (Fieblinger et al., 2014; Suárez et al., 2014; Graves and Surmeier, 2019). Interestingly, spine loss following dopamine depletion is significantly delayed in D1-MSNs and cannot be restored by L-DOPA treatment, whereas D2-MSN spine pruning occurs early and is reversed by L-DOPA treatment (Suárez et al., 2014; Graves and Surmeier, 2019). This suggests that while D2-MSN spine loss is a homeostatic adaptation, D1-MSN spine loss may instead be the result of dendritic degeneration.

1.4 Dopamine and plasticity in motor learning

1.4.1 Reinforcement learning

Dopamine signaling in the striatum has long been associated with reinforcement learning and motor skill acquisition (Wise, 2004). When an action is met with an unexpected reward, midbrain dopamine neurons briefly fire in bursts that result in a short phasic increase in dopamine signaling in the striatum, which transiently activates low-affinity D1Rs (Richfield et al., 1989; Schultz, 1998). This phasic activation is believed to encode a reward prediction error. While unexpected rewards elicit dopamine neuron activation, predicted rewards elicit no response, and the absence of a predicted reward results in a pause in activity that halts D2R activation, leading to disinhibition of D2-MSNs (Schultz, 2007). In the context of behavior, actions that are represented as cortical inputs to striatum are modulated by nigrostriatal dopamine signals that serve to reinforce or suppress the action through these mechanisms via the direct and indirect pathways (Schultz, 2007).

1.4.2 Plasticity in motor learning

Striatum-dependent motor learning is mediated by changes in plasticity at corticostriatal synapses in the dorsal striatum (Yin and Knowlton, 2006). Several studies over the past decade have examined the changes in striatal activity associated with different stages of learning. The links between motor skill acquisition and striatal plasticity at different learning stages were first demonstrated both *in vivo* and *ex vivo* with mice that were trained on an accelerating rotarod (Yin et al., 2009). In this study, *in vivo* recording of MSN activity showed that the dorsomedial striatum (DMS) displayed increased firing activity at early stages of training while the DLS displayed increased activity in the late phase of training. Furthermore, LTP was observed in

DMS slices taken from mice early in training and in DLS slices from mice late in training, suggesting that the DMS is more strongly engaged during initial acquisition while the DLS is more important for consolidation (Yin et al., 2009). Consistent with these findings, a study of T-maze learning in rats found that task-related plasticity appeared early in the DMS and later in the DLS (Hawes et al., 2015). Mouse dorsal striatal neurons also exhibit increased firing during the late phase of learning an abstract neuroprosthetic-mediated task, and this type of learning is dependent on NMDAR-mediated corticostriatal plasticity (Koralek et al., 2012). In humans, neuroimaging studies have shown increased activity in the putamen over the course of motor skill acquisition (Lohse et al., 2014). Interestingly, *in vivo* fiber photometric measures of mouse corticostriatal activity during rotarod training show that both cortico-DMS and cortico-DLS projections disengage over the course of training, which runs somewhat counter to the reports of increased DLS activity after training (Kupferschmidt et al., 2017). One possibility is that motor learning involves a refinement of presynaptic cortical inputs together with postsynaptic potentiation in dorsal striatum.

Motor learning can also modulate plasticity differently between D1- and D2-MSNs. In the DMS, learning of a goal-directed task results in AMPA/NMDA ratios that are increased in D1-MSNs and decreased in D2-MSNs (Shan et al., 2014). DLS D2-MSNs in mice exhibit LTD following learning of a lever-pressing task, while D1-MSNs show no change (Shan et al., 2015). Serial order tasks, in which mice learn and perform an ordered sequence of responses, require D1-MSN activation and lead to potentiation of corticostriatal synapses at D1-MSNs but not D2-MSNs (Rothwell et al., 2015).

Many studies have demonstrated how learning modulates striatal plasticity, but fewer studies have examined the reverse, that is, how striatal plasticity shapes learning. The recent

advancements in *in vivo* optogenetics have allowed researchers to directly manipulate striatal activity in behaving animals in order to draw causal links between plasticity and behavior (Pascoli et al., 2012; Ma et al., 2018). In some of the first studies to induce long-lasting, striatum-dependent behavioral changes with optogenetic stimulation, locomotor sensitization to cocaine was abolished by optogenetic induction of corticostriatal LTD in the nucleus accumbens (Pascoli et al., 2012; Creed et al., 2015). Repeated stimulation of corticostriatal terminals in the ventromedial striatum in mice led to increased firing and persistent increases in grooming behavior associated with obsessive-compulsive disorder (Ahmari et al., 2013). In a more recent study, direct induction of corticostriatal LTP in the DMS was shown to cause a long-lasting increase in alcohol self-administration, while LTD was shown to decrease the behavior (Ma et al., 2018). While not directly examining the mechanisms underlying motor learning, these studies still provide insight into how striatum-dependent motor behaviors are shaped by neural circuitry.

1.4.3 Inhibitory motor learning in Parkinson's disease

Given dopamine's critical role in shaping striatal plasticity and learning, it is not surprising that its loss results in significant impairments in motor function. Animal models of PD that rely on irreversible damage to dopamine neurons, such those using 6-OHDA- or MPTP-lesioned mice, make it difficult to dissociate dysfunctional motor learning from acute motor impairments. One alternative to the toxin-based models is the Pitx3 knockout mouse which has a selective loss of nigrostriatal neurons and only mild impairments in motor performance (Hwang et al., 2003, 2005). Pitx3-deficient mice show impaired learning on the accelerating rotarod, despite indicating no initial impairment in performance on the first day of training when

compared to controls (Beeler et al., 2010). These learning deficits can be prevented by administering L-DOPA during training. Interestingly, Pitx3-deficient mice that were treated with L-DOPA during training continue to perform well on the rotarod after cessation of L-DOPA treatment. Following the removal of L-DOPA, performance degrades gradually rather than mirroring the abrupt loss of dopamine (Beeler et al., 2010). This performance pattern strongly resembles the decline of the LDR following cessation of L-DOPA treatment in human patients (Zhuang et al., 2013). This data suggests that learning programs can take place both with and without L-DOPA in PD, and that the learning that occurs without L-DOPA is inhibitory.

Another alternative to toxin-based PD models is the use of pharmacological agents that reversibly block dopamine receptors in wild-type mice. The blockade of D1Rs and D2Rs essentially mimics a loss of nigrostriatal signaling, as dopamine is unable to modulate MSN activity in the presence of antagonists at its receptors. An advantage of this approach is that long-lasting learning effects can easily be dissociated from acute impairments in performance. When mice are given a cocktail of D1R and D2R antagonists (SCH23390 and eticlopride, respectively) and trained on the accelerating rotarod, the acute effects of receptor blockade are apparent in their poor performance compared to controls. When these mice are tested again in the absence of drugs, their performance continues to be poor, and only gradually improves over the course of several days (Beeler et al., 2012). These mice perform even worse than naïve controls despite having normal dopamine signaling restored. This persistent motor inhibition appears to be mediated by the D2R-expressing indirect pathway, as training with the D2R antagonist, but not D1R antagonist, is sufficient to induce a lasting motor impairment (Figure 1.3). This study suggests that mice trained under D2R blockade undergo an aberrant, inhibitory learning process that can impede normal learning when dopamine is restored.

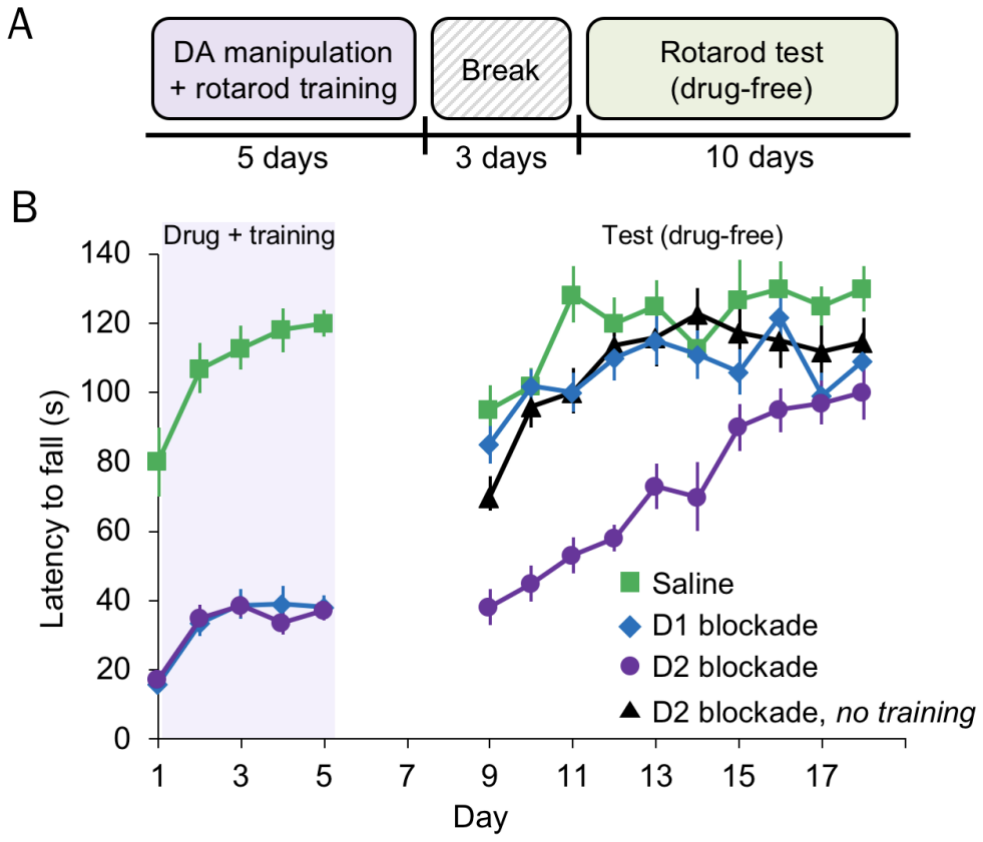

Figure 1.3. Motor experience under D2 receptor blockade results in inhibitory motor learning.
(A) Mice were administered daily injections of either D1R antagonist, D2R antagonist, or saline, and trained on an accelerating rotarod. Following a 3-day break, subsequent rotarod performance was tested under drug-free conditions. Each daily session consisted of 5 trials.
(B) Both D1R and D2R blockades (blue and purple, respectively) result in impairment during the initial training phase compared to saline (green). In the subsequent drug-free test phase, only the D2 blockade group continue to demonstrate lasting impairment. Black triangles show mice that previously received D2R blockade without motor training. Error bars: s.e.m. Adapted from Beeler et al. (2012).

The long-lasting nature of these motor impairments suggests that these behaviors are driven by changes in plasticity that occur under dopamine-deficient conditions (Zhuang et al., 2013). According to the classical model of basal ganglia function, the loss of dopamine signaling results in hypoactivity of the direct pathway and hyperactivity of the indirect pathway (Albin et al., 1989; DeLong, 1990). Under D2R blockade, D2-MSNs are more excitable by cortical inputs due to the D2R's inability to modulate glutamatergic signals, and are therefore unable to support LTD (Shen et al., 2008). Furthermore, D2R blockade, or downstream effects of D2R blockade such as elevated cAMP, facilitate the induction of LTP in brain slices (Shen et al., 2008; Beeler et al., 2012; Augustin et al., 2014). Based on this data, our laboratory has proposed that inhibitory motor learning is caused by aberrant corticostriatal LTP in D2-MSNs (Figure 1.4). This irregular plasticity may be responsible for some PD motor symptoms and could explain the temporal pattern of the LDR with L-DOPA treatment.

D2-MSNs also express A2ARs which have been shown as necessary for LTP induction (Shen et al., 2008). Co-administration of A2AR antagonist theophylline during training blocks the induction of inhibitory motor learning (Beeler et al., 2012). Theophylline is only beneficial when administered during induction, as it is ineffective when given after inhibitory motor learning has already been induced. Our laboratory has also found that caffeine, another A2AR antagonist, protects mice against the induction of inhibitory motor learning (Figure 1.5; unpublished data). As with theophylline, caffeine is only protective if administered during training; caffeine given during recovery has no effect. Given that A2AR antagonists can block induction of LTP in D2-MSNs, this data provides further support for the view that corticostriatal LTP underlies aberrant inhibitory motor learning.

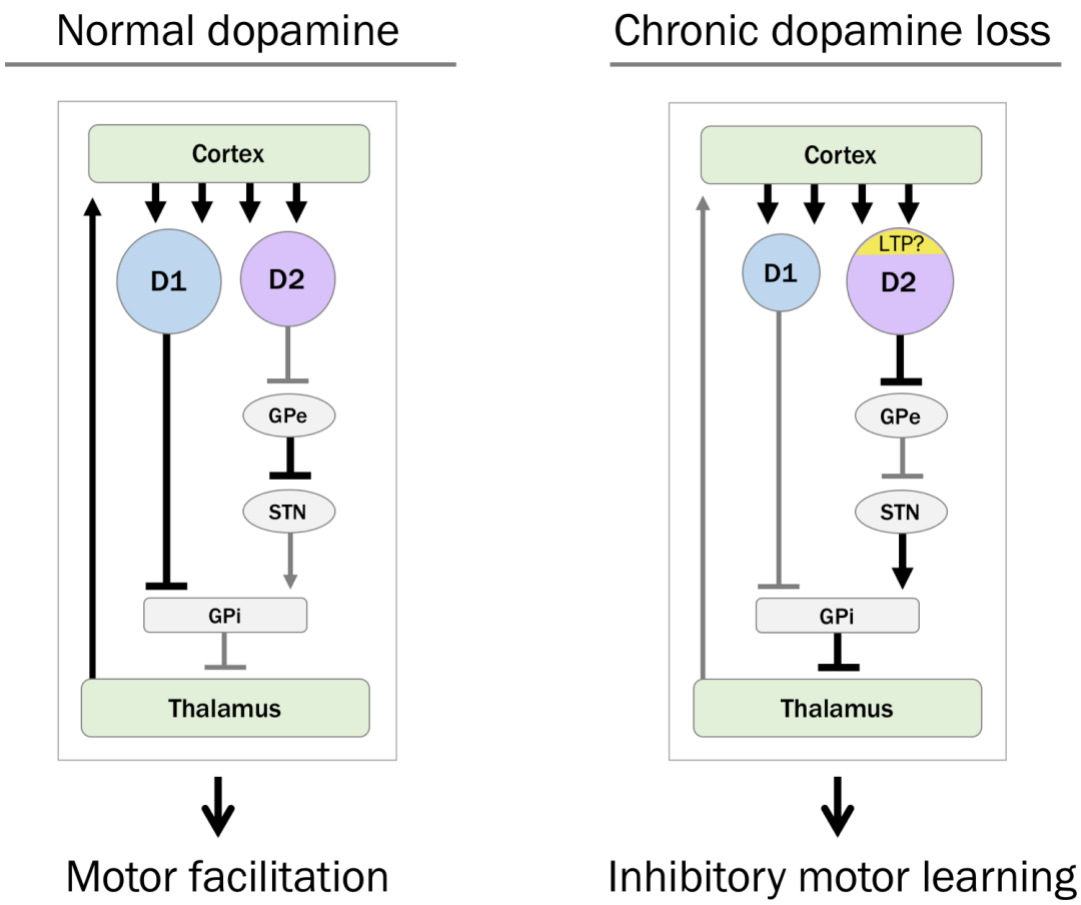

Figure 1.4. Proposed synaptic plasticity underlying inhibitory motor learning.
(Left) Normal dopamine signaling in the striatum facilitates activation of the D1R-expressing direct pathways and suppression of the D2R-expressing indirect pathways. This promotes output from the cortico-basal-ganglia loop to facilitate movement. (Right) The loss of dopamine signaling facilitates increased activation of the indirect pathway and hypoactivity in the direct pathway. With persistent cortical input to D2-MSNs, aberrant corticostriatal LTP is proposed to develop in D2-MSNs to drive aberrant motor learning.

1.5 Experimental aims

In this thesis I examine the mechanisms of striatal synaptic plasticity that contribute to the long-lasting deterioration of motor output in PD. The loss of dopamine signaling in the striatum is thought to decrease activity of the basal ganglia's direct pathway and increase the

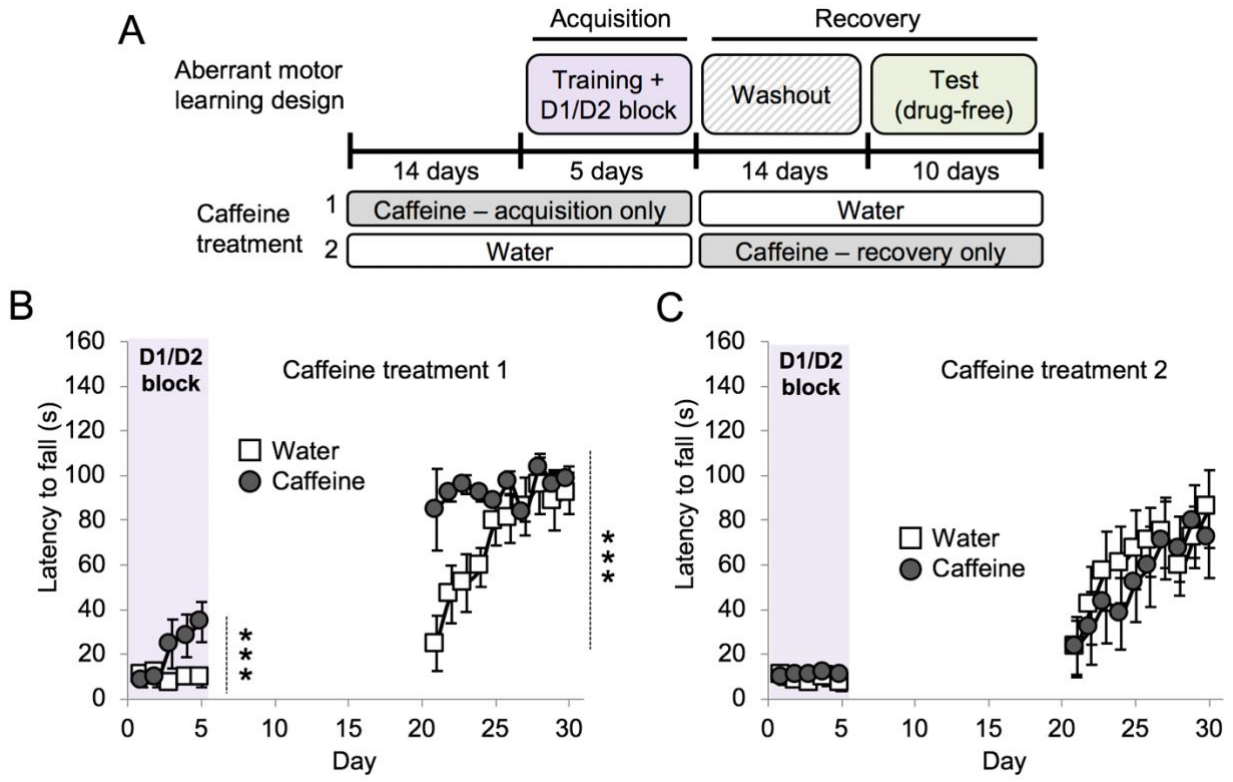

Figure 1.5. Chronic caffeine treatment prevents induction of inhibitory motor learning.
(A) Mice were pretreated with either caffeine or plain drinking water for 14 days. At the start of rotarod training, mice were administered a cocktail of D1R and D2R antagonists. Following training, mice were given either caffeine or plain drinking water for another 14 days. Their performance was then tested on the rotarod.
(B) Mice that were given chronic caffeine prior to rotarod training are protected from developing inhibitory motor learning compared to control mice that received only water prior to training.
(C) Mice that received caffeine after training only show no protection from inhibitory motor learning. Error bars: s.e.m. (X.Z. unpublished results.)

activity of the indirect pathway, leading to a suppression of motor output (Albin et al., 1989). While much is already known about dopaminergic modulation of basal ganglia activity, changes in synaptic states following chronic dopamine loss have received less attention. Studies from our laboratory have shown that the loss of D2R signaling in the striatum combined with concurrent motor experience leads to a long-lasting motor impairment that slows normal learning even after

restoration of dopamine signaling (Beeler et al., 2012). We hypothesize that what underlies this inhibitory motor learning is irregular corticostriatal plasticity, specifically aberrant LTP in the D2R-expressing indirect pathway. The research presented in this thesis addresses the proposed link between parkinsonian motor behavior and aberrant plasticity.

Until recently, limitations in our ability to control specific pre- and post-synaptic neuronal populations have impeded the study of corticostriatal plasticity both *in vivo* and in brain slices. In Chapter 2 of this thesis, I describe optogenetic approaches to more selectively characterize corticostriatal plasticity. Using genetically modified mice to specifically isolate corticostriatal projections in the dorsolateral striatum, I test protocols to be used for assessing plasticity with optogenetics and electrophysiology in mouse brain slices. In Chapter 3, I examine changes in corticostriatal plasticity *ex vivo* following induction of inhibitory motor learning. I also examine the causal link between aberrant LTP and motor impairments. In the final chapter, I discuss future directions of this research and potential implications for PD treatment.

CHAPTER 2

OPTOGENETIC APPROACHES TO CHARACTERIZING CORTICOSTRIATAL PLASTICITY IN THE MOUSE DORSOLATERAL STRIATUM

2.1 Abstract

Afferent connections to the striatum consist of a number of different cell types originating from multiple sources within the brain. This heterogeneity in inputs has, until recently, limited the specificity with which striatal plasticity could be studied and impeded our ability to link various behaviors to specific synaptic events. Advances in transgenics and optogenetics have provided new opportunities to precisely manipulate and record activity in defined pre- and postsynaptic cell types which has enhanced our approaches to studying plasticity in the brain. Here, we used genetically targeted channelrhodopsin-2 (ChR2), a light-sensitive cation channel, to better understand plasticity specifically at corticostriatal synapses in D2-MSNs. I tested previously established *in vitro* protocols for inducing corticostriatal LTP in D2-MSNs and found that optogenetic stimulation could not reproduce the effects of electrically induced LTP protocols in brain slices. I also established an *in vitro* optogenetic LTD protocol that induces postsynaptic corticostriatal depression in D2-MSNs. Unlike previously reported forms of striatal LTD, this light-mediated LTD is CB1R-independent and does not alter presynaptic glutamate release. Moreover, it does not require the activation of NMDA or mGluR5 receptors. This data describes a post-synaptic form of striatal LTD that can be used to examine synaptic strength in D2-MSNs and uncovers differences between electrical and optogenetic

approaches to studying corticostriatal plasticity.

2.2 Introduction

Learning, drug exposure, and other salient experiences are proposed to drive changes in behavior through modulation of synaptic plasticity in the brain. Approaches to assessing how these experiences influence synaptic strength involve either *in vivo* recording in behaving animals or *ex vivo* analysis of various proxies for plasticity, such as LTP/LTD occlusion or depotentiation, AMPAR/NMDAR ratios, or miniature excitatory postsynaptic currents (mEPSCs). Current established protocols for striatal LTP and LTD are primarily based on studies involving electrical stimulation and pharmacology to effect changes in striatal circuitry. Notably, several of these studies have discovered the precise timing requirements and signaling mechanisms necessary for bidirectional plasticity in MSNs (Calabresi et al., 1992; Kreitzer and Malenka, 2007; Shen et al., 2008; Lerner and Kreitzer, 2012; Augustin et al., 2014). A feature of the electrical stimulation used in these studies is the ability to stimulate a large population of afferents which can evoke robust postsynaptic responses in MSNs. However, a significant disadvantage of this technique is that stimulation cannot be limited to axons of a certain cell type, nor can it avoid also depolarizing cell bodies and dendrites within the electrode's field of stimulation. A stimulating electrode positioned within the DLS is expected to evoke release from cortical, thalamic, and dopaminergic afferents, as well as activate local GABAergic interneurons, cholinergic interneurons, and MSNs themselves. This assortment makes it difficult to characterize the individual contributions of striatal inputs and can complicate the ultimate interpretation of synaptic events.

The past decade has seen immense progress in molecular genetic and optogenetic

technologies that have rapidly refined our approaches to studying brain circuitry (Kim et al., 2017). One of these approaches involves the cell-type-specific expression of fluorescent proteins and opsins using mouse transgenic Cre-recombinase driver lines. Through the GENSAT project, there are now hundreds of bacterial artificial chromosomal (BAC) transgenic mouse lines that express Cre through gene-specific promoters in neuronal populations throughout the nervous system (Gong et al., 2007; Gerfen et al., 2013). Within one of these Cre mice, ChR2 can be expressed by either a Cre-dependent transgene or Cre-dependent viral vector, typically adeno-associated virus (AAV), that encodes ChR2. The resulting subtype-specific expression of ChR2 allows for stimulation of distinct axonal subpopulations within highly heterogeneous brain regions (Kim et al., 2017). AAV-mediated delivery of ChR2 is especially useful for also achieving anatomical precision for a particular experiment. Studies using optogenetics also have the potential to reveal findings about plasticity that challenge previous theories formed with conventional electrical stimulation data. For example, while electrical stimulation could previously only induce eCB-LTD in D2-MSNs (Kreitzer and Malenka, 2007), Wu et. al (2015) demonstrated that precise corticostriatal stimulation with optogenetics could in fact induce eCB-LTD in both MSN subtypes (Wu et al., 2015). This finding was likely uncovered by the elimination of inadvertent co-activation of dopaminergic and/or cholinergic inputs. While tonic dopaminergic signaling at higher-affinity D2Rs promotes eCB-LTD in both types of MSNs, stronger evoked release likely activates lower-affinity D1Rs that instead block LTD and promote LTP in D1-MSNs (Shen et al., 2008; Wu et al., 2015). Though studies using pharmacological tools combined with electrical stimulation can still provide some clues toward this end (Wang et al., 2006; Shen et al., 2008), optogenetics is a simpler and more effective approach to isolating inputs and understanding synaptic connectivity in the striatum.

The data presented in this chapter show attempts to reproduce previously established electrical LTP induction protocols by selectively targeting corticostriatal terminals only via optogenetics. I also characterize a form of corticostriatal LTD previously unattainable with electrical stimulation. This work lays the foundation for the experiments presented in Chapter 3.

2.3 Methods

2.3.1 Animals

Several existing BAC Cre lines target distinct subpopulations of neurons just within cerebral cortex, many of which project to striatum. For our work, we took advantage of the Rbp4-Cre mouse line (GENSAT KL100) which selectively expresses Cre recombinase in layer 5 excitatory neurons, including both PT and IT (Gerfen et al., 2013). Rbp4-Cre mice were crossed to a BAC transgenic Drd2-EGFP line (GENSAT S118) (Gong et al., 2003) in order to generate Rbp4Cre;Drd2-EGFP double transgenic mice. All double transgenic mice used in experiments were hemizygous for each transgene. The presence of each transgene was determined by genotyping using PCR primer sequences obtained from MMRRC.

Male and female mice 8-16 weeks of age were used for all experiments. Mice were housed on a 12-hour light/dark cycle and allowed ad libitum access to standard food and water. All animal procedures performed in these experiments were approved by the Institutional Animal Care and Use Committee of the University of Chicago.

2.3.2 Surgery and AAV injection

Rbp4-Cre;Drd2-EGFP mice at least 8 weeks of age were anesthetized with 2% vaporized isoflurane and positioned into a stereotaxic apparatus (Kopf Instruments). Anesthesia was then

maintained at 1-1.5% and mice were kept warm on a heating pad throughout the remainder of the procedure. Fur was removed from the scalp with an electric clipper and Betadine was applied to the bare scalp prior to incision. The mouse's eyes were treated with ophthalmic ointment to prevent corneal drying. An incision was made through the scalp midline and the skull was exposed for identification of bregma. Two holes were drilled into the skull and a total volume of 500 nl of AAV5-Ef1a-DIO-hChR2(H134R)-mCherry-WPRE-pA (University of North Carolina Vector Core) was injected into each hole with a 33-gauge needle at a rate of 120 nl/min. Injections were made in cortex at the following stereotaxic coordinates: AP: +0.25, ML: ±1.5, DV: -1.25. At the end of each injection, the needle was kept in the same position in the brain for an additional 5 minutes to allow the AAV to diffuse. The scalp was then sutured closed at the end of surgery and mice were administered buprenorphine (0.1 mg/kg subcutaneous) and meloxicam (1 mg/kg subcutaneous) for postoperative analgesia. Mice were not used for experiments until at least 4 weeks after AAV injections.

2.3.3 Brain slice preparation

To prepare slices for recordings, mice were deeply anesthetized with isoflurane and then decapitated. The brain was rapidly dissected out of the skull and submerged in an ice-cold, oxygenated (95% O_2, 5% CO_2) artificial cerebrospinal fluid (ACSF) solution containing the following (in mM): 92 *N*-methyl-D-glucamine, 2.5 KCl, 1.2 NaH_2PO_4, 30 $NaHCO_3$, 25 glucose, 12 *N*-acetyl-L-cysteine, 20 HEPES, 5 sodium ascorbate, 2 thiourea, 3 sodium pyruvate, 10 $MgSO_4$ ($7H_2O$), and 0.5 $CaCl_2$. The solution was brought to pH 7.3-7.4 with 12N HCl and osmolarity was adjusted to 305-315 mOsm. The brain was sliced in ice-cold oxygenated ACSF into 250 µm thick coronal sections using a vibratome (Leica VT1000S). Brain slices were then

transferred to a holding chamber containing 32°C ACSF continuously oxygenated for 12-15 minutes. Slices were then transferred again to a new holding chamber at room temperature containing a different oxygenated ACSF consisting of the following (in mM): 92 NaCl, 2.5 KCl, 1.2 NaH_2PO_4, 30 $NaHCO_3$, 25 glucose, 20 HEPES, 5 sodium ascorbate, 2 thiourea, 3 sodium pyruvate, 2 $MgSO_4$ ($7H_2O$), and 2 $CaCl_2$. The solution was brought to pH 7.3-7.4 with 10N NaOH and osmolarity was adjusted to 305-315 mOsm. The slices were incubated for at least 60 minutes before recording.

The method of slice preparation described here (Ting et al., 2014) differs from the slice preparation procedure previously used by our laboratory (Kheirbek et al., 2009; Beeler et al., 2012; Augustin et al., 2014). While the standard sucrose-based recovery method is sufficient for preparing healthy slices from young mice under 8 weeks of age, I have found this method to be inadequate at preserving the health of adult striatal neurons (data not shown). The neuroprotective recovery method used for electrophysiology experiments in this thesis instead uses a sodium replacement approach that protects against excitotoxicity and significantly improves the survival and health of neurons from older brain slices. Furthermore, the inclusion of N-acetyl-L-cysteine, a neuron-permeable precursor to the antioxidant glutathione, has been shown to protect slices from oxidative-stress-related damage (Ting et al., 2014). Because the animals used in my experiments were at least 12 weeks old by the time of recording, I chose to use this strategy over the traditional sucrose-based method previously used in our laboratory.

2.3.4 Electrophysiology

Individual brain slices were transferred to a recording chamber and perfused at a rate of 2-4 ml/min with room temperature recording ACSF consisting of the following (in mM): 125

NaCl, 2.5 KCl, 1 $MgCl_2(6H_2O)$, 2.5 $CaCl_2$, 20 glucose, 1 NaH_2PO_4, 25 $NaHCO_3$. Picrotoxin (Sigma-Aldrich) was also added to recording ACSF at 50 µM to block $GABA_A$ receptors. For some LTP induction experiments, $MgCl_2$ was excluded from the recording ACSF. MSNs in the dorsolateral striatum were visually identified under infrared illumination using an Olympus BX-51W1 microscope equipped with DIC optics and a 60X water-immersion objective. EGFP-expressing neurons and mCherry-expressing axons were identified with epifluorescence (Excelitas X-Cite 120Q).

Whole-cell voltage-clamp recordings were made with borosilicate glass patch electrodes (3-6 MΩ) filled with an internal solution consisting of (in mM): 120 cesium gluconate, 10 TEA-Cl, 10 HEPES, 10 glucose, 5 NaCl, 0.5 EGTA, 4 MgCl2, 4 ATP-K, 0.3 GTP-Na, 5 QX-314. Solution was adjusted to pH 7.3 and 285-290 mOsm. For some LTP induction experiments, 20 µM Sp-cAMPS was included in the pipette solution.

Recording data was obtained with a Multiclamp 700B amplifier, digitized with Digidata 1440A, and viewed with pCLAMP 10.6 software (Molecular Devices). Signals were digitized at 10 kHz and filtered at 4 kHz. Patched cells were clamped at -70 mV and series and input resistances were monitored throughout the recording by applying 10 mV depolarizing pulses. Data was excluded if the series resistance went over 25 MΩ or changed by more than 20%, or if the input resistance increased by more than 20%.

To stimulate ChR2 in corticostriatal terminals, 470 nm light pulses were produced by a collimated LED (Thorlabs), passed through a GFP filter, and delivered through the 60X objective to the brain slice. A 2 ms pulse duration was set by a Master-8 pulse stimulator (A.M.P.I). Light intensity was adjusted with an LED driver (Thorlabs) to evoke a baseline excitatory postsynaptic current (EPSC) of 100 – 400 pA.

Baseline EPSCs were recorded for at least 10 minutes to ensure that the 5 minutes immediately preceding plasticity induction were stable. Baseline and post-conditioning EPSCs were measured by applying one 2 ms light pulse every 30 seconds. Paired pulse ratios (PPRs) were measured by applying two pulses at 10 Hz and calculated by dividing the peak of the second EPSC by the first. AMPA/NMDA ratios were measured by stimulating at -70 mV and +40 mV for the AMPAR- and NMDAR-mediated currents, respectively. The NMDAR-mediated component was measured by sampling a 5 ms window 50 ms after the light stimulus at +40 mV. Average traces for AMPA and NMDA currents were obtained by averaging 5 EPSCs from each holding potential.

For Sp-cAMPS LTP induction, 20 µM Sp-cAMPS (Tocris) was included in the pipette solution. Cells were stimulated once at -70 mV, then depolarized to +40 mV for 50 ms, stimulated once, then held at +40 mV for an additional 500 ms. This was repeated 5 times at 0.5 Hz (Augustin et al., 2014). The Mg^{2+}-free LTP induction protocol was adapted from Calabresi et al. 1992 and consisted of three trains (3 second duration, 10 Hz, 20 second intervals) with $MgCl_2$ excluded from the recording medium. The $MgCl_2$-free medium was applied 10 minutes before the conditioning stimulus. The LTD induction protocol consisted of light stimulation at 1 Hz for 10 minutes with the cell clamped at -70 mV throughout. Blockade of CB1 receptors was achieved by adding 2 µM AM-251 (Tocris) to the bath. Blockade of NMDA receptors was achieved by adding 50 µM D-APV to the bath. To block mGluR5 receptors, 20 µM MPEP (Tocris) was added to the bath.

2.3.5 Data analysis

For LTP and LTD experiments, EPSCs recorded after the induction stimuli were

normalized to the average EPSC from the last 5 minutes of recorded baseline. Cells from each animal were averaged before performing statistical analysis, unless specified otherwise. Average amplitudes from 20-30 minutes following plasticity induction were compared between groups using Student's unpaired *t*-test. Comparison of AMPA/NMDA ratios, PPRs, and within-group EPSCs before and after plasticity induction were performed with a paired *t*-test. Statistical significance was assigned to p-values smaller than 0.05.

2.4 Results

2.4.1 Functional ChR2 expression in DLS corticostriatal terminals

Rbp4-Cre;Drd2-EGFP mice were injected with AAV-Ef1a-DIO-ChR2-mCherry bilaterally into layer 5 motor cortex, a region dense with striatal-projecting glutamatergic neurons. Following at least 4 weeks for expression to reach terminals in striatum, slices showed strong ChR2-mCherry expression in cortex and axons in the DLS (Figure 2.1).

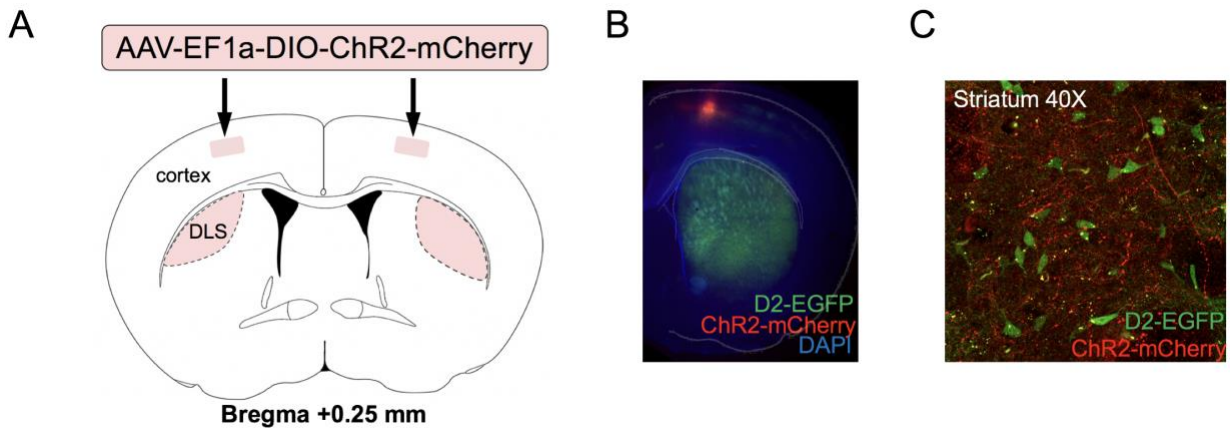

Figure 2.1. AAV-mediated expression of ChR2 in corticostriatal terminals in the DLS.
(A) Schematic of AAV injection in Rbp4-Cre; D2-EGFP mice.
(B) ChR2-mCherry expression in layer 5 of cortex 4 weeks after AAV injection.
(C) Confocal image of dorsolateral striatum showing ChR2-mCherry-positive axons surrounding EGFP-positive D2-MSNs.

Functional expression of ChR2 was confirmed using whole-cell patch clamp electrophysiology in brain slices. Whole-cell recordings from mCherry-positive cortical neurons showed reliably evoked action potentials in response to 470 nm light stimulation. In addition, optical stimulation of mCherry-positive axon terminals in the DLS reliably evoked EPSCs in D2-MSNs (Figure 2.2).

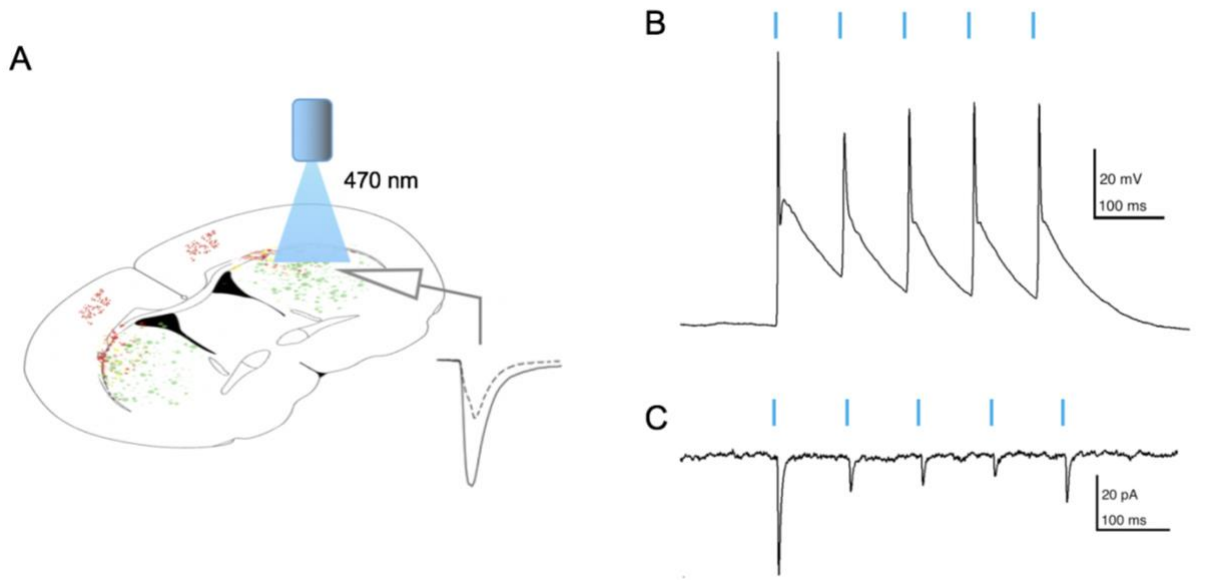

Figure 2.2. ChR2-mediated excitatory responses in cortex and striatum.
(A) Schematic of DLS stimulation with 470 nm light.
(B) Action potentials recorded in current-clamp from ChR2-expressing cortical neurons stimulated with 470 nm light at 10 Hz.
(C) EPSCs recording in voltage-clamp from D2-MSNs in response to stimulation of ChR2-expressing cortical axons in DLS.

2.4.2 LTP attempts

Our laboratory recently reported that bidirectional synaptic plasticity in D2-MSNs is regulated by intracellular cAMP signaling (Augustin et al., 2014). This study directly manipulated cAMP signaling in D2-MSNs by adding a reactive cAMP analog, Sp-cAMPS, to

the patch pipette internal solution. High levels of Sp-cAMPS (20 µM) were shown to promote robust LTP when combined with brief depolarization and low-frequency electrical stimulation. To determine if ChR2-mediated corticostriatal stimulation could also induce LTP under the same conditions, I applied the same low-frequency stimulation (LFS) protocol reported by Augustin et al. (2014) using light on ChR2-expressing terminals in the DLS (Figure 2.3A). Optical LFS with depolarization did not induce any potentiation in D2-MSNs (Figure 2.3B; n = 3 mice/6 cells).

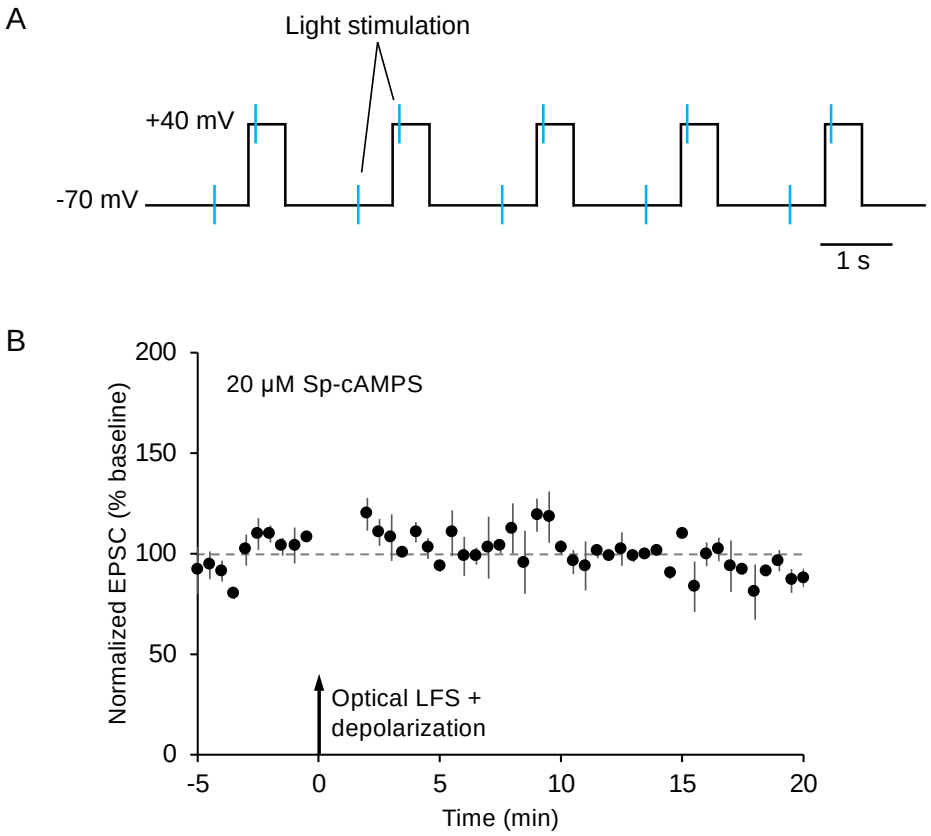

Figure 2.3. Optical LFS with depolarization does not induce LTP in D2-MSNs with high cAMP.
(A) Schematic of LFS with depolarization adapted from Augustin et al. (2014).
(B) EPSC amplitude as a function of time. Sp-cAMPS (20 µM) in the recording pipette with LFS and depolarization did not promote LTP in D2-MSNs (n = 3 mice/6 cells). Error bars: s.e.m.

I next tested an LTP protocol described by Calabresi et al. (1992) with which LTP was reportedly induced by applying tetanic electrical stimulation in a Mg^{2+}-free recording bath (Calabresi et al., 1992). The tetanic stimulation used by Calabresi et al. was applied at a frequency of 100 Hz, which far exceeds the highest frequency at which ChR2 can drive action potentials (Lin et al., 2009). In addition, ChR2-mediated postsynaptic currents have been shown to depress at high frequencies more than those evoked by electrical stimulation, in part due to an increased probability of initial release at the presynaptic boutons (Zhang and Oertner, 2007). In the DLS, ChR2-mediated corticostriatal stimulation failed to reliably evoke EPSCs at frequencies above 20 Hz, and significant current attenuation was observed at frequencies above 10 Hz (data not shown). Consequently, stimulation for this experiment was restricted to 10 Hz. Three trains of 10 Hz stimulation under Mg^{2+}-free extracellular conditions produced no lasting potentiation in D2-MSNs. A short-duration increase in EPSC amplitude following the conditioning stimulus was gradually reversed following reintroduction of the standard Mg^{2+}-containing bath solution (Figure 2.4).

2.4.3 Low frequency optogenetic stimulation of corticostriatal terminals induces LTD in D2 MSNs

Nearly all reported forms of LTD in the DLS involve eCB-mediated depression of presynaptic release, while most reported forms of LTP occur at postsynaptic sites (Kreitzer and Malenka, 2007; Shen et al., 2008; Augustin et al., 2014). In order to measure corticostriatal LTP using *ex vivo* LTD or depotentiation as a proxy, we needed an LTD protocol that induced reliable postsynaptic depression at corticostriatal synapses. The only postsynaptic corticostriatal LTD reported to date was observed in the nucleus accumbens (Pascoli et al., 2012). I tested whether

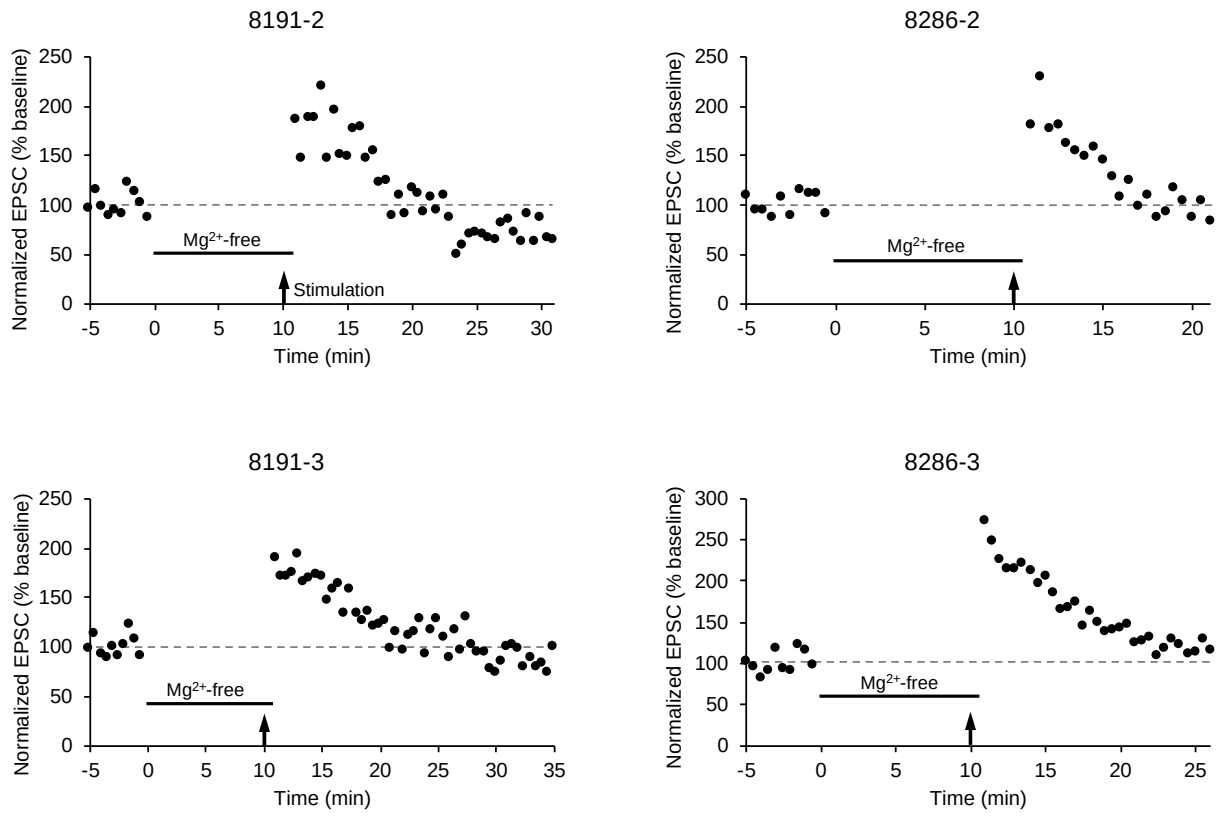

Figure 2.4. Optical stimulation under magnesium-free extracellular conditions.
Plots show EPSC amplitudes over time for individual cells. Optical stimulation of DLS corticostriatal terminals in Mg^{2+}-free medium does not promote LTP in D2-MSNs. Top label indicates cell number.

this approach could induce LTD at D2-MSN corticostriatal synapses in the DLS. Light pulses applied at 1 Hz for 10 minutes strongly depressed transmission in D2-MSNs (Figure 2.5A; 44% ± 8% of baseline, n = 6 mice/10 cells, $t_{(5)} = -7.33$, $p < 0.001$). PPRs were not changed following the LTD induction protocol (Figure 2.5B; n = 10 cells, mean change = -0.04, n = 10 cells, $t_{(9)} = 0.84$, $p = 0.42$), consistent with results reported from the nucleus accumbens (Pascoli et al., 2012). AMPAR/NMDAR ratios were not significantly different following LTD induction (Figure 2.5C; mean change = -0.56, n = 9 cells, $t_{(8)} = -1.3$, $p = 0.23$).

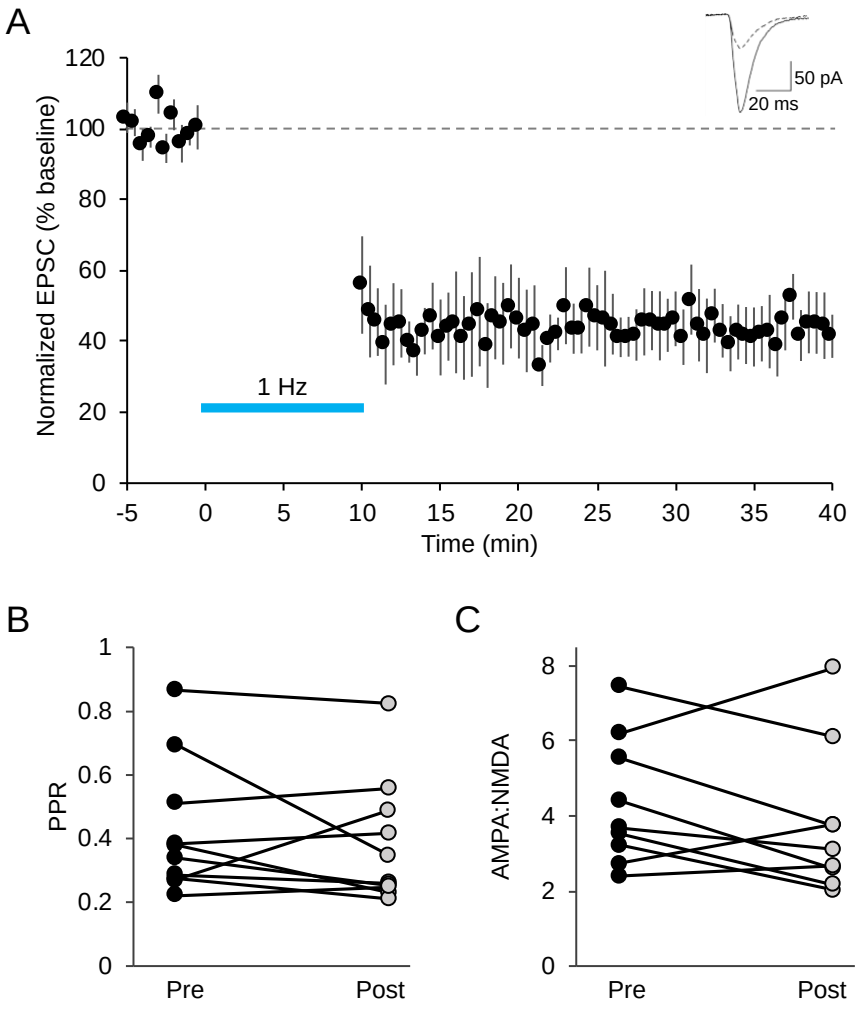

Figure 2.5. Low-frequency corticostriatal stimulation induces LTD in D2-MSNs.
(A) Plot shows EPSC amplitude over time. 1 Hz optical stimulation for 10 minutes induced strong LTD (44% ± 8% of baseline, n = 6 mice/10 cells, $t_{(5)} = -7.33$, $p < 0.001$). Inset shows averaged EPSC traces (10 trials) from before (solid line) and after (dashed line) LTD induction. Error bars: s.e.m.
(B) PPRs were unchanged following LTD induction (mean change = -0.04, n = 10 cells, $t_{(9)} = 0.84$, $p = 0.42$.
(C) AMPAR/NMDAR ratios were unchanged following LTD induction (mean change = -0.56, n = 9 cells, $t_{(8)} = -1.3$, $p = 0.23$.

2.4.4 Optically induced corticostriatal LTD is not dependent on CB1, NMDA, or mGluR5 receptors

The absence of change in PPR suggested that presynaptic release was not affected by the LTD induction protocol. To further verify this, I tested whether this LTD was dependent on CB1R activation. Bath application of the CB1R antagonist AM-251 (2 µM) had no effect on LTD induction (Figure 2.6; Control: 44% ± 8% of baseline, n = 6 mice/10 cells; AM-251: 45% ± 13% of baseline, n = 2 mice/5 cells, $t_{(6)} = 0.07$, p = 0.95).

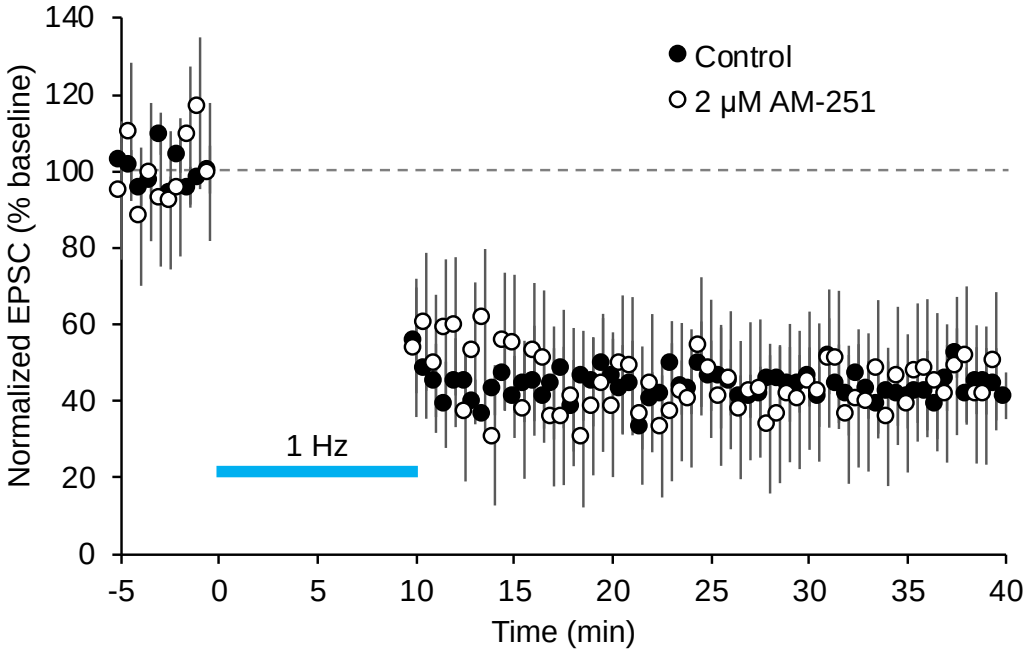

Figure 2.6. Optogenetic LFS LTD is not blocked by CB1R antagonist.
Application of CB1R antagonist AM-251 (2 µM) had no effect on magnitude of LTD in D2-MSNs (Control: 44% ± 8% of baseline, n = 6 mice/10 cells; AM-251: 45% ± 13% of baseline, n = 2 mice/5 cells, $t_{(6)} = 0.07$, p = 0.95). Error bars: s.e.m.

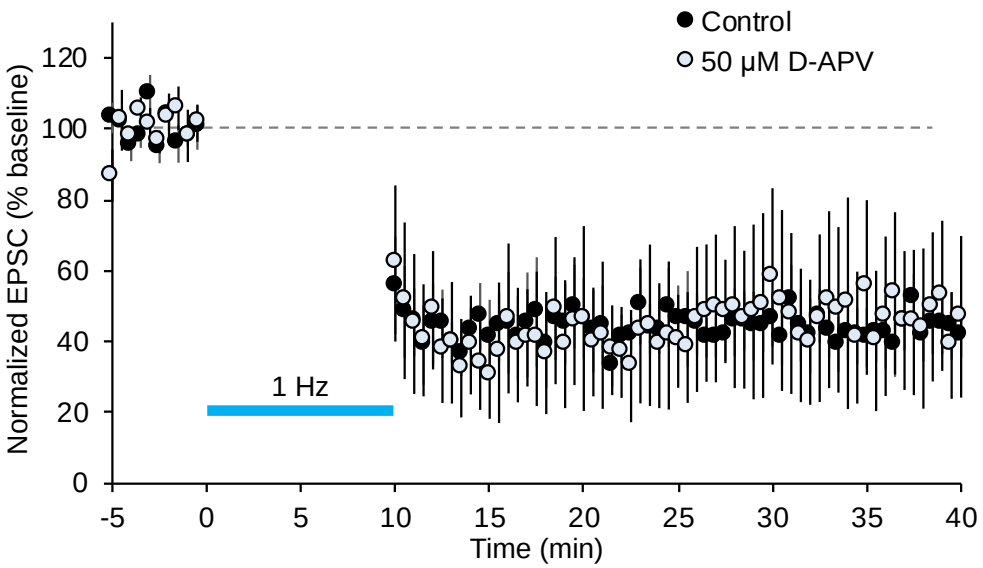

Figure 2.7. Optogenetic LFS LTD is not blocked by NMDAR antagonist.
Application of NMDAR antagonist D-APV (50 µM) had no effect on magnitude of LTD in D2-MSNs (Control: 44% ± 8% of baseline, n = 6 mice/10 cells; D-APV: 47% ± 22% of baseline, n = 3 mice/6 cells, $t_{(3)} = 0.14$, p = 0.89). Error bars: s.e.m.

Next, I tested whether this LTD was NMDAR-dependent. Bath application of NMDAR antagonist D-APV (50 µM) had no effect on LTD induction (Figure 2.7; Control: 44% ± 8% of baseline, n = 6 mice/10 cells; D-APV: 47% ± 22% of baseline, n = 3 mice/6 cells, $t_{(3)} = 0.14$, p = 0.89), unlike the optogenetic LTD reported in the nucleus accumbens (Pascoli et al., 2012).

I then tested whether the optogenetic LFS LTD was dependent on Group I mGluR activation, an important regulator of eCB-LTD. Bath application of the mGluR5 antagonist MPEP (20 µM) also had no effect on the magnitude of LTD induction (Figure 2.8; Control: 33% ± 8% of baseline, n = 3 mice/3 cells; MPEP: 43% ± 9% of baseline, n = 3 mice/3 cells, $t_{(4)} = -0.87$, p = 0.43). Together, the results shown here demonstrate that this optogenetic LFS-induced LTD is not dependent on CB1R, NMDAR, or mGluR5 activation.

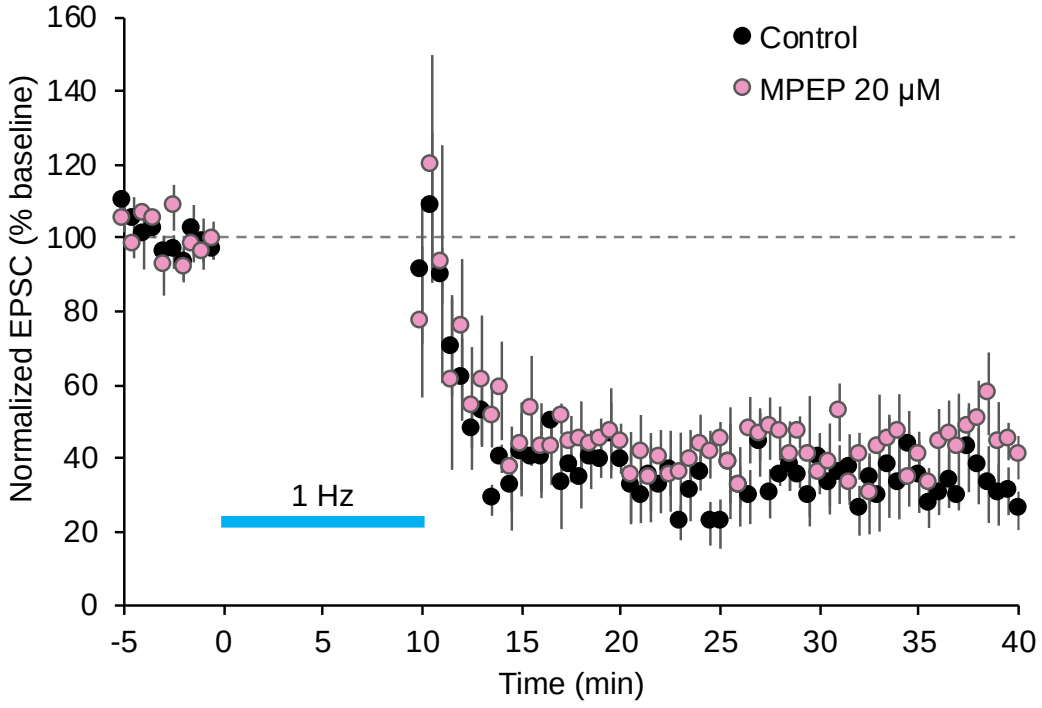

Figure 2.8. Optogenetic LFS LTD is not blocked by mGluR5 antagonist.
Application of mGluR5 antagonist MPEP (20 µM) had no effect on induction of LTD in D2-MSNs (Control: 33% ± 8% of baseline, n = 3 mice/3 cells; MPEP: 42% ± 9% of baseline, n = 3 mice/3 cells, $t_{(4)} = -0.87$, $p = 0.43$). Error bars: s.e.m.

2.5 Discussion

The experiments presented in this chapter took advantage of optogenetics and BAC transgenic mice to examine striatal synaptic plasticity with both presynaptic and postsynaptic cell-type specificity. The approach taken here allowed for selective stimulation of glutamatergic axons originating from cortex without activation of other intermingled modulatory systems. I demonstrated that two reported striatal LTP protocols that used electrical stimulation could not be reproduced when using optogenetic corticostriatal stimulation. I also characterized an optogenetic LTD protocol that did not affect presynaptic release like eCB-LTD. These results

highlight the importance of cell-type specificity in electrophysiology and provide a new method for assessing plasticity *ex vivo* in the DLS.

Corticostriatal eCB-LTD has been observed in brain slices with both electrical and optogenetic corticostriatal stimulation, and reported stimulation frequencies have ranged from 5 Hz to 100 Hz, illustrating the flexibility with which this form of plasticity is induced (Lovinger, 2010; Wu et al., 2015). Here, I applied 1 Hz corticostriatal stimulation to induce a robust LTD that was previously unreported in the DLS and that was neither eCB-dependent nor associated with altered presynaptic release. This optogenetic LFS LTD, which was first reported in the nucleus accumbens (Pascoli et al., 2012), eliminates coactivation of inputs that may be responsible for promoting eCB-LTD, thereby uncovering eCB-independent plasticity. Notably, eCB-LTD in D2-MSNs is known to depend on dopamine signaling at D2Rs (Wang et al., 2006; Kreitzer and Malenka, 2007; Lerner and Kreitzer, 2012). In previous studies where 1 Hz electrical stimulation was applied in the striatum for several minutes, no lasting changes in plasticity were observed in MSNs (Bonsi et al., 2003; Singla et al., 2007). The form of corticostriatal LTD characterized in this chapter may likely have only been possible by using optogenetics.

In addition to not being dependent on CB1R or mGluR5 activation, the LTD described here is not dependent on NMDAR activation either. This finding is at odds with a previous study in which optogenetic LFS LTD was found to be NMDAR-dependent in MSNs of the nucleus accumbens (Pascoli et al., 2012). The source of this discrepancy remains unclear, though anatomical subregion, gene expression, local circuitry, recording conditions, or other sources could all potentially have an impact on the results from these experiments. It is still unknown what the exact synaptic mechanism governing this LTD is in the DLS, but it is clear from the

findings presented here that it is fundamentally different from the mechanism that underlies the more common eCB-LTD.

Because LTP in the striatum has primarily been reported to occur postsynaptically, a corticostriatal LTD that does not alter presynaptic release, like the one described here, can conceivably be used to measure LTP by reversing the mechanisms that led to potentiation. This is especially useful for *ex vivo* studies that measure changes in synaptic strength associated with behavior, and for *in vivo* studies that aim to manipulate plasticity in order to influence changes in striatum-dependent behaviors.

In this chapter, I also tested optogenetic protocols for corticostriatal LTP. LTP in the DLS has historically been more challenging to induce than LTD, with far fewer published reports on the former. Some reported protocols for inducing LTP in the striatum have included the application of a magnesium-free extracellular medium (Calabresi et al., 1992), high intracellular cAMP (Augustin et al., 2014), STDP stimulation (Shen et al., 2008), or the addition of neurotrophic factors (Flajolet et al., 2008). Notably, most protocols for LTP induction have relied on electrical stimulation to activate corticostriatal afferents and the release of glutamate. Here, I tested two LTP protocols, one using low extracellular magnesium, and another using high intracellular cAMP, to determine if striatal potentiation could also be induced with optogenetics. LTP induced under magnesium-free conditions is attributed to the removal of the voltage-dependent magnesium block in NMDAR channels (Calabresi et al., 1992). High intracellular cAMP delivered through the patch pipette has been shown to promote LTP in D2-MSNs when combined with electrical LFS and postsynaptic depolarization (Augustin et al., 2014). Using optogenetics, I found that corticostriatal stimulation with either magnesium-free conditions or high intracellular cAMP was unable to induce LTP in D2-MSNs.

In the optogenetic experiments shown in this chapter, there were a few notable differences from the protocols reported by Calabresi et al. (1992) and Augustin et al. (2014) that may explain the failure to induce LTP reported here. First, the frequency of stimulation used by Calabresi et al. (1992) was 100 Hz, while my own stimulation was limited to 10 Hz due to the kinetics of ChR2. It is possible that the conditions provided by unblocking NMDARs are not indiscriminately permissive to LTP, and that high-frequency tetanic stimulation is still necessary for synaptic strengthening to occur under these conditions. While increases in spontaneous activity have been reported in hippocampal neurons following removal of magnesium from the recording bath (Herron et al., 1985), the dominant potassium conductances inherent to MSNs may serve to hamper any depolarization events facilitated by unblocked NMDAR channels. Moreover, the increase in intracellular calcium resulting from high frequency stimulation, which normally facilitates eCB-LTD under regular magnesium concentrations, may be necessary for triggering biochemical changes that are critical for LTP (Lovinger, 2010). The second notable difference in my experiments from the previous studies is that the optogenetic stimulation used in my study eliminated many inputs that may have contributed to LTP induction. Many factors can regulate striatal plasticity, and with electrical stimulation one can activate a large, heterogeneous body of inputs that encompasses all the necessary elements for inducing LTP in MSNs. It is possible that a convergence of afferents beyond the small subset expressing ChR2 is required for sufficient activation of striatal MSNs. For example, expression of ChR2 via local AAV injection may not cover a large enough volume of tissue to realistically mirror the activation of cortical afferents during behavior. Furthermore, the activation of thalamostriatal afferents or cholinergic neurons could potentially help drive potentiation together with corticostriatal inputs. The exclusion of many excitatory afferents when using optogenetics may

also lead to insufficient depolarization of distal MSN dendrites that cannot be depolarized with somatic current injection alone (Surmeier et al., 2009). This notion was supported by a recent study in which optogenetic depolarization of MSNs, which can directly depolarize distal dendritic processes, was far more effective than somatic current injection at promoting corticostriatal LTP in the DMS (Ma et al., 2018). Future studies using optogenetic manipulation of both pre- and postsynaptic targets may be required to fully understand the individual contributions to LTP in D2-MSNs. Overall, the results in this chapter highlight both advantages and disadvantages of using optogenetics for studying plasticity in the striatum. These findings set the groundwork for experiments described later in this thesis by providing an important tool for studying cell-type-specific synaptic plasticity relevant to learning and behavior.

CHAPTER 3

NEURAL CORRELATES OF INHIBITORY MOTOR LEARNING IN MICE

3.1 Abstract

The long-lasting deterioration of motor output in Parkinson's disease is thought to arise from the degeneration of midbrain dopamine neurons and the subsequent loss of dopamine signaling in the striatum. While much is already known about dopaminergic modulation of basal ganglia activity, changes in synaptic plasticity following chronic dopamine loss have received less attention. Here, I examine the striatal synaptic plasticity mechanisms that contribute to parkinsonian motor behaviors. Previous studies from our laboratory have suggested that the loss of dopamine signaling in the striatum may lead to motor decline through aberrant plasticity at corticostriatal synapses in the dopamine D2R-expressing indirect pathway. To test this, I used optogenetics and whole-cell recordings to assess changes in corticostriatal plasticity in mice that underwent motor training with a pharmacological D2R blockade. I observed that this treatment resulted in enhanced *ex vivo* corticostriatal LTD in D2R-expressing MSNs, suggesting that aberrant LTP had previously occurred at these synapses during inhibitory motor learning. Furthermore, co-administration of an adenosine A2AR antagonist, which has previously been shown to block corticostriatal LTP *in vitro*, was sufficient to prevent the induction of aberrant corticostriatal plasticity during training. To further examine the link between impaired behavior and plasticity, I applied *in vivo* corticostriatal stimulation with D2R blockade to induce aberrant LTP at D2-MSNs and observed a mild impairment in rotarod performance following stimulation.

Together, these results implicate aberrant corticostriatal plasticity in the development of parkinsonian motor symptoms and provide support for therapeutic strategies that target altered plasticity in PD and other neuropsychiatric disorders.

3.2 Introduction

PD is a progressive neurodegenerative disease in which the selective loss of nigrostriatal dopamine neurons leads to motor symptoms such as resting tremor, bradykinesia, and rigidity. The most commonly used clinical treatment for PD consists of dopamine replacement with levodopa (L-DOPA) which remains the most effective pharmacological therapy today. However, the response to L-DOPA begins to fluctuate over time in PD patients and the beneficial effects of the drug start to diminish (Nutt et al., 1992). Moreover, adverse side effects stemming from prolonged use of the drug, such as dyskinesia, begin to emerge (Fabbrini et al., 2007). Therefore, there is a continued need for developing new treatments for PD that remain effective over time with fewer adverse side effects.

Dysfunctional basal ganglia circuitry is thought to have a significant role in the motor symptoms of PD due to the loss of dopamine signaling in the striatum. Reduced signaling at D1- and D2Rs is thought to decrease output from the direct pathway while increasing output from the indirect pathway, resulting in an overall suppression of movement (Albin et al., 1989; DeLong, 1990). While several studies have shown intrinsic and homeostatic adaptations in MSNs in PD models (Day et al., 2006; Fieblinger et al., 2014; Nishijima et al., 2014), few have directly examined the role of experience-dependent synaptic plasticity in PD motor symptoms. Previous studies from our laboratory suggest that the loss of dopamine signaling in the striatum may lead to motor decline through aberrant plasticity at corticostriatal synapses in the indirect pathway

(Beeler et al., 2010, 2012). Animals that engage in motor activity while under D2R blockade develop a long-lasting motor inhibition that persists even after normal dopamine signaling is restored. We propose that this motor inhibition is the outcome of an aberrant learning process through which active motor programs are suppressed rather than reinforced. With the loss of signaling at D2Rs, normal inhibition of the indirect pathway is relieved as intracellular cAMP levels rise in D2-MSNs. We hypothesize that this allows excitatory cortical input to potentiate synapses on D2-MSNs during motor activity, eventually leading to motor suppression. The blockade of A2ARs, which prevents inhibitory motor learning in mice, may help protect against motor inhibition via mitigation of corticostriatal LTP. The study presented in this chapter examines the synaptic mechanisms behind inhibitory motor learning and provides support for a causal link between aberrant corticostriatal plasticity and parkinsonian motor inhibition. The prevention or reversal of aberrant plasticity may serve as a potential therapeutic approach to treating PD motor symptoms.

3.3 Methods

3.3.1 Animals

Rbp4-Cre transgenic mice were crossed to a Drd2-EGFP transgenic mouse line (Gong et al., 2003) in order to generate Rbp4Cre;Drd2-EGFP double transgenic mice. All double transgenic mice used in experiments were hemizygous for each transgene. The presence of each transgene was determined by genotyping using PCR primer sequences obtained from MMRRC.

Male and female mice 8-16 weeks of age were used for all experiments. Mice were housed on a 12-hour light/dark cycle and allowed ad libitum access to standard food and water. All animal procedures performed in these experiments were approved by the Institutional Animal

Care and Use Committee of the University of Chicago.

3.3.2 Drug administration

Drugs were administered by intraperitoneal (i.p.) injections delivered 30 minutes before the start of each rotarod session during the training phase, or 30 minutes before the start of stimulation for *in vivo* experiments. Eticlopride (Sigma-Aldrich) was administered at 0.016 mg/kg of body weight and theophylline (Sigma-Aldrich) at 60 mg/kg. Drugs were prepared in 0.9% normal saline.

3.3.3 Behavioral tests

Mice were trained on the accelerating rotarod (Columbus Instruments) with a 7 cm diameter rod programmed to accelerate from 4 to 40 rotations per minute (rpm). The training phases consisted of 5 consecutive trials per day (session) for a total of 5 training sessions. For assessing motor performance after training or optogenetic stimulation, mice were tested for 1 session before electrophysiological experiments or for 10 sessions after optogenetic conditioning experiments. Mice were returned to their home cages after each session.

Open field chambers (Med Associates) were 40 x 40 cm with lighting at 21 lux. Locomotor activity was tracked in each mouse with infrared beams and recorded with Med Associates software. Mice were returned to their home cages at the end of testing.

3.3.4 Surgery and AAV injection

Rbp4-Cre;Drd2-EGFP mice at least 8 weeks of age were anesthetized with 2% vaporized isoflurane and positioned into a stereotaxic apparatus (Kopf Instruments). Anesthesia was then

maintained at 1-1.5% and mice were kept warm on a heating pad throughout the remainder of the procedure. Fur was removed from the scalp with an electric clipper and Betadine was applied to the bare scalp prior to incision. The mouse's eyes were treated with ophthalmic ointment to prevent corneal drying. An incision was made through the scalp midline and the skull was exposed for identification of bregma. Two holes were drilled into the skull and a total volume of 500 nl of AAV5-Ef1a-DIO-hChR2(H134R)-mCherry-WPRE-pA (University of North Carolina Vector Core) was injected into each hole with a 33-gauge needle at a rate of 120 nl/min. Injections were made in cortex at the following stereotaxic coordinates: AP: +0.25, ML: ±1.5, DV: -1.25. These coordinates target the forelimb and hindlimb regions of mouse primary motor cortex (Tennant et al., 2011). At the end of each injection, the needle was kept in the same position in the brain for an additional 5 minutes to allow the AAV to diffuse. For *in vivo* optogenetic stimulation experiments, a 200 µm core multimode optical fiber (Thorlabs) attached to a ceramic ferrule was implanted unilaterally into the right dorsolateral striatum at the following stereotaxic coordinates: AP: +0.8, ML: +2.2, DV: -2.7. Positioning the fiber in the DLS rather than cortex allowed us to avoid direct stimulation of brainstem-projecting PT neurons in motor cortex. The fiber and ferrule were secured in place with glue (Loctite) and dental acrylic (Ortho-Jet). The scalp was then sutured closed at the end of surgery and mice were administered buprenorphine (0.1 mg/kg subcutaneous) and meloxicam (1 mg/kg subcutaneous) for postoperative analgesia. Mice were not used for experiments until at least 4 weeks after surgery.

3.3.5 Brain slice preparation

To prepare slices for recordings, mice were deeply anesthetized with isoflurane and then

decapitated. The brain was rapidly dissected out of the skull and submerged in an ice-cold, oxygenated (95% O_2, 5% CO_2) artificial cerebrospinal fluid (ACSF) solution containing the following (in mM): 92 *N*-methyl-D-glucamine, 2.5 KCl, 1.2 NaH_2PO_4, 30 $NaHCO_3$, 25 glucose, 12 *N*-acetyl-L-cysteine, 20 HEPES, 5 sodium ascorbate, 2 thiourea, 3 sodium pyruvate, 10 $MgSO_4$ ($7H_2O$), and 0.5 $CaCl_2$. The solution was brought to pH 7.3-7.4 with 12N HCl and osmolarity was adjusted to 305-315 mOsm. The brain was sliced in ice-cold oxygenated ACSF into 250 µm thick coronal sections using a vibratome (Leica VT1000S). Brain slices were then transferred to a holding chamber containing 32°C ACSF continuously oxygenated for 12-15 minutes. Slices were then transferred again to a new holding chamber at room temperature containing a different oxygenated ACSF consisting of the following (in mM): 92 NaCl, 2.5 KCl, 1.2 NaH_2PO_4, 30 $NaHCO_3$, 25 glucose, 20 HEPES, 5 sodium ascorbate, 2 thiourea, 3 sodium pyruvate, 2 $MgSO_4$ ($7H_2O$), and 2 $CaCl_2$. The solution was brought to pH 7.3-7.4 with 10N NaOH and osmolarity was adjusted to 305-315 mOsm. The slices were incubated for at least 60 minutes before recording.

3.3.6 Electrophysiology

Individual brain slices were transferred to a recording chamber and perfused at a rate of 2-4 ml/min with room temperature recording ACSF consisting of the following (in mM): 125 NaCl, 2.5 KCl, 1 $MgCl_2$($6H_2O$), 2.5 $CaCl_2$, 20 glucose, 1 NaH_2PO_4, 25 $NaHCO_3$. Picrotoxin (Sigma-Aldrich) was also added to recording ACSF at 50 µM to block $GABA_A$ receptors. For some LTP induction experiments, $MgCl_2$ was excluded from the recording ACSF. MSNs in the dorsolateral striatum were visually identified under infrared illumination using an Olympus BX-51W1 microscope equipped with DIC optics and a 60X water-immersion objective. EGFP-

expressing neurons and mCherry-expressing axons were identified with epifluorescence.

Whole-cell voltage-clamp recordings were made with borosilicate glass patch electrodes (3-6 MΩ) filled with an internal solution consisting of (in mM): 120 cesium gluconate, 10 TEA-Cl, 10 HEPES, 10 glucose, 5 NaCl, 0.5 EGTA, 4 MgCl2, 4 ATP-K, 0.3 GTP-Na, 5 QX-314. Solution was adjusted to pH 7.3 and 285-290 mOsm. For some LTP induction experiments, 20 µM Sp-cAMPS was included in the pipette solution.

Recording data was obtained with a Multiclamp 700B amplifier, digitized with Digidata 1440A, and viewed with pCLAMP 10.6 software (Molecular Devices). Signals were digitized at 10 kHz and filtered at 4 kHz. Patched cells were clamped at -70 mV and series and input resistances were monitored throughout the recording by applying 10 mV depolarizing pulses. Data was excluded if the series resistance went over 25 MΩ or changed by more than 20%, or if the input resistance increased by more than 20%.

To stimulate ChR2 in corticostriatal terminals, 470 nm light pulses were produced by a collimated LED (Thorlabs), passed through a GFP filter, and delivered through the 60X objective to the brain slice. A 2 ms pulse duration was set by a Master-8 pulse stimulator (A.M.P.I). Light intensity was adjusted with an LED driver (Thorlabs) to evoke a baseline excitatory postsynaptic current (EPSC) of 100 – 400 pA.

Baseline EPSCs were recorded for at least 10 minutes to ensure that the 5 minutes immediately preceding plasticity induction were stable. Baseline and post-conditioning EPSCs were measured by applying one 2 ms light pulse every 30 seconds. Paired pulse ratios (PPRs) were measured by applying two pulses at 10 Hz and calculated by dividing the peak of the second EPSC by the first. AMPA/NMDA ratios were measured by stimulating at -70 mV and +40 mV for the AMPAR- and NMDAR-mediated currents, respectively. The NMDAR-mediated

component was measured by sampling a 5 ms window 50 ms after the light stimulus at +40 mV. Average traces for AMPA and NMDA currents were obtained by averaging 5 EPSCs from each holding potential. The LTD induction protocol consisted of light stimulation at 1 Hz for 10 minutes with the cell clamped at -70 mV throughout.

Miniature EPSCs (mEPSCs) were recorded in the presence of 0.5 µM tetrodotoxin. Signals were filtered at 2 kHz and analyzed with Clampex software (Molecular Devices).

3.3.7 In vivo optogenetic stimulation

Implanted fibers were connected to a 473 nm solid-state laser (Shanghai Laser & Optics Century Co.) by a rotary joint patch cable (Thorlabs). Mice were placed in an open field arena and stimulated with 10 ms pulses at 10 Hz for 10 minutes, repeated 3 times with a 1-minute inter-train interval daily for a total of 5 days. Stimulation frequency and duration were controlled with a Master-9 pulse stimulator (A.M.P.I.). Mice were returned to their home cages at the end of stimulation.

3.3.8 Data analysis

EPSCs recorded after LTD induction were normalized to the average EPSC from the last 5 minutes of recorded baseline. Cells from each animal were averaged before performing statistical analysis. Average amplitudes from 20-30 minutes following LTD induction were compared between groups using Student's unpaired *t*-test. Comparison of AMPA/NMDA ratios and PPRs were performed with unpaired *t*-test. Analysis of mEPSC amplitude and frequency was done with Mann-Whitney *U* test. Rotarod performance was analyzed with two-way ANOVA with repeated measures. Statistical significance was assigned to p-values smaller than 0.05.

3.4 Results

3.4.1 Ex vivo LTD is enhanced following training with D2R antagonist

To determine whether corticostriatal synaptic strength was changed in D2-MSNs in mice with inhibitory motor learning, I performed *ex vivo* recordings from mice that underwent rotarod training with various drug treatments (Figure 3.1A). As reported previously (Beeler et al., 2012),

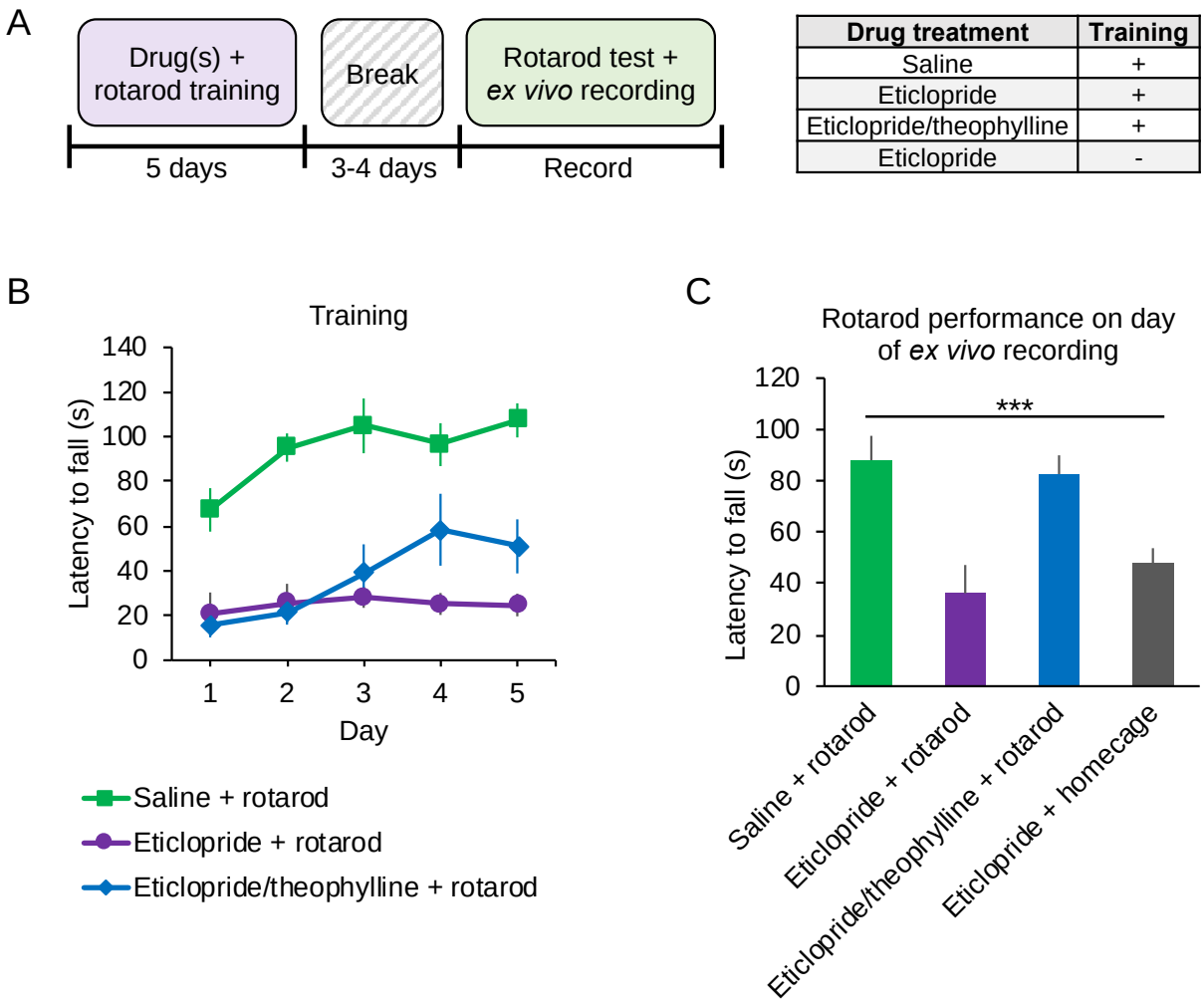

Figure 3.1. Inhibitory motor learning experiment design.
(A) Schedule of rotarod training and drug treatment (left) and treatment conditions (right).
(B) Rotarod performance during training phase. Group main effect: $F_{(2,17)} = 31.91$, $p < 0.0001$.
(C) Rotarod performance on day of recording. Group main effect: $F_{(3,25)} = 7.78$, $p < 0.001$. n = 8 saline, 7 eticlopride+rotarod, 7 eticlopride/theophylline+rotarod, 8 eticlopride+homecage. Error bars: s.e.m.

mice that were administered the D2R antagonist eticlopride during the training phase were significantly impaired compared to saline controls (Figure 3.1B; group main effect: $F_{(2,17)}$ = 31.91, $p < 0.0001$). To determine whether mice had developed inhibitory motor learning before performing whole-cell recording, they were tested on the rotarod for a single session in the absence of any drug. As expected, mice that were previously trained with eticlopride showed a persistent impairment on the rotarod on the day of recording (Figure 3.1C; group main effect: $F(3,25) = 7.78$, $p < 0.001$).

Following the testing session, acute brain slices were prepared for *ex vivo* recording. Using the low-frequency optogenetic LTD induction protocol characterized earlier (see Chapter 2.4.3), I observed a significantly larger magnitude of corticostriatal depression in D2-MSNs of mice that were trained under eticlopride treatment compared to saline controls (Figure 3.2A; eticlopride: n = 5 mice/6 cells, 26% ± 4% of baseline; saline: n = 5 mice/7 cells, 57% ± 10% of baseline, $t_{(8)} = 3.01$, $p = 0.017$). Mice that were trained under D2R blockade also displayed a larger magnitude of LTD compared to untrained mice (Figure 3.2B; homecage: n = 7 mice/9 cells, 65% ± 13% of baseline, $t_{(7)} = 2.94$, $p = 0.022$). *Ex vivo* measures of AMPAR/NMDAR ratio showed no difference between groups (Figure 3.2C; group main effect: $F_{(2,15)} = 0.41$, $p = 0.67$). Similarly, there were no differences in PPR associated with treatment (Figure 3.2D; group main effect: $F_{(2,17)} = 0.395$, $p = 0.68$).

3.4.2 mEPSC amplitude and frequency in D2-MSNs are not changed by inhibitory motor learning

To further examine the effects of inhibitory motor learning on synaptic transmission in D2-MSNs, I recorded mEPSCs. Mean amplitude of mEPSCs in mice trained under D2R

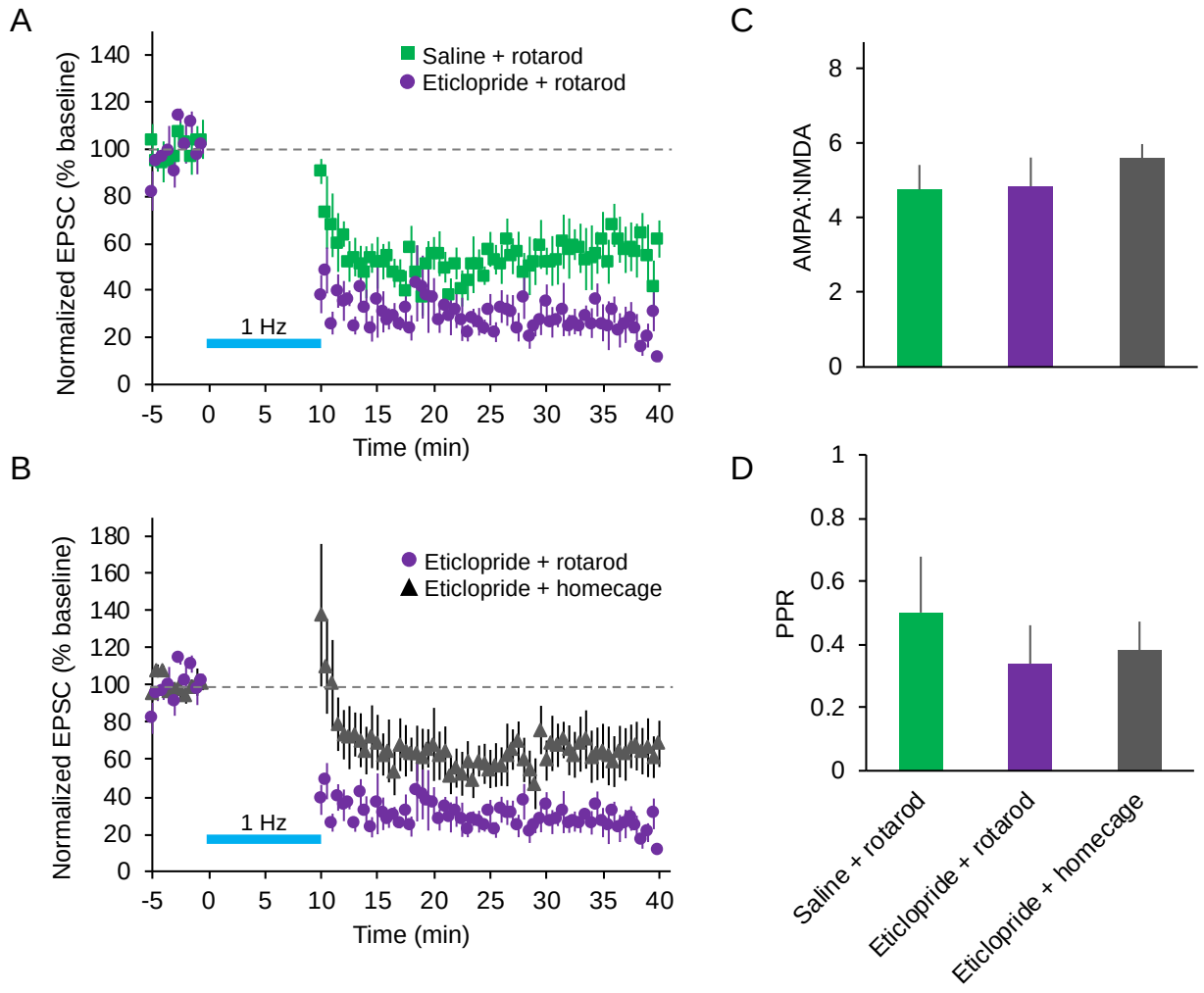

Figure 3.2. *Ex vivo* corticostriatal LTD is enhanced in mice trained under eticlopride.
(A, B) Optogenetic LTD is enhanced in D2-MSNs from mice trained under eticlopride (n = 5 mice/6 cells, 26% ± 4% of baseline) compared to **(A)** saline (n = 5 mice/7 cells, 57% ± 10% of baseline; $t_{(8)} = 3.01$, p = 0.017) or **(B)** untrained (n = 7 mice/9 cells, 65% ± 13% of baseline, $t_{(7)} = 2.94$, p = 0.022).
(C) Mean ratio of AMPAR- to NMDAR-mediated currents is unaffected by treatment (n = 7 saline, 6 eticlopride, 5 homecage; group main effect: $F_{(2,15)} = 0.41$, p = 0.67).
(D) Mean PPR (100 ms inter-pulse interval) is unaffected by treatment (n = 6 saline, 6 eticlopride, 8 homecage; group main effect: $F_{(2,17)} = 0.395$, p = 0.68). Error bars: s.e.m.

blockade showed no difference compared to mEPSCs from saline (W = 8, p = 0.63) or untrained (W = 4, p > 0.99) groups (Figure 3.3A,B). Mean mEPSC frequency was also unchanged in eticlopride/rotarod mice compared to saline (W = 6, p > 0.99) or untrained (W = 2, p = 0.40) mice, indicating no significant differences in presynaptic transmission (Figure 3.3C,D). These

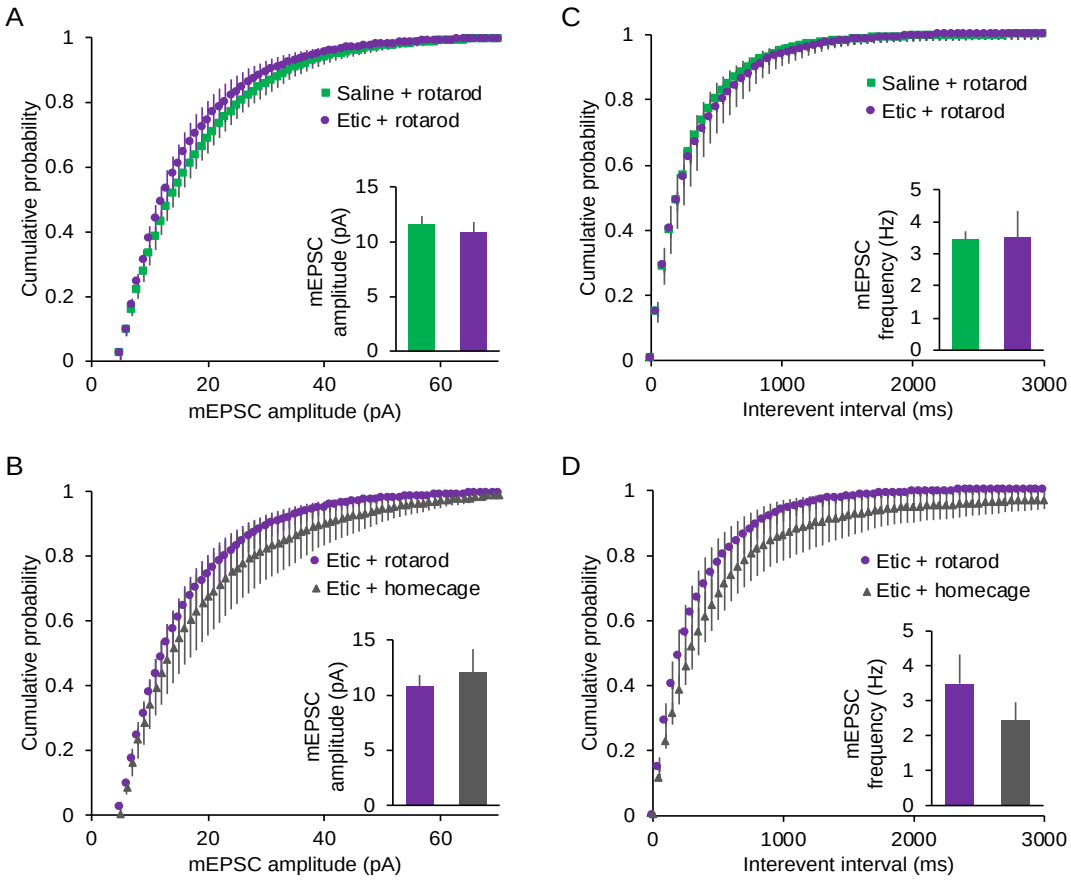

Figure 3.3. mEPSC amplitude and frequency are unaffected by aberrant motor learning. **(A, B)** Plots show cumulative probability distribution and mean amplitude of mEPSCs recorded from D2-MSNs. Mice trained on rotarod under eticlopride showed no difference in mean mEPSC amplitude compared to saline (W = 8, p = 0.63) or untrained mice (W = 4, p > 0.99). **(C, D)** Cumulative probabilities of mEPSC interevent intervals and mean frequency. There were no differences in mEPSC frequency in mice trained under eticlopride compared to saline (W = 6, p > 0.99) or untrained mice (W = 2, p = 0.40). Eticlopride rotarod n = 3 mice/10 cells; Saline rotarod n = 4 mice/10 cells; Eticlopride untrained n = 3 mice/6 cells. Error bars: s.e.m.

results suggest that while inhibitory motor learning is associated with enhanced corticostriatal LTD, these observations may reflect a selective strengthening of corticostriatal synapses that is not present at the majority of synapses in D2-MSNs.

3.4.3 A2AR antagonist mitigates induction of aberrant plasticity

The A2AR antagonist theophylline has been shown to prevent the induction of inhibitory motor learning in mice (Figure 3.1C; Beeler et al., 2012). To determine whether this effect was associated with protection against aberrant corticostriatal plasticity, mice were trained on the rotarod with both eticlopride and theophylline and then subjected to *ex vivo* recording. Mice that were co-administered theophylline showed a significantly smaller magnitude of LTD than mice that were trained with eticlopride alone (Figure 3.4A; eticlopride: n = 5 mice/6 cells, 26% ± 4%

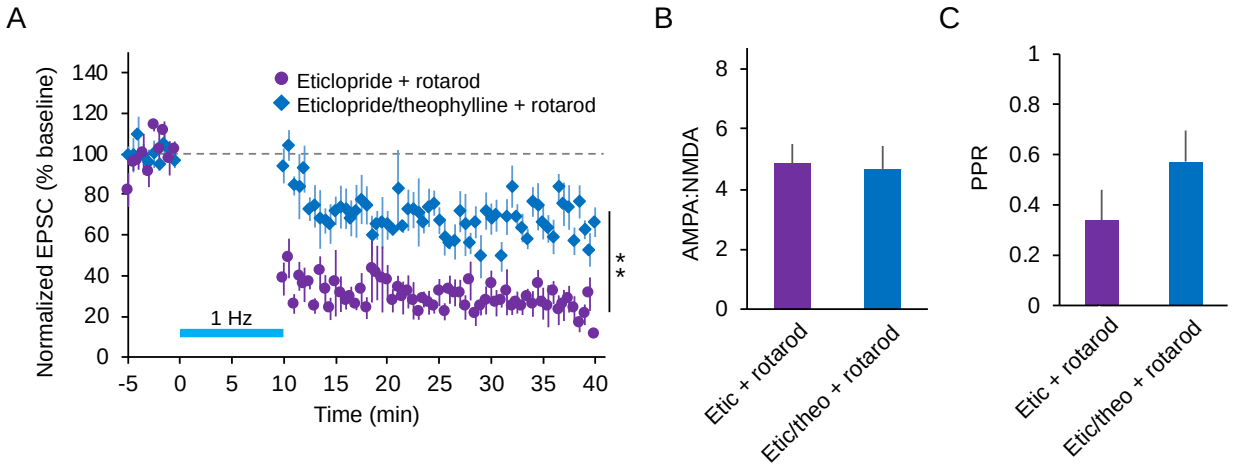

Figure 3.4. A2AR antagonist theophylline mitigates aberrant corticostriatal plasticity.
(A) Magnitude of LTD is reduced in mice trained with eticlopride/theophylline (eticlopride: n = 5 mice/6 cells, 26% ± 4% of baseline; theophylline: n = 4 mice/6 cells, 67% ± 4% of baseline, $t_{(7)} = 7.1$, $p < 0.001$).
(B) Mean AMPA/NMDA ratio is not affected by theophylline (n = 6 eticlopride, 6 theophylline, $t_{(10)} = 0.2$, $p = 0.84$).
(C) Mean PPR (100 ms inter-pulse interval) is unaffected by treatment (n = 6 eticlopride, 6 theophylline, $t_{(10)} = 1.35$, $p = 0.21$).

of baseline; theophylline: n = 4 mice/6 cells, 67% ± 4% of baseline, $t_{(7)} = -7.1$, $p < 0.001$). Neither the AMPAR/NMDAR ratio nor PPR differed between the two groups (Figure 3.4B,C; AMPA/NMDA: $t_{(10)} = 0.2$, $p = 0.84$; PPR: $t_{(10)} = 1.35$, $p = 0.21$). mEPSC analysis also found no difference in mean mEPSC amplitude or frequency between the two groups (Figure 3.5; amplitude: W = 5, p = 0.86; frequency: W = 5, p = 0.86).

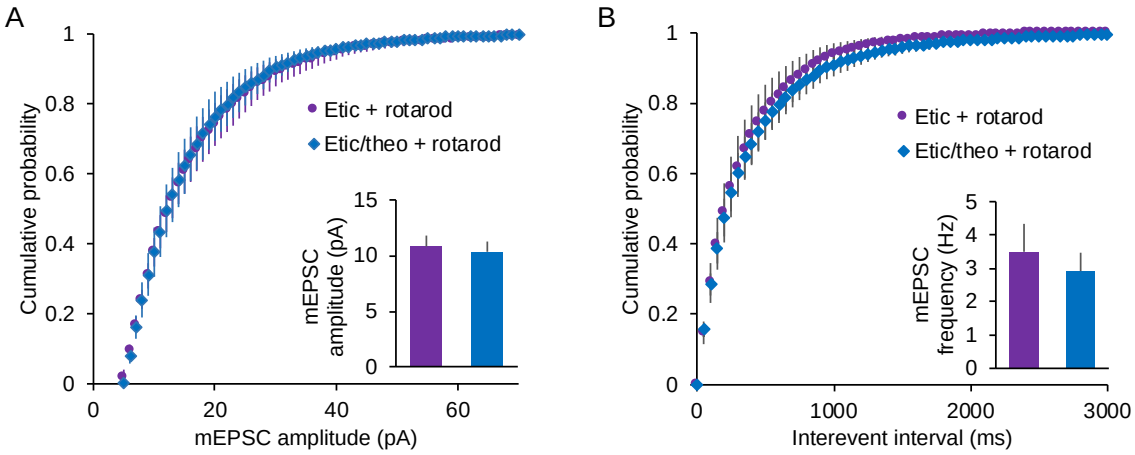

Figure 3.5. A2AR antagonist has no effect on mEPSC amplitude or frequency.
(A) Plots show cumulative probability distribution and mean amplitude of mEPSCs from mice trained with eticlopride only or both eticlopride and theophylline (W = 5, p = 0.86).
(B) Cumulative probability distribution of interevent intervals and mean frequency of mEPSCs from mice trained with eticlopride only or both eticlopride and theophylline (W = 5, p = 0.86). Eticlopride n = 3 mice/10 cells, theophylline n = 4 mice/6 cells. Error bars: s.e.m.

3.4.4 Establishing a link between aberrant plasticity and inhibitory motor learning

Given the strong correlation between inhibitory motor learning and aberrant corticostriatal plasticity, we wanted to more directly establish a causal link between the synaptic mechanism and behavior. To address this, optical fibers were surgically implanted into the DLS of mice expressing ChR2 in corticostriatal projections. We replaced motor experience with

optogenetic stimulation to directly activate corticostriatal synapses in awake behaving mice. We hypothesized that the combination of D2R antagonist with corticostriatal stimulation would lead to aberrant corticostriatal LTP in D2 MSNs and a long-lasting motor impairment in mice. Mice were treated with eticlopride or saline and stimulated with three 10-minute trains of 10 Hz per day for 5 days (Figure 3.6A). Following the fifth day of stimulation, mice were given a 3-day

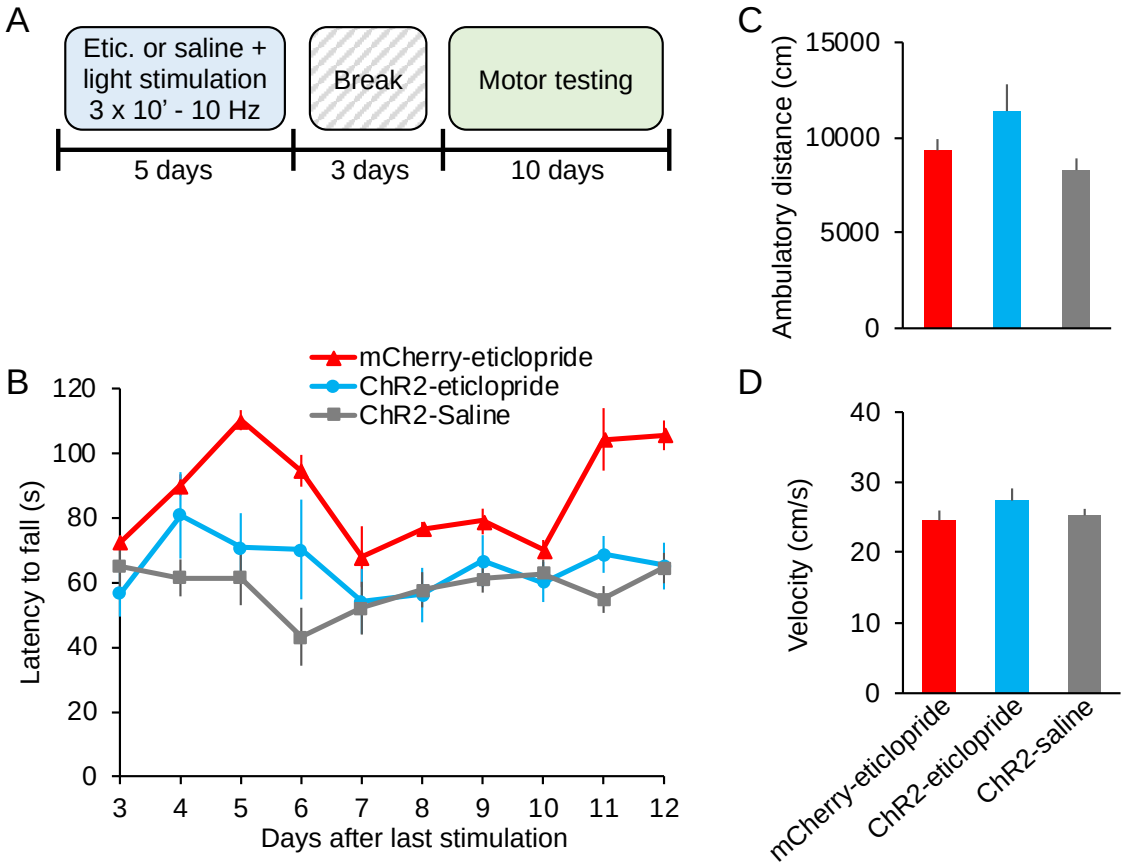

Figure 3.6. Corticostriatal stimulation induces impairment in rotarod performance.
(A) Schedule of stimulation and testing. Mice received daily 10 Hz optogenetic stimulation while under eticlopride or saline. Motor performance was tested following a 3-day drug-free break.
(B) Rotarod performance after stimulation. Group x day: $F_{(18,81)} = 2.14$; $p = 0.011$. n = 3 mCherry-eticlopride, 5 ChR2-eticlopride, 5 ChR2-saline.
(C,D) Open field test of general locomotor activity. No difference in ambulatory distance (top) or velocity (bottom). Error bars: s.e.m.

break that was followed with motor behavioral testing. Control mice expressing mCherry instead of ChR2 performed better on the rotarod compared to ChR2-expressing mice from both eticlopride- or saline-treated groups (Figure 3.6B; group x day: $F_{(18,81)} = 2.14$, $p = 0.011$). In spite of their impaired performances on the rotarod, the ChR2-expressing groups showed no other motor deficits (Figure 3.6C,D; open field distance: $F_{(2,11)} = 2.3$, $p = 0.16$; velocity: $F_{(2,11)}$: 0.91, $p = 0.44$). These findings suggest that repeated corticostriatal stimulation can induce a mild motor impairment with or without D2R blockade.

3.5 Discussion

The findings presented in this chapter uncover a potential synaptic mechanism underlying motor impairments in PD. Our lab previously reported that a dopamine signaling deficiency can induce D2R-mediated aberrant learning that promotes long-lasting motor inhibition similar to PD motor symptoms (Beeler et al., 2010, 2012). Here, I performed whole-cell recordings in brain slices from mice with inhibitory motor learning to assess changes in synaptic transmission in D2-MSNs of the DLS. Using precise optogenetic stimulation of corticostriatal terminals, I found that mice that were rotarod-trained under D2R blockade demonstrated enhanced LTD in D2-MSNs, and that this enhancement could be blocked by theophylline co-administration. Together with previous studies, these findings strongly suggest that inhibitory motor learning is encoded by aberrant corticostriatal LTP in D2-MSNs. Dopamine signaling has a well-documented role in modulating plasticity in both the direct and indirect pathways (Lovinger, 2010). Changes in corticostriatal plasticity can subsequently alter the output of each pathway, ultimately influencing striatum-dependent motor learning and behavior. It is likely that corticostriatal LTP in the indirect pathway occurs as a part of normal learning processes and not solely under pathological

conditions. The well-established role of dopamine in reinforcement learning serves to influence behavioral outcomes through both faciliatory and inhibitory learning (Schultz, 2007). When dopamine neuron firing increases in response to an unexpected reward, activation of striatal D1 and D2Rs promotes LTP in the direct pathway and LTD in the indirect pathway. However, when a predicted reward is omitted, there is a pause in dopamine neuron firing that subsequently reduces activation of dopamine receptors in the striatum. The pause in D2R activation allows for cAMP to increase in D2-MSNs, thereby promoting LTP in the indirect pathway and enhancing the inhibitory output from the cortico-basal-ganglia loop. We propose that this inhibitory mechanism becomes exaggerated under chronic dopamine depletion, such that any motor program active under these conditions is ultimately suppressed rather than facilitated.

The observed lack of change in mEPSC amplitude or frequency despite enhanced corticostriatal LTD in mice with inhibitory motor learning suggests a highly selective strengthening of a minority of D2-MSN synapses. Because our site of AAV injection limited ChR2 expression only to neurons in motor cortex, a brain region known to be highly active during rotarod learning (Cao et al., 2015; Kupferschmidt et al., 2017), LTD was primarily mediated by a subset of behaviorally-relevant axons in striatum. On the other hand, mEPSC recordings captured a much broader subset of synapses that received inputs from multiple cortical regions as well as thalamus. Therefore, behaviorally relevant synapses expressing aberrant LTP may have constituted only a fraction of total recorded mEPSCs. We also observed no change in AMPAR/NMDAR ratio, another frequently used measure of synaptic strength. The significance of this measure is premised on the assumption of dynamic AMPAR expression but static NMDAR expression at the synapse of interest. In the striatum, however, both AMPAR and NMDAR expression have been shown to change with motor learning or drug exposure (Yin et

al., 2009; Wang et al., 2010; Ma et al., 2017; Xia et al., 2017) thereby making the AMPAR/NMDAR ratio difficult to interpret. Thus, it is not possible to rule out expression changes for either receptor based on AMPAR/NMDAR alone.

Corticostriatal LTP in D2-MSNs is dependent on A2AR activation and its coupling to cAMP production (Shen et al., 2008; Peterson et al., 2012). Here, I demonstrated that co-administration of the A2AR antagonist theophylline during D2R blockade prevented induction of aberrant plasticity in D2-MSNs. This data provides further support for the role of aberrant LTP in inhibitory motor learning, and provides insight into a mechanism for caffeine's protection against PD. A2AR antagonists have already been shown to prevent or mitigate parkinsonian motor symptoms in animal models of PD (Marcellino et al., 2010; Beeler et al., 2012), and several have undergone clinical testing as a potential therapy for PD (Zheng et al., 2018). It should be noted that theophylline is not strictly selective for A2ARs, so it is possible that other adenosine receptors contribute to the behavioral and physiological effects we have observed. However, given that selective A2AR antagonism is sufficient to block LTP in D2-MSNs *in vitro* (Shen et al., 2008), we propose that theophylline and caffeine deliver protection against motor inhibition and aberrant plasticity predominantly through A2AR blockade.

The selective A2AR antagonist istradefylline has very recently been approved for use in the United States as an adjunctive treatment for PD (Voelker, 2019), but this and several other A2AR antagonists, such as preladenant, have repeatedly faced difficulties gaining approval for market due to inconsistent clinical results (Fernandez-Duenas et al., 2018; Zheng et al., 2018). While several factors may have contributed to the observed lack of clinical efficacy, there are some reports suggesting that A2AR antagonism may be most efficacious in protecting against the initial development of parkinsonian motor impairments. A2AR-deficient mice are protected

against haloperidol-induced catalepsy (El Yacoubi et al., 2001; Taura et al., 2018), and our own laboratory has found that sensitization of catalepsy in response to repeated haloperidol exposure can be blocked by co-administration of theophylline (data not shown). We have also reported that induction of inhibitory motor learning is blocked by co-administration of theophylline, but theophylline has no therapeutic effect after aberrant learning has already taken place (Beeler et al., 2012). Similarly, chronic caffeine treatment, which can mitigate the acquisition of inhibitory motor learning, has no discernable effect on performance when administered during recovery only (Figure 1.5). These findings suggest that the benefits of A2AR antagonism are primarily preventive in nature and may be most effective at earlier stages of dopamine depletion. Interestingly, istradefylline has been found to improve PD symptoms during the OFF periods between L-DOPA doses after several weeks of treatment (Dungo and Deeks, 2013). A2AR antagonists could potentially induce an LDR-like therapeutic effect by progressively mitigating aberrant corticostriatal plasticity in the indirect pathway. It will be important for future studies to address A2AR function in the context of pre-existing aberrant plasticity, particularly as it applies to more advanced stages of PD.

We have so far demonstrated a strong correlation between aberrant corticostriatal plasticity and parkinsonian motor deficits, but what remains to be shown is a direct causal link between the two. In the present study, we used *in vivo* optogenetic stimulation to directly activate corticostriatal synapses in the DLS of behaving mice. Though we initially predicted that the combination of stimulation and D2R blockade would be necessary to induce a motor impairment, we also observed a lasting rotarod impairment in mice that received only saline. Given that we were unable to limit the corticostriatal stimulation to just D2-MSNs, it is possible that aberrant changes occurred in both direct and indirect pathways which could be driving the motor

impairment. In order to determine whether this impairment was caused by LTP in the indirect pathway, future studies will need to measure changes in synaptic strength following stimulation with either *ex vivo* or *in vivo* recording. As suggested in the previous chapter, induction of a robust LTP in D2-MSNs may be difficult to achieve with corticostriatal stimulation alone. A recent study demonstrated a method for manipulating striatal plasticity *in vivo* using a dual-channel optogenetic approach (Ma et al., 2018). By expressing the opsins Chronos in prefrontal cortical neurons and Chrimson in the DMS, they were able to pair presynaptic stimulation with postsynaptic depolarization *in vivo* to induce changes in plasticity and alcohol-seeking behavior in mice (Ma et al., 2018). As optogenetic technology continues to advance, complex approaches like dual-channel optogenetics may soon become the norm for studying causal links between plasticity and behavior.

CHAPTER 4

DISCUSSION

4.1 Summary

Dopamine modulates both intrinsic excitability and synaptic plasticity in MSNs, which ultimately influences an animal's behavioral output. The loss of this modulation in PD models triggers a range of physiological changes, both homeostatic and maladaptive. The research presented in this thesis describes the aberrant synaptic changes that underlie motor impairments associated with dopamine loss. In this chapter, I will briefly summarize the results from Chapters 2 and 3 and follow with a discussion on how these findings may be relevant to human PD symptoms and treatment.

4.1.1 Postsynaptic corticostriatal LTD is uncovered by low-frequency optogenetic stimulation

In Chapter 2, I tested optogenetic stimulation protocols for corticostriatal plasticity in brain slices. I showed that a previously reported LTP protocol that used low extracellular magnesium and electrical stimulation could not induce LTP with optogenetic corticostriatal stimulation. I also demonstrated that optogenetic stimulation could not induce LTP with a protocol using high intracellular cAMP and low frequency electrical stimulation. These results indicate that cell-type-specific stimulation is essential for understanding the precise mechanisms of striatal plasticity. In Chapter 2, I also characterized an optogenetic corticostriatal LTD that is distinct from the well-characterized presynaptic LTD seen in the striatum. This LTD is induced by low-frequency optical stimulation, and does not depend on CB1R, NMDAR, or mGluR5

activation. Furthermore, it is not associated with a change in PPR, suggesting that its locus of depression is postsynaptic.

4.1.2 Aberrant corticostriatal plasticity underlies inhibitory motor learning

In Chapter 3, I demonstrated mice that experienced inhibitory motor learning showed aberrant corticostriatal plasticity in indirect pathway MSNs. By using the optogenetic LTD induction protocol characterized in Chapter 2, I found mice that received rotarod training while under D2R blockade showed enhanced corticostriatal LTD in D2-MSNs compared to mice that received either training or D2R blockade alone. This finding suggests that animals experiencing inhibitory motor learning develop aberrant corticostriatal LTP that may underlie impaired performance. Furthermore, mice that were co-administered an A2AR antagonist during motor training showed a smaller magnitude of LTD in slice, suggesting that A2AR blockade protects against inhibitory motor learning by blocking the induction of aberrant corticostriatal LTP. In Chapter 3 I also showed that direct corticostriatal stimulation could induce a lasting motor impairment in mice. Together, these findings highlight aberrant plasticity as a significant component in the pathophysiology of PD and uncover a potential mechanism for caffeine's protective effects against PD.

4.2 Targeting aberrant plasticity as a therapeutic approach for Parkinson's disease

Most clinical studies of motor learning in human PD patients typically examine only the early stages of skill acquisition, making it difficult to predict the quality of future performance. However, there are two studies of motor learning conducted over extended periods that strongly suggest that aberrant corticostriatal plasticity and inhibitory motor learning are highly relevant to

human PD. In one study, PD patients were asked to perform different motor learning tasks during both the ON phase (soon after the morning dose) and OFF phase (before the morning dose) of L-DOPA treatment (Anderson et al., 2014). Patients that trained during the ON phase demonstrated a progressive improvement in motor performance over the week of training. However, when these patients were subsequently tested during the OFF phase, they showed a progressive decline in performance. This result is indicative of an inhibitory motor learning process that occurred during the OFF phase of dopamine replacement. Another study examined the role of motor experience in the LDR response of L-DOPA treatment (Kang and Auinger, 2012). The pre-dose performance in a finger-tapping task was measured over the course of 40 weeks in PD patients being treated with L-DOPA. The authors found that the dominant hand demonstrated a greater pre-dose LDR compared to the non-dominant hand in L-DOPA-treated patients, while placebo-treated patients showed no changes in response. Furthermore, L-DOPA patients' scores remained improved over baseline after a brief withdrawal of medication. Their findings demonstrate that the combination of motor activity with dopamine treatment enhances the LDR, while the LDR from L-DOPA without activity is relatively smaller (Kang and Auinger, 2012).

These clinical studies and recent computational models (Beeler et al., 2012; Ursino and Baston, 2018) strongly suggest that the LDR in PD is regulated by dopamine-dependent corticostriatal plasticity, while the gradual decline in motor performance following cessation of L-DOPA is instead due to aberrant plasticity. Moreover, given our own data suggests that the prevention of aberrant LTP can protect against inhibitory motor learning, the reversal of aberrant corticostriatal plasticity could be an effective therapeutic strategy for PD. While L-DOPA already appears to ameliorate aberrant plasticity, as evidenced by the LDR, long-term use of the

drug can lead to adverse side effects such as dyskinesia. Other approaches may include the use of DBS, which is currently used to treat several neurological and psychiatric disorders including PD, epilepsy, Tourette's syndrome, OCD, and depression (Herrington et al., 2016). Chronic DBS has already been shown to induce structural and anatomical changes in the brain (Van Hartevelt et al., 2014), as well as persistent changes in metabolic activity following long-term treatment in various brain regions (Herrington et al., 2016). Finally, non-dopaminergic drugs that target signaling molecules involved in aberrant plasticity could be a novel alternative to current therapies. Our laboratory has previously reported that AC5 knock-out mice show impaired corticostriatal plasticity (Kheirbek et al., 2009), suggesting that molecules that are either involved in or downstream of the cAMP pathway could serve as potential pharmacological targets for treating PD-related plasticity.

4.3 Future directions

A critical step in establishing causality between aberrant corticostriatal plasticity and inhibitory motor learning will be to demonstrate bidirectional control of motor behaviors with both LTP and LTD in mice *in vivo*. Not only would this solidify the causal link between plasticity and behavior, it would also demonstrate that aberrant corticostriatal plasticity is a viable therapeutic target for PD. Recent studies have demonstrated that optogenetics can be used to reverse both potentiation and depression *in vivo* to influence drug-related behaviors or recall of memories (Nabavi et al., 2014; Creed et al., 2015; Ma et al., 2018). The optogenetic LTD protocol described in Chapter 2, which requires no specific extracellular or intracellular perturbations to execute, can be used to induce postsynaptic corticostriatal LTD in animals with inhibitory motor learning. Moreover, the therapeutic effects of LTD should be tested in a more

traditional model of PD, such as 6-OHDA-lesioned mice. Further work will be needed to uncover a reliable optogenetic LTP protocol that can reverse LTD both in slice and *in vivo*. Opsins with faster kinetics than ChR2, such as ChIEF (Lin et al., 2009), may be required to achieve the necessary stimulation frequency for inducing corticostriatal potentiation.

One concern with the experiments proposed above is the lack of specificity for behaviorally relevant cells during *in vivo* stimulation. A recently developed transgenic mouse tool, targeted recombination in active populations (TRAP), allows expression of a fluorescent label or opsin in active neuronal populations (Guenthner et al., 2013; DeNardo et al., 2019). TRAP targets recombination with an IEG promoter (FosTRAP or ArcTRAP), driving expression of CreER, a tamoxifen-inducible form of Cre recombinase. By taking advantage of brain c-Fos expression, FosTRAP mice could be used to express ChR2 in neurons that were active during rotarod training. This would allow for subsequent depotentiation and repotentiation experiments to limit stimulation to behaviorally relevant cells or axons in the striatum. More generally, FosTRAP mice could also be used to label activity in MSNs to provide insight into how aberrant striatal activity is distributed during different phases of inhibitory motor learning.

4.4 Conclusions

The research presented in this thesis revealed aberrant synaptic changes underlying motor impairments associated with PD. Motor activity engaged under deficient dopamine signaling results in corticostriatal LTP in D2-MSNs, which is proposed to drive inhibitory motor learning in mice. Furthermore, A2AR antagonists, such as caffeine and theophylline, protect against inhibitory motor learning by blocking the induction of aberrant corticostriatal LTP in the indirect pathway. These findings provide new insight into not only the deterioration of motor output in

PD, but also the mechanisms of the LDR in L-DOPA treatment and protective effects of caffeine in PD. Therapeutic strategies that target aberrant synaptic plasticity could deliver significant, long-lasting improvements in the motor symptoms of PD.

REFERENCES

Aguiar LMV, Nobre H V., Macêdo DS, Oliveira AA, Freitas RM, Vasconcelos SM, Cunha GMA, Sousa FCF, Viana GSB (2006) Neuroprotective effects of caffeine in the model of 6-hydroxydopamine lesion in rats. Pharmacol Biochem Behav 84:415–419.

Ahmari SE, Spellman T, Douglass NL, Kheirbek MA, Simpson HB, Deisseroth K, Gordon JA, Hen R (2013) Repeated cortico-striatal stimulation generates persistent OCD-like behavior. Science 340:1234–1239.

Albin RL, Young AB, Penney JB (1989) The functional anatomy of basal ganglia disorders. Trends Neurosci 12:366–375.

Alloway KD, Smith JB, Watson GDR (2014) Thalamostriatal projections from the medial posterior and parafascicular nuclei have distinct topographic and physiologic properties. J Neurophysiol 111:36–50.

Anderson ED, Horak FB, Lasarev MR, Nutt JG (2014) Performance of a motor task learned on levodopa deteriorates when subsequently practiced off. Mov Disord 29:54–60.

Ascherio A, Weisskopf MG, O'Reilly EJ, McCullough ML, Calle EE, Rodriguez C, Thun MJ (2004) Coffee consumption, gender, and Parkinson's disease mortality in the Cancer Prevention Study II cohort: The modifying effects of estrogen. Am J Epidemiol 160:977–984.

Ascherio A, Zhang SM, Hernán MA, Kawachi I, Colditz GA, Speizer FE, Willett WC (2001) Prospective study of caffeine consumption and risk of Parkinson's disease in men and women. Ann Neurol 50:56–63.

Assous M, Faust TW, Assini R, Shah F, Sidibe Y, Tepper JM (2018) Identification and characterization of a novel spontaneously active bursty gabaergic interneuron in the mouse striatum. J Neurosci 38:5688–5699.

Augustin SM, Beeler JA, McGehee DS, Zhuang X (2014) Cyclic AMP and afferent activity govern bidirectional synaptic plasticity in striatopallidal neurons. J Neurosci 34:6692–6699.

Augustin SM, Chancey JH, Lovinger DM (2018) Dual Dopaminergic Regulation of Corticostriatal Plasticity by Cholinergic Interneurons and Indirect Pathway Medium Spiny Neurons. Cell Rep 24:2883–2893.

Augustin SM, Lovinger DM (2018) Functional Relevance of Endocannabinoid-Dependent Synaptic Plasticity in the Central Nervous System. ACS Chem Neurosci.

Averbeck BB, Lehman J, Jacobson M, Haber SN (2014) Estimates of projection overlap and zones of convergence within frontal-striatal circuits. J Neurosci 34:9497–9505.

Barbato L, Stocchi F, Monge A, Vacca L, Ruggieri S, Nordera G, Marsden CD (1997) The long-duration action of levodopa may be due to a postsynaptic effect. Clin Neuropharmacol 20:394–401.

Beeler JA, Cao ZFH, Kheirbek MA, Ding Y, Koranda J, Murakami M, Kang UJ, Zhuang X (2010) Dopamine-dependent motor learning: Insight into levodopa's long-duration response. Ann Neurol 67:639–647.

Beeler JA, Frank MJ, McDaid J, Alexander E, Turkson S, Bernardez MS, McGehee DS, Zhuang X (2012) A role for dopamine-mediated learning in the pathophysiology and treatment of Parkinson's disease. Cell Rep 2:1747–1761.

Bennett BD, Callaway JC, Wilson CJ (2000) Intrinsic membrane properties underlying spontaneous tonic firing in neostriatal cholinergic interneurons. J Neurosci 20:8493–8503.

Björklund A, Dunnett SB (2007) Dopamine neuron systems in the brain: an update. Trends Neurosci 30:194–202.

Bolam JP, Hanley JJ, Booth PA, Bevan MD (2000) Synaptic organisation of the basal ganglia. J Anat 196:527–542.

Bonsi P, Pisani A, Bernardi G, Calabresi P (2003) Stimulus frequency, calcium levels and striatal synaptic plasticity. Neuroreport 14:419–422.

Calabresi P, Filippo M Di, Ghiglieri V, Tambasco N, Picconi B (2010) Levodopa-induced dyskinesias in patients with Parkinson's disease: Filling the bench-to-bedside gap. Lancet Neurol 9:1106–1117.

Calabresi P, Misgeld U, Dodt HU (1987) Intrinsic membrane properties of neostriatal neurons can account for their low level of spontaneous activity. Neuroscience 20:293–303.

Calabresi P, Picconi B, Tozzi A, Di Filippo M (2007) Dopamine-mediated regulation of corticostriatal synaptic plasticity. Trends Neurosci 30:211–219.

Calabresi P, Pisani A, Mercuri NB, Bernardi G (1992) Long-term Potentiation in the Striatum is Unmasked by Removing the Voltage-dependent Magnesium Block of NMDA Receptor Channels. Eur J Neurosci 4:929–935.

Cao VY, Ye Y, Mastwal S, Ren M, Coon M, Liu Q, Costa RM, Wang KH (2015) Motor Learning Consolidates Arc-Expressing Neuronal Ensembles in Secondary Motor Cortex. Neuron 86:1385–1392.

Cao X, Yasuda T, Uthayathas S, Watts RL, Mouradian MM, Mochizuki H, Papa SM (2010) Striatal Overexpression of FosB Reproduces Chronic Levodopa-Induced Involuntary Movements. J Neurosci 30:7335–7343.

Carvey PM, Punati A, Newman MB (2006) Progressive dopamine neuron loss in Parkinson's

disease: the multiple hit hypothesis. Cell Transpl 15:239–250.

Casas M, Ferre S, Guix T, Jane F (1988) Theophylline reverses haloperidol-induced catalepsy in the rat possible relevance to the pharmacological treatment of psychosis. Biol Psychiatry 24:642–648.

Cepeda C, André VM, Yamazaki I, Wu N, Kleiman-Weiner M, Levine MS (2008) Differential electrophysiological properties of dopamine D1 and D2 receptor-containing striatal medium-sized spiny neurons. Eur J Neurosci 27:671–682.

Chen JF, Xu K, Petzer JP, Staal R, Xu YH, Beilstein M, Sonsalla PK, Castagnoli K, Castagnoli N, Schwarzschild MA (2001) Neuroprotection by caffeine and A2A adenosine receptor inactivation in a model of Parkinson's disease. J Neurosci 21:1–6.

Chiken S, Nambu A (2016) Mechanism of Deep Brain Stimulation: Inhibition, Excitation, or Disruption? Neuroscientist 22:313–322.

Cotzias GC, Papvasiliou PS, Gellene R (1969) Modification of Parkinsonism--Chronic Treatment with L-Dopa. N Engl J Med 280:337–345.

Cowan RL, Wilson CJ (1994) Spontaneous firing patterns and axonal projections of single corticostriatal neurons in the rat medial agranular cortex. J Neurophysiol 71:17–32.

Creed M, Pascoli VJ, Lüscher C (2015) Refining deep brain stimulation to emulate optogenetic treatment of synaptic pathology. Science 347:659–664.

Cui Y, Paillé V, Xu H, Genet S, Delord B, Fino E, Berry H, Venance L (2015) Endocannabinoids mediate bidirectional striatal spike-timing-dependent plasticity. J Physiol 593.13:2833–2849.

Cui Y, Prokin I, Xu H, Delord B, Genet S, Venance L, Berry H (2016) Endocannabinoid dynamics gate spike- timing dependent depression and potentiation. Elife 5:e13185.

Currie LJ, Harrison MB, Trugman JM, Bennett JP, Wooten GF (2004) Postmenopausal estrogen use affects risk for Parkinson disease. Arch Neurol 61:886–888.

Day M, Wang Z, Ding J, An X, Ingham CA, Shering AF, Wokosin D, Ilijic E, Sun Z, Sampson AR, Mugnaini E, Deutcch AY, Sesack SR, Arbuthnott GW, Surmeier DJ (2006) Selective elimination of glutamatergic synapses on striatopallidal neurons in Parkinson disease models. Nat Neurosci 9:251–259.

De Mei C, Ramos M, Iitaka C, Borrelli E (2009) Getting specialized: presynaptic and postsynaptic dopamine D2 receptors. Curr Opin Pharmacol 9:53–58.

DeLong MR (1990) Primate models of movement disorders of basal ganglia origin. Trends Neurosci 13:281–285.

DeNardo LA, Liu CD, Allen WE, Adams EL, Friedmann D, Fu L, Guenthner CJ, Tessier-Lavigne M, Luo L (2019) Temporal evolution of cortical ensembles promoting remote memory retrieval. Nat Neurosci 22:460–469.

Ding J, Guzman JN, Tkatch T, Chen S, Goldberg JA, Ebert PJ, Levitt P, Wilson CJ, Hamm HE, Surmeier DJ (2006) RGS4-dependent attenuation of M4 autoreceptor function in striatal cholinergic interneurons following dopamine depletion. Nat Neurosci 9:832–842.

Ding Y, Won L, Britt JP, Lim SAO, McGehee DS, Kang UJ (2011) Enhanced striatal cholinergic neuronal activity mediates L-DOPA-induced dyskinesia in parkinsonian mice. Proc Natl Acad Sci U S A 108:840–845.

Donoghue JP, Herkenham M (1986) Neostriatal projections from individual cortical fields conform to histochemically distinct striatal compartments in the rat. Brain Res 365:397–403.

Donoghue JP, Kitai ST (1981) A collateral pathway to the neostriatum from corticofugal neurons of the rat sensory-motor cortex: An intracellular HRP study. J Comp Neurol 201:1–13.

Dubach M, Schmidt R, Kunkel D, Bowden DM, Martin R, German DC (1987) Primate neostriatal neurons containing tyrosine hydroxylase: Immunohistochemical evidence. Neurosci Lett 75:205–210.

Dumartin B, Doudnikoff E, Gonon F, Bloch B (2007) Differences in ultrastructural localization of dopaminergic D1 receptors between dorsal striatum and nucleus accumbens in the rat. Neurosci Lett 419:273–277.

Dungo R, Deeks ED (2013) Istradefylline: First global approval. Drugs 73:875–882.

Eblen F, Graybiel AM (1995) Highly restricted origin of prefrontal cortical inputs to striosomes in the macaque monkey. J Neurosci 15:5999–6013.

El Yacoubi M, Ledent C, Parmentier M, Costentin J, Vaugeois JM (2001) Adenosine A2A receptor knockout mice are partially protected against drug-induced catalepsy. Neuroreport 12:983–986.

Engeln M, Bastide MF, Toulmé E, Dehay B, Bourdenx M, Doudnikoff E, Li Q, Gross CE, Boué-Grabot E, Pisani A, Bezard E, Fernagut PO (2016) Selective Inactivation of Striatal FosB/ΔFosB-Expressing Neurons Alleviates L-DOPA–Induced Dyskinesia. Biol Psychiatry 79:354–361.

Fabbrini G, Brotchie JM, Grandas F, Nomoto M, Goetz CG (2007) Levodopa-induced dyskinesias. Mov Disord 22:1379–1389.

Faust TW, Assous M, Shah F, Tepper JM, Koós T (2015) Novel fast adapting interneurons mediate cholinergic-induced fast GABA<inf>A</inf> inhibitory postsynaptic currents in striatal spiny neurons. Eur J Neurosci 42:1764–1774.

Ferger B, Spratt C, Earl CD, Teismann P, Oertel WH, Kuschinsky K (1998) Effects of nicotine on hydroxyl free radical formation in vitro and on MPTP-induced neurotoxicity in vivo. Naunyn Schmiedebergs Arch Pharmacol 358:351–359.

Fernandez-Duenas V, Ferre S, Ciruela F (2018) Adenosine A2A-dopamine D2 receptor heteromers operate striatal function: Impact on Parkinson's disease pharmacotherapeutics. Neural Regen Res 13:241–243.

Fernández-Dueñas V, Taura JJ, Cottet M, Gómez-Soler M, López-Cano M, Ledent C, Watanabe M, Trinquet E, Pin JP, Luján R, Durroux T, Ciruela F (2015) Untangling dopamine-adenosine receptor-receptor assembly in experimental parkinsonism in rats. DMM Dis Model Mech 8:57–63.

Ferré S, Quiroz C, Orru M, Guitart X, Navarro G, Cortés A, Casadó V, Canela EI, Lluis C, Franco R (2011) Adenosine A2A receptors and A2A receptor heteromers as key players in striatal function. Front Neuroanat 5:1–8.

Fieblinger T, Graves SM, Sebel LE, Alcacer C, Plotkin JL, Gertler TS, Chan CS, Heiman M, Greengard P, Cenci MA, Surmeier DJ (2014) Cell type-specific plasticity of striatal projection neurons in parkinsonism and L-DOPA-induced dyskinesia. Nat Commun 5:5316.

Flajolet M, Wang Z, Futter M, Shen W, Nuangchamnong N, Bendor J, Wallach I, Nairn AC, Surmeier DJ, Greengard P (2008) FGF acts as a co-transmitter through adenosine A2A receptor to regulate synaptic plasticity. Nat Neurosci 11:1402–1409.

Ford CP (2014) The role of D2-autoreceptors in regulating dopamine neuron activity and transmission. Neuroscience 282:13–22.

Gerfen CR (1992) The neostriatal mosaic: Multiple levels of compartmental organization. Annu Rev Neurosci 15:285–320.

Gerfen CR, Paletzki R, Heintz N (2013) GENSAT BAC cre-recombinase driver lines to study the functional organization of cerebral cortical and basal ganglia circuits. Neuron 80:1368–1383.

Gerfen CR, Surmeier DJ (2011) Modulation of striatal projection systems by dopamine. Annu Rev Neurosci 34:441–466.

Gertler TS, Chan CS, Surmeier DJ (2008) Dichotomous Anatomical Properties of Adult Striatal Medium Spiny Neurons. J Neurosci 28:10814–10824.

Girasole AE, Lum MY, Nathaniel D, Luo L, Kreitzer AC, Nelson AB (2018) A Subpopulation of Striatal Neurons Mediates Levodopa-Induced Dyskinesia. Neuron 97:787-795.e6.

Giros B, Sokoloff P, Martres MP, Riou JF, Emorine LJ, Schwartz JC (1989) Alternative splicing directs the expression of two D2 dopamine receptor isoforms. Nature 342:923–926.

Gokce O, Stanley G, Treutlein B, Neff N, Camp JG, Malenka RC, Rothwell PE, Fuccillo M V., Sudhof TC, Quake SR (2016) Cellular Taxonomy of the Mouse Striatum as Revealed by Single Cell RNA Sequencing. Cell Rep 16:1126–1137.

Goldberg JA, Ding JB, Surmeier DJ (2012) Muscarinic modulation of striatal function and circuitry. Handb Exp Pharmacol 208:223–241.

Gong S, Doughty M, Harbaugh CR, Cummins A, Hatten ME, Heintz N, Gerfen CR (2007) Targeting Cre recombinase to specific neuron populations with bacterial artificial chromosome constructs. J Neurosci 27:9817–9823.

Gong S, Zheng C, Doughty ML, Losos K, Didkovsky N, Schambra UB, Nowak NJ, Joyner A, Leblanc G, Hatten ME, Heintz N (2003) A gene expression atlas of the central nervous system based on bacterial artificial chromosomes. Nature 425.

Gorell JM, Rybicki BA, Johnson CC, Peterson EL (1999) Smoking and Parkinson's disease: A dose-response relationship. Neurology 52:115–119.

Grace AA, Bunney BS (1983) Intracellular and extracellular electrophysiology of nigral dopaminergic neurons. Neuroscience 10:301–315.

Grady S, Marks MJ, Wonnacott S, Collins AC (1992) Characterization of Nicotinic Receptor-Mediated [3H]Dopamine Release from Synaptosomes Prepared from Mouse Striatum. J Neurochem 59:848–856.

Graves SM, Surmeier DJ (2019) Delayed spine pruning of direct pathway spiny projection neurons in a mouse model of parkinson's disease. Front Cell Neurosci 13:32.

Graybiel AM, Aosaki T, Flaherty AW, Kimura M (1994) The basal ganglia and adaptive motor control. Science 265:1826–1831.

Greif GJ, Lin YJ, Liu JC, Freedman JE (1995) Dopamine-modulated potassium channels on rat striatal neurons: Specific activation and cellular expression. J Neurosci 15:4533–4544.

Guenthner CJ, Miyamichi K, Yang HH, Heller HC, Luo L (2013) Permanent genetic access to transiently active neurons via TRAP: targeted recombination in active populations. Neuron 78:773–784.

Haber SN (2016) Corticostriatal circuitry. Dialogues Clin Neurosci 18:7–21.

Haber SN, Kim KS, Mailly P, Calzavara R (2006) Reward-related cortical inputs define a large striatal region in primates that interface with associative cortical connections, providing a substrate for incentive-based learning. J Neurosci 26:8368–8376.

Hawes SL, Evans RC, Unruh BA, Benkert EE, Gillani F, Dumas TC, Blackwell KT (2015) Multimodal plasticity in dorsal striatum while learning a lateralized navigation task. J Neurosci 35:10535–10549.

Heiman M, Schaefer A, Gong S, Peterson JD, Day M, Ramsey KE, Suárez-Fariñas M, Schwarz C, Stephan DA, Surmeier DJ, Greengard P, Heintz N (2008) A Translational Profiling Approach for the Molecular Characterization of CNS Cell Types. Cell 135:738–748.

Heimer L, Zahm DS, Churchill L, Kalivas PW, Wohltmann C (1991) Specificity in the projection patterns of accumbal core and shell in the rat. Neuroscience 41:89–125.

Hernández-Echeagaray E, Starling AJ, Cepeda C, Levine MS (2004) Modulation of AMPA currents by D2 dopamine receptors in striatal medium-sized spiny neurons: Are dendrites necessary? Eur J Neurosci 19:2455–2463.

Hernández-López S, Tkatch T, Perez-Garci E, Galarraga E, Bargas J, Hamm H, Surmeier DJ (2000) D2 dopamine receptors in striatal medium spiny neurons reduce L-type Ca2+ currents and excitability via a novel PLCβ1-IP3-Calcineurin-signaling cascade. J Neurosci 20:8987–8995.

Herrington TM, Cheng JJ, Eskandar EN (2016) Mechanisms of deep brain stimulation. J Neurophysiol 115:19–38.

Herron CE, Lester RAJ, Coan EJ, Collingridge GL (1985) Intracellular demonstration of an N-methyl-d-aspartate receptor mediated component of synaptic transmission in the rat hippocampus. Neurosci Lett 16:19–23.

Higley MJ, Sabatini BL (2010) Competitive regulation of synaptic Ca2+ influx by D2 dopamine and A2A adenosine receptors. Nat Neurosci 13:958–966.

Hooks BM, Papale AE, Paletzki RF, Feroze MW, Eastwood BS, Couey JJ, Winnubst J, Chandrashekar J, Gerfen CR (2018) Topographic precision in sensory and motor corticostriatal projections varies across cell type and cortical area. Nat Commun 9.

Huerta-Ocampo I, Mena-Segovia J, Bolam JP (2014) Convergence of cortical and thalamic input to direct and indirect pathway medium spiny neurons in the striatum. Brain Struct Funct 219:1787–1800.

Hwang DY, Ardayfio P, Kang UJ, Semina E V., Kim KS (2003) Selective loss of dopaminergic neurons in the substantia nigra of Pitx3-deficient aphakia mice. Mol Brain Res 114:123–131.

Hwang DY, Fleming SM, Ardayfio P, Moran-Gates T, Kim H, Tarazi FI, Chesselet MF, Kim KS (2005) 3,4-Dihydroxyphenylalanine reverses the motor deficits in Pitx3-deficient Aphakia mice: Behavioral characterization of a novel genetic model of Parkinson's disease. J Neurosci 25:2132–2137.

Ibáñez-Sandoval O, Tecuapetla F, Unal B, Shah F, Koós T, Tepper JM (2011) A novel functionally distinct subtype of striatal neuropeptide Y interneuron. J Neurosci 31:16757–16769.

Joghataie MT, Roghani M, Negahdar F, Hashemi L (2004) Protective effect of caffeine against neurodegeneration in a model of Parkinson's disease in rat: Behavioral and histochemical evidence. Park Relat Disord 10:465–468.

Kang UJ, Auinger P (2012) Activity enhances dopaminergic long-duration response in Parkinson disease. Neurology 78:1146–1149.

Kheirbek MA, Britt JP, Beeler JA, Ishikawa Y, McGehee DS, Zhuang X (2009) Adenylyl cyclase type 5 contributes to corticostriatal plasticity and striatum-dependent learning. J Neurosci 29:12115–12124.

Khwaja M, McCormack A, McIntosh JM, Di Monte DA, Quik M (2007) Nicotine partially protects against paraquat-induced nigrostriatal damage in mice; link to α6β2* nAChRs. J Neurochem 100:180–190.

Kim CK, Adhikari A, Deisseroth K (2017) Integration of optogenetics with complementary methodologies in systems neuroscience. Nat Rev Neurosci 18:222–235.

Kincaid AE, Wilson CJ (1996) Corticostriatal innervation of the patch and matrix in the rat neostriatum. J Comp Neurol 374:578–592.

Koralek AC, Jin X, Long JD, Costa RM, Carmena JM (2012) Corticostriatal plasticity is necessary for learning intentional neuroprosthetic skills. Nature 483:331–335.

Koranda JL, Cone JJ, McGehee DS, Roitman MF, Beeler JA, Zhuang X (2014) Nicotinic receptors regulate the dynamic range of dopamine release in vivo. J Neurophysiol 111:103–111.

Koranda JL, Krok AC, Xu J, Contractor A, McGehee DS, Beeler JA, Zhuang X (2016) Chronic Nicotine Mitigates Aberrant Inhibitory Motor Learning Induced by Motor Experience under Dopamine Deficiency. J Neurosci 36:5228–5240.

Kravitz A V., Freeze BS, Parker PRL, Kay K, Thwin MT, Deisseroth K, Kreitzer AC (2010) Regulation of parkinsonian motor behaviours by optogenetic control of basal ganglia circuitry. Nature 466:622–626.

Kravitz A V., Tye LD, Kreitzer AC (2012) Distinct roles for direct and indirect pathway striatal neurons in reinforcement. Nat Neurosci 15:816–818.

Kreitzer AC (2009) Physiology and pharmacology of striatal neurons. Annu Rev Neurosci 32:127–147.

Kreitzer AC, Malenka RC (2005) Dopamine modulation of state-dependent endocannabinoid release and long-term depression in the striatum. J Neurosci 25:10537–10545.

Kreitzer AC, Malenka RC (2007) Endocannabinoid-mediated rescue of striatal LTD and motor deficits in Parkinson's disease models. Nature 445:643–647.

Kress GJ, Yamawaki N, Wokosin DL, Wickersham IR, Shepherd GMG, Surmeier DJ (2013) Convergent cortical innervation of striatal projection neurons. Nat Neurosci 16:665–667.

Kupferschmidt DA, Juczewski K, Cui G, Johnson KA, Lovinger DM (2017) Parallel, but Dissociable, Processing in Discrete Corticostriatal Inputs Encodes Skill Learning. Neuron 96:476-489.e5.

La Manno G, Gyllborg D, Codeluppi S, Nishimura K, Salto C, Zeisel A, Borm LE, Stott SRW, Toledo EM, Villaescusa JC, Lönnerberg P, Ryge J, Barker RA, Arenas E, Linnarsson S (2016) Molecular Diversity of Midbrain Development in Mouse, Human, and Stem Cells. Cell 167:566–580.

Leranth C, Roth RH, Elsworth JD, Naftolin F, Horvath TL, Redmond DE (2000) Estrogen Is Essential for Maintaining Nigrostriatal Dopamine Neurons in Primates: Implications for Parkinson's Disease and Memory. J Neurosci 20:8604–8609.

Lerner TN, Kreitzer AC (2012) RGS4 Is Required for Dopaminergic Control of Striatal LTD and Susceptibility to Parkinsonian Motor Deficits. Neuron 73:347–359.

Lichtensteiger W, Hefti F, Felix D, Huwyler T, Melamed E, Schlumpf M (1982) Stimulation of nigrostriatal dopamine neurones by nicotine. Neuropharmacology 21:963–968.

Lim SAO, Kang UJ, McGehee DS (2014) Striatal cholinergic interneuron regulation and circuit effects. Front Synaptic Neurosci 6:1–23.

Lin JY, Lin MZ, Steinbach P, Tsien RY (2009) Characterization of engineered channelrhodopsin variants with improved properties and kinetics. Biophys J 96:1803–1814.

Little S, Beudel M, Zrinzo L, Foltynie T, Limousin P, Hariz M, Neal S, Cheeran B, Cagnan H, Gratwicke J, Aziz TZ, Pogosyan A, Brown P (2016) Bilateral adaptive deep brain stimulation is effective in Parkinson's disease. J Neurol Neurosurg Psychiatry 87:717–721.

Lobo MK, Karsten SL, Gray M, Geschwind DH, Yang XW (2006) FACS-array profiling of striatal projection neuron subtypes in juvenile and adult mouse brains. Nat Neurosci 9:433–452.

Lohse KR, Wadden K, Boyd LA, Hodges NJ (2014) Motor skill acquisition across short and long time scales: A meta-analysis of neuroimaging data. Neuropsychologia 59:130–141.

Lovinger DM (2010) Neurotransmitter roles in synaptic modulation, plasticity and learning in the dorsal striatum. Neuropharmacology 58:951–961.

Lovinger DM, Tyler EC, Merritt A (1993) Short- and long-term synaptic depression in rat neostriatum. J Neurophysiol 70:1937–1949.

Lynd-Balta E, Haber SN (1994) The organization of midbrain projections to the striatum in the primate: Sensorimotor-related striatum versus ventral striatum. Neuroscience 59:625–640.

Ma T, Barbee B, Wang X, Wang J (2017) Alcohol induces input-specific aberrant synaptic plasticity in the rat dorsomedial striatum. Neuropharmacology 123:46–54.

Ma T, Cheng Y, Hellard ER, Wang X, Lu J, Gao X, Huang CCY, Wei X, Ji J, Wang J (2018) Bidirectional and long-lasting control of alcohol-seeking behavior by corticostriatal LTP and LTD. Nat Neurosci.

Mandhane SN, Chopde CT, Ghosh AK (1997) Adenosine A2 receptors modulate haloperidol-induced catalepsy in rats. Eur J Pharmacol 328:135–141.

Marcellino D, Lindqvist E, Schneider M, Müller CE, Fuxe K, Olson L, Galter D (2010) Chronic A2A antagonist treatment alleviates parkinsonian locomotor deficiency in MitoPark mice. Neurobiol Dis 40:460–466.

Marras C, Beck JC, Bower JH, Roberts E, Ritz B, Ross GW, Abbott RD, Savica R, Van Den Eeden SK, Willis AW, Tanner C (2018) Prevalence of Parkinson's disease across North America. npj Park Dis 4:1–7.

Martiros N, Burgess AA, Graybiel AM (2018) Inversely Active Striatal Projection Neurons and Interneurons Selectively Delimit Useful Behavioral Sequences. Curr Biol 28:560–573.

Moo-Puc RE, Góngora-Alfaro JL, Alvarez-Cervera FJ, Pineda JC, Arankowsky-Sandoval G, Heredia-López F (2003) Caffeine and muscarinic antagonists act in synergy to inhibit haloperidol-induced catalepsy. Neuropharmacology 45:493–503.

Moro E, Esselink RJA, Xie J, Hommel M, Benabid AL, Pollak P (2002) The impact on Parkinson's disease of electrical parameter settings in STN stimulation. Neurology 59:706–713.

Nabavi S, Fox R, Proulx CD, Lin JY, Tsien RY, Malinow R (2014) Engineering a memory with LTD and LTP. Nature 511:348–352.

Neve KA, Seamans JK, Trantham-Davidson H (2004) Dopamine receptor signaling. J Recept Signal Transduct 24:165–205.

Nisenbaum ES, Mermelstein PG, Wilson CJ, Surmeier DJ (1998) Selective blockade of a slowly inactivating potassium current in striatal neurons by (±) 6-chloro-APB hydrobromide (SKF82958). Synapse 23:213–224.

Nishijima H, Suzuki S, Kon T, Funamizu Y, Ueno T, Haga R, Suzuki C, Arai A, Kimura T, Suzuki C, Meguro R, Miki Y, Yamada J, Migita K, Ichinohe N, Ueno S, Baba M, Tomiyama M (2014) Morphologic changes of dendritic spines of striatal neurons in the levodopa-induced dyskinesia model. Mov Disord 29:336–343.

Nutt JG, Woodward WR, Carter JH, Gancher ST (1992) Effect of long-term therapy on the pharmacodynamics of levodopa: Relation to on-off phenomenon. Arch Neurol 49:1123–1130.

Owen SF, Berke JD, Kreitzer AC (2018) Fast-Spiking Interneurons Supply Feedforward Control of Bursting, Calcium, and Plasticity for Efficient Learning. Cell 172:683–695.

Palacios N, Gao X, McCullough ML, Schwarzschild MA, Shah R, Gapstur S, Ascherio A (2012) Caffeine and risk of Parkinson's disease in a large cohort of men and women. Mov Disord 27:1276–1282.

Pan WX, Mao T, Dudman JT (2010) Inputs to the dorsal striatum of the mouse reflect the parallel circuit architecture of the forebrain. Front Neuroanat 4:1–13.

Park H, Popescu A, Poo M (2014) Essential Role of Presynaptic NMDA Receptors in Activity-Dependent BDNF Secretion and Corticostriatal LTP. Neuron 84:1009–1022.

Parker PRL, Lalive AL, Kreitzer AC (2016) Pathway-Specific Remodeling of Thalamostriatal Synapses in Parkinsonian Mice. Neuron 89:734–740.

Pascoli V, Turiault M, Lüscher C (2012) Reversal of cocaine-evoked synaptic potentiation resets drug-induced adaptive behaviour. Nature 481:71–75.

Pawlak V, Kerr JND (2008) Dopamine receptor activation is required for corticostriatal spike-timing-dependent plasticity. J Neurosci 28:2435–2446.

Peterson JD, Goldberg JA, Surmeier DJ (2012) Adenosine A2a receptor antagonists attenuate striatal adaptations following dopamine depletion. Neurobiol Dis 45:409–416.

Phillips PEM, Hancock PJ, Stamford JA (2002) Time window of autoreceptor-mediated inhibition of limbic and striatal dopamine release. Synapse 44:15–22.

Pisani A, Bonsi P, Centonze D, Calabresi P, Bernardi G (2000) Activation of D2-like dopamine receptors reduces synaptic inputs to striatal cholinergic interneurons. J Neurosci 20:RC69.

Pollock BG, Wylie M, Stack JA, Sorisio DA, Thompson DS, Kirshner MA, Folan MM, Condifer KA (1999) Inhibition of caffeine metabolism by estrogen replacement therapy in postmenopausal women. J Clin Pharmacol 39:936–940.

Postuma RB, Anang J, Pelletier A, Joseph L, Moscovich M, Grimes D, Furtado S, Munhoz RP, Appel-Cresswell S, Moro A, Borys A, Hobson D, Lang AE (2017) Caffeine as symptomatic treatment for Parkinson disease (Café-PD). Neurology 89:1795–1803.

Poulin JF, Caronia G, Hofer C, Cui Q, Helm B, Ramakrishnan C, Chan CS, Dombeck DA, Deisseroth K, Awatramani R (2018) Mapping projections of molecularly defined dopamine neuron subtypes using intersectional genetic approaches. Nat Neurosci 21:1260–1271.

Poulin JF, Zou J, Drouin-Ouellet J, Kim KYA, Cicchetti F, Awatramani RB (2014) Defining midbrain dopaminergic neuron diversity by single-cell gene expression profiling. Cell Rep 9:930–943.

Prensa L, Parent A (2001) The nigrostriatal pathway in the rat: A single-axon study of the relationship between dorsal and ventral tier nigral neurons and the striosome/matrix striatal compartments. J Neurosci 21:7247–7260.

Quik M, Parameswaran N, McCallum SE, Bordia T, Bao S, McCormack A, Kim A, Tyndale RF, Langston JW, Di Monte DA (2006) Chronic oral nicotine treatment protects against striatal degeneration in MPTP-treated primates. J Neurochem 98:1866–1875.

Ramanathan S, Hanley JJ, Deniau JM, Bolam JP (2002) Synaptic convergence of motor and somatosensory cortical afferents onto GABAergic interneurons in the rat striatum. J Neurosci 22:8158–8169.

Redgrave P, Gurney K (2006) The short-latency dopamine signal: A role in discovering novel actions? Nat Rev Neurosci 7:967–975.

Redgrave P, Rodriguez M, Smith Y, Rodriguez-Oroz MC, Lehericy S, Bergman H, Agid Y, DeLong MR, Obeso JA (2010) Goal-directed and habitual control in the basal ganglia: implications for Parkinson's disease. Nat Rev Neurosci 11:760–772.

Reeve A, Simcox E, Turnbull D (2014) Ageing and Parkinson's disease: Why is advancing age the biggest risk factor? Ageing Res Rev 14:19–30.

Richfield EK, Penney JB, Young AB (1989) Anatomical and affinity state comparisons between dopamine D1 and D2 receptors in the rat central nervous system. Neuroscience 30:767–777.

Ross GW, Abbott RD, Petrovitch H, Morens DM, Grandinetti A, Tung KH, Tanner CM, Masaki KH, Blanchette PL, Curb JD, Popper JS, White LR (2000) Association of coffee and caffeine intake with the risk of Parkinson disease. J Am Med Assoc 283:2674–2679.

Rothwell PE, Hayton SJ, Sun GL, Fuccillo M V., Lim BK, Malenka RC (2015) Input- and Output-Specific Regulation of Serial Order Performance by Corticostriatal Circuits. Neuron 88:345–356.

Rymar V V, Sasseville R, Luk KC, Sadikot AF (2004) Neurogenesis and Stereological Morphometry of Calretinin-Immunoreactive GABAergic Interneurons of the Neostriatum. J Comp Neurol 469:325–339.

Schiffmann SN, Lledo PM, Vincent JD (1995) Dopamine D1 receptor modulates the voltage-gated sodium current in rat striatal neurones through a protein kinase A. J Physiol 483:95–107.

Schultz W (1998) Predictive reward signal of dopamine neurons. J Neurophysiol 80:1–27.

Schultz W (2007) Behavioral dopamine signals. Trends Neurosci 30:203–210.

Selemon LD, Goldman-Rakic PS (1985) Longitudinal topography and interdigitation of corticostriatal projections in the rhesus monkey. J Neurosci 5:776–794.

Shan Q, Christie MJ, Balleine BW (2015) Plasticity in striatopallidal projection neurons mediates the acquisition of habitual actions. Eur J Neurosci 42:2097–2104.

Shan Q, Ge M, Christie MJ, Balleine BW (2014) The acquisition of goal-directed actions generates opposing plasticity in direct and indirect pathways in dorsomedial striatum. J Neurosci 34:9196–9201.

Shen W, Flajolet M, Greengard P, Surmeier DJ (2008) Dichotomous Dopaminergic Control of Striatal Synaptic Plasticity. Science 321:848–851.

Shen W, Plotkin JL, Francardo V, Ko WKD, Xie Z, Fieblinger T, Wess J, Neubig RR, Lindsley CW, Jeffrey P, Greengard P, Bezard E, Cenci MA, Surmeier DJ (2015) M4 muscarinic receptor signaling ameliorates striatal plasticity deficits in models of L-DOPA-induced dyskinesia. Neuron 88:762–773.

Shen W, Tian X, Day M, Ulrich S, Tkatch T, Nathanson NM, Surmeier DJ (2007) Cholinergic modulation of Kir2 channels selectively elevates dendritic excitability in striatopallidal neurons. Nat Neurosci 10:1458–1466.

Shepherd GMG (2013) Corticostriatal connectivity and its role in disease. Nat Rev Neurosci 14:278–291.

Singla S, Kreitzer AC, Malenka RC (2007) Mechanisms for synapse specificity during striatal long-term depression. J Neurosci 27:5260–5264.

Smith JB, Klug JR, Ross DL, Howard CD, Hollon NG, Ko VI, Hoffman H, Callaway EM, Gerfen CR, Jin X (2016) Genetic-Based Dissection Unveils the Inputs and Outputs of Striatal Patch and Matrix Compartments. Neuron 91:1069–1084.

Smith Y, Bevan MD, Shink E, Bolam JP (1998) Microcircuitry of the direct and indirect pathways of the basal ganglia. Neuroscience 86:353–387.

Smith Y, Raju D V., Pare JF, Sidibe M (2004) The thalamostriatal system: A highly specific network of the basal ganglia circuitry. Trends Neurosci 27:520–527.

Spieles-Engemann AL, Steece-Collier K, Behbehani MM, Collier TJ, Wohlgenant SL, Kemp CJ, Cole-Strauss A, Levine ND, Gombash SE, Thompson VB, Lipton JW, Sortwell CE (2011) Subthalamic nucleus stimulation increases brain derived neurotrophic factor in the nigrostriatal system and primary motor cortex. J Parkinsons Dis 1:123–136.

Stanley G, Gokce O, Malenka RC, Südhof TC, Quake SR (2019) Discrete and Continuous Cell Identities of the Adult Murine Striatum. bioRxiv Preprint:. https://doi.org/10.1101/591396.

Stephenson-Jones M, Samuelsson E, Ericsson J, Robertson B, Grillner S (2011) Evolutionary conservation of the basal ganglia as a common vertebrate mechanism for action selection. Curr Biol 21:1081–1091.

Suárez LM, Solís O, Caramés JM, Taravini IR, Solís JM, Murer MG, Moratalla R (2014) L-DOPA treatment selectively restores spine density in dopamine receptor D2-expressing projection neurons in dyskinetic mice. Biol Psychiatry 75:711–722.

Sulzer D (2007) Multiple hit hypotheses for dopamine neuron loss in Parkinson's disease. Trends Neurosci 30:244–250.

Sunahara RK, Taussig R (2002) Isoforms of mammalian adenylyl cyclase: multiplicities of signaling. Mol Interv 2:168–184.

Surmeier DJ, Bargas J, Hemmings HC, Nairn AC, Greengard P (1995) Modulation of calcium currents by a D1 dopaminergic protein kinase/phosphatase cascade in rat neostriatal neurons. Neuron 14:385–397.

Surmeier DJ, Graves SM, Shen W (2014) Dopaminergic modulation of striatal networks in health and Parkinson's disease. Curr Opin Neurobiol 29:109–117.

Surmeier DJ, Kitai ST (1993) D1 and D2 dopamine receptor modulation of sodium and potassium currents in rat neostriatal neurons. Prog Brain Res 99:309–324.

Surmeier DJ, Plotkin J, Shen W (2009) Dopamine and synaptic plasticity in dorsal striatal circuits controlling action selection. Curr Opin Neurobiol 19:621–628.

Sveinbjornsdottir S (2016) The clinical symptoms of Parkinson's disease. J Neurochem 139:318–324.

Svenningsson P, Nishi A, Fisone G, Girault J-A, Nairn AC, Greengard P (2004) DARPP-32: An Integrator of Neurotransmission. Annu Rev Pharmacol Toxicol 44:269–296.

Tan EK, Tan C, Fook-Chong SMC, Lum SY, Chai A, Chung H, Shen H, Zhao Y, Teoh ML, Yih Y, Pavanni R, Chandran VR, Wong MC (2003) Dose-dependent protective effect of coffee, tea, and smoking in Parkinson's disease: A study in ethnic Chinese. J Neurol Sci 216:163–167.

Tanimura A, Du Y, Kondapalli J, Wokosin DL, Surmeier DJ (2019) Cholinergic Interneurons Amplify Thalamostriatal Excitation of Striatal Indirect Pathway Neurons in Parkinson's Disease Models. Neuron 101:444–458.

Tanimura A, Pancani T, Lim SAO, Tubert C, Melendez AE, Shen W, Surmeier DJ (2018) Striatal cholinergic interneurons and Parkinson's disease. Eur J Neurosci 47:1148–1158.

Tanner CM, Goldman SM, Aston DA, Ottman R, Ellenberg J, Mayeux R, Langston JW (2002) Smoking and Parkinson's disease in twins. Neurology 58:581–588.

Taura J, Valle-León M, Sahlholm K, Watanabe M, Van Craenenbroeck K, Fernández-Dueñas V, Ferré S, Ciruela F (2018) Behavioral control by striatal adenosine A2A-dopamine D2 receptor heteromers. Genes, Brain Behav 17:e12432.

Tennant KA, Adkins DL, Donlan NA, Asay AL, Thomas N, Kleim JA, Jones TA (2011) The organization of the forelimb representation of the C57BL/6 mouse motor cortex as defined by intracortical microstimulation and cytoarchitecture. Cereb Cortex 21:865–876.

Tepper JM, Tecuapetla F, Koós T, Ibáñez-Sandoval O (2010) Heterogeneity and diversity of striatal GABAergic interneurons. Front Neuroanat 4:1–18.

Tepper JM, Wilson CJ, Koós T (2008) Feedforward and feedback inhibition in neostriatal GABAergic spiny neurons. Brain Res Rev 58:272–281.

Ting JT, Daigle TL, Chen Q, Feng G (2014) Acute brain slice methods for adult and aging animals: Application of targeted patch clamp analysis and optogenetics. Patch-Clamp Methods Protoc (from Methods Mol Biol 1183:221–242.

Toda H, Hamani C, Fawcett AP, Hutchison WD, Lozano AM (2008) The regulation of adult rodent hippocampal neurogenesis by deep brain stimulation. J Neurosurg 108:132–138.

Tozzi A, De Iure A, Di Filippo M, Tantucci M, Costa C, Borsini F, Ghiglieri V, Giampà C, Fusco FR, Picconi B, Calabresi P (2011) The distinct role of medium spiny neurons and cholinergic interneurons in the D2/A2A receptor interaction in the striatum: Implications for Parkinson's disease. J Neurosci 31:1850–1862.

Ursino M, Baston C (2018) Aberrant learning in Parkinson's disease: A neurocomputational study on bradykinesia. Eur J Neurosci 47:1563–1582.

Van Hartevelt TJ, Cabral J, Deco G, Møller A, Green AL, Aziz TZ, Kringelbach ML (2014) Neural plasticity in human brain connectivity: The effects of long term deep brain stimulation of the subthalamic nucleus in Parkinson's disease. PLoS One 9:e86496.

Voelker R (2019) News from the food and drug administration. JAMA 322:1246.

Wang J, Lanfranco MF, Gibb SL, Yowell Q V., Carnicella S, Ron D (2010) Long-lasting adaptations of the NR2B-containing NMDA receptors in the dorsomedial striatum play a crucial role in alcohol consumption and relapse. J Neurosci 30:10187–10198.

Wang Z, Kai L, Day M, Ronesi J, Yin HH, Ding J, Tkatch T, Lovinger DM, Surmeier DJ (2006) Dopaminergic Control of Corticostriatal Long-Term Synaptic Depression in Medium Spiny Neurons Is Mediated by Cholinergic Interneurons. :443–452.

Wiesendanger E, Clarke S, Kraftsik R, Tardif E (2004) Topography of cortico-striatal connections in man: Anatomical evidence for parallel organization. Eur J Neurosci 20:1915–1922.

Wilson CJ (1987) Morphology and synaptic connections of crossed corticostriatal neurons in the rat. J Comp Neurol 263:567–580.

Wilson CJ, Groves PM (1980) Fine structure and synaptic connections of the common spiny

neuron of the rat neostriatum: A study employing intracellular injection of horseradish peroxidase. J Comp Neurol 194:599–615.

Wilson CJ, Kawaguchi Y (1996) The origins of two-state spontaneous membrane potential fluctuations of neostriatal spiny neurons. J Neurosci 16:2387–2410.

Wirdefeldt K, Adami HO, Cole P, Trichopoulos D, Mandel J (2011) Epidemiology and etiology of Parkinson's disease: A review of the evidence. Eur J Epidemiol 26:S1–S58.

Wise RA (2004) Dopamine, learning and motivation. Nat Rev Neurosci 5:483–494.

Wu Y-W, Kim J-I, Tawfik VL, Lalchandani RR, Scherrer G, Ding JB (2015) Input- and Cell-Type-Specific Endocannabinoid-Dependent LTD in the Striatum. Cell Rep 10:75–87.

Xia J, Meyers AM, Beeler JA (2017) Chronic Nicotine Alters Corticostriatal Plasticity in the Striatopallidal Pathway Mediated By NR2B-Containing Silent Synapses. Neuropsychopharmacology:1–11.

Xu H, Perez S, Cornil A, Detraux B, Prokin I, Cui Y, Degos B, Berry H, de Kerchove d'Exaerde A, Venance L (2018) Dopamine–endocannabinoid interactions mediate spike-timing-dependent potentiation in the striatum. Nat Commun 9:. 10.1038/s41467-018-06409-5.

Xu K, Xu Y, Brown-Jermyn D, Chen J, Ascherio A, Dluzen D, Schwarzschild M (2006) Estrogen Prevents Neuroprotection by Caffeine in the Mouse 1-Methyl-4-Phenyl-1,2,3,6-Tetrahydropyridine Model of Parkinson's Disease. J Neurosci 26:535–541.

Yagishita S, Hayashi-Takagi A, Ellis-Davies GCR, Urakubo H, Ishii S, Kasai H (2014) A critical time window for dopamine actions on the structural plasticity of dendritic spines. Science 345:1616–1620.

Yin HH, Knowlton BJ (2006) The role of the basal ganglia in habit formation. Nat Rev Neurosci 7:464–476.

Yin HH, Mulcare SP, Hilário MRF, Clouse E, Holloway T, Davis MI, Hansson AC, Lovinger DM, Costa RM (2009) Dynamic reorganization of striatal circuits during the acquisition and consolidation of a skill. Nat Neurosci 12:333–341.

Zhang YP, Oertner TG (2007) Optical induction of synaptic plasticity using a light-sensitive channel. Nat Methods 4:139–141.

Zheng J, Zhang X, Zhen X (2018) Development of Adenosine A2A Receptor Antagonists for the Treatment of Parkinson's Disease: A Recent Update and Challenge. ACS Chem Neurosci 10:783–791.

Zhuang X, Belluscio L, Hen R (2000) G(olf)alpha mediates dopamine D1 receptor signaling. J Neurosci 20:RC91.

Zhuang X, Mazzoni P, Kang UJ (2013) The role of neuroplasticity in dopaminergic therapy for Parkinson disease. Nat Rev Neurol 9:248–256.